2012

DEPARTAMENTO DE CIÊNCIAS DA VIDA

FACULDADE DE CIÊNCIAS E TECNOLOGIA
UNIVERSIDADE DE COIMBRA

Calcium Mobilisation in Human Sperm and its Effects on Mobility

Calcium Mobilisation in Human Sperm and its Effects on Motility

Leonor Cruz Fernandes

Leonor Cruz Fernandes

2012

DEPARTAMENTO DE CIÊNCIAS DA VIDA

FACULDADE DE CIÊNCIAS E TECNOLOGIA
UNIVERSIDADE DE COIMBRA

Calcium Mobilisation in Human Sperm and its Effects on Motility

Dissertação apresentada à Universidade de Coimbra para cumprimento dos requisitos necessários à obtenção do grau de Mestre em Biologia Celular e Molecular, realizada sob a orientação científica do Professor Doutor Stephen Publicover (Universidade de Birmingham) e do Professor Doutor João Ramalho-Santos (Universidade de Coimbra)

Leonor Cruz Fernandes

2012

Acknowledgments

À minha família. Em especial aos meus pais Eduardo e Ana Paula, irmão Miguel e avó Lurdinhas por estarem sempre lá, por me apoiarem em tudo o que fiz, faço e farei e por terem total confiança em mim e nas minhas capacidades. Agradeço-lhes do fundo do coração todo o amor e ensinamentos que me transmitiram e que me transformaram na mulher que sou hoje. Ao meu avô Arménio, que sei que estaria imensamente orgulhoso da sua neta primogénita por completar mais uma etapa importante da sua vida.

To Prof. Dr. Steve Publicover, for guiding me through the whole process. For all the suggestions, advice and help provided. For accepting me on his group, allowing me to explore new techniques and acquire knowledge on several areas.

Ao Prof. Dr. João Ramalho-Santos, pela ajuda disponibilizada sempre que necessitada, quer em sugestões de organização da tese como em opiniões sobre a mesma.

I am deeply grateful to Dr. João Correia, for all the advice and experience shared, for always being there for me, happy to help whenever I needed and for keeping my Portuguese alive on a daily basis. Muito obrigada João por tudo! Also to Jennifer Morris, for turning my times in the imaging room less lonely, for all the talks and funny moments, for the cakes and muffins, for the company in general and assistance whenever the microscope/cells didn't want to cooperate. Thank you for everything Jen!

A todos aqueles dos quais me orgulho de chamar amigos e que, de uma maneira ou de outra, estiveram presentes na minha vida. Dos tempos de licenciatura no Porto, na FCUP, um especial agradecimento à Cláudia, Nádia Silva, Nádia Ferreira, Marta, Pedro e Ricardo pelos bons momentos passados e amizade que ainda se mantém até hoje e a qual conto prolongar pela vida fora. Do mestrado na FCTUC, um obrigado à Ana Farinha, Ana Padilha, Eva, Marcos, Miguel, Ricardo, Sara, Susana e Teresa pela companhia e cumplicidade essenciais no decorrer do curto ano que vivi e estudei em Coimbra. Não me posso esquecer também das meninas da Casa da Ladeira, a minha morada em Coimbra, Cátia, Joana, Maria Luís e Raquel, um grande beijinho para vós.

Por fim, entre o Porto e V.N.Gaia, Andreia, Bárbara, Cecília, Miguel e Ricardo, vocês também cá têm um espacinho no meu coração, obrigada pela vossa amizade.

I would also like to thank to those who made my life much brighter and happier in Birmingham, my housemates and international friends An, Arantxa, Costanza, Eduardo, German, Isabel, Jan, Javier Monedero, Javier Díaz, José, Karen, Kim, Laura Bach, Laura van Beijnen, Manollo, Marta, Max, Miguel, Nicole, Renata, Sabine, Sarah, Sebastian, Thibault and Tiago. Thank you for the pool games, the meal times, the goings to the Tavern/Goose/Broad St and for all the laughters and great times we shared. I love you all!

And finally to Eduardo, for being the best thing that happened to me in Birmingham and one of the best things in my whole life. Por acreditares sempre em mim, me apoiares e incentivares.

List of abbreviations

4-AP : 4-aminopyridine

AC : adenylate cyclase

AMP : adenosine monophosphate

BSA : bovine serum albumin

cAMP : cyclic adenosine monophosphate

CCE : capacitative Ca^{2+} entry

cGMP : cyclic guanosine monophosphate

CICR : Ca^{2+}-induced Ca^{2+} release

CNG : cyclic nucleotide-gated Ca^{2+} channels

dCCV : dense calreticulin-containing vesicle

EBSS : Earle's balanced salt solution

ICS : intracellular Ca^{2+} stores

IP_3R : inositol 1,4,5-triphosphate receptor

lCCV : light calreticulin-containing vesicle

M : Mibefradil dihydrochloride hydrate

NCX : Na^{+}-Ca^{2+} exchanger

NNC : NNC 55-0396 dihydrochloride

ORAI1 : Ca^{2+} release-activated Ca^{2+} modulator 1

P4 : progesterone

PLC : phospholipase C

PKA : protein kinase A

PMC plasma membrane channels

PMCA : plasma membrane Ca^{2+} ATPase

PRC : procaine

RNE : redundant nuclear envelope

RyR : ryanodine receptor

SERCA : sarcoplasmic-endoplasmic reticulum Ca^{2+} ATPase

SOC : store-operated Ca^{2+} channels

SPCA : secretory pathway Ca^{2+} ATPase

STIM1 : stromal interaction molecule 1

TMA : trimethylamine hydrochloride

TMS : thimerosal

TRPC : transient receptor potential channel

VG : voltage-gated Ca^{2+} channels

VOCC : voltage-operated Ca^{2+} channels

ZP : zona pellucida

% : percentage

[ ] concentration

$[Ca^{2+}]_I$: intracellular calcium concentration

Resumo

O Ca^{2+} presente nos espermatozóides pode provenir de duas fontes: uma extracelular, mediada por canais de Ca^{2+} na membrana plasmática e uma intracelular devido à abertura de canais libertadores de Ca^{2+} em dois reservatórios de Ca^{2+} - o acrossoma e o envelope nuclear redundante (RNE). Existem dois tipos de canais membranares de Ca^{2+} presentes nos espermatozoides: uns responsáveis pelo seu influxo tais como CatSper, VOCC, SOC e CNG e outros pela sua dispersão para o meio envolvente como PMCA e NCX. Os reservatórios intracelulares de Ca^{2+} também possuem canais para o seu efluxo (IP_3R e RyR) e para a dispersão de Ca^{2+} citoplasmática / inclusão nos reservatórios (SERCAs e SPCAs).

Estudos em reservatórios, canais, bombas e permutadores de Ca^{2+} bem como as suas interacções internas e efeitos em actividades do espermatozoide requerem o uso de moduladores farmacológicos quer para inibir ou induzir transporte de Ca^{2+} ou simplesmente afectar directamente a mobilidade ou reacção acrossómica do espermatozóide. No presente estudo, seis moduladores foram usados por forma a esclarecer a intercomunicação entre CatSper e os reservatórios intracelulares de Ca^{2+} (especialmente o RNE) e os seus efeitos na motilidade do espermatozóide humano; progesterona - um indutor geral da concentração de Ca^{2+} intracelular), Mibefradil dihydrochloride hydrate e NNC 55-0396 dihydrochloride - inibidores de CatSper e, consequentemente, influxo de Ca^{2+}, thimerosal e 4-aminopyridine - mobilizadores de Ca^{2+} armazenado e indutores de influxo de Ca^{2+} e trimethylamine hydrochloride - um indutor alcalino do influxo de Ca^{2+}.

Com este trabalho, foi possível concluir que o TMA induz eficientemente o influxo de Ca^{2+} através de CatSper, enquanto que o Mibefradil e o NNC actuam negativamente nestes canais, interferindo com o influxo bem como a resposta induzida pela progesterona; ademais, o thimerosal e a 4-aminopyridine causam um aumento do Ca^{2+} intracelular que parece ser parcialmente mediado pelos reservatórios de Ca^{2+}, nomeadamente o RNE. Nos estudos de motilidade, os espermatozóides tratados com TMA, Mibefradil e NNC apresentaram uma mudança no seu movimento: velocidade aumentada quando estimulados com TMA e Mibefradil e velocidade

diminuída com NNC. As diferenças encontradas entre o controlo (com sEBSS) e o tratamento com thimerosal ou 4-aminopyridine não foram significativas, segundo o teste t de Student. Assim sendo, existe uma intercomunicação relevante entre CatSper e reservatórios intracelulares de Ca^{2+} que previne a descida de Ca^{2+} intracelular para níveis anormais e também afecta a mobilidade espermática, quando interrompida.

Palavras-chave: espermatozóides humanos; sinalização de Ca^{2+}; CatSper; reservatórios intracelulares de Ca^{2+}; motilidade.

Abstract

Ca^{2+} in sperm can come from two sources: an extracellular one, mediated by plasma membrane Ca^{2+} channels and an intracellular one due to the opening of Ca^{2+}-release channels in the two Ca^{2+} stores - the acrosome and the RNE. There are two types of plasma membrane channels present in sperm: the ones responsible for Ca^{2+} influx such as CatSper, VOCC, SOC and CNG and those accountable for Ca^{2+} clearance to the surrounding medium like PMCA and NCX. Intracellular Ca^{2+} stores also possess channels for Ca^{2+} efflux (IP_3R and RyR) and for cytoplasmic Ca^{2+} clearance/inclusion into the stores (SERCAs and SPCAs).

Studies of Ca^{2+} stores, channels, pumps and exchangers as well as its internal interactions and effects on sperm activities require the use of pharmacological modulators either to inhibit or induce Ca^{2+} transportation or simply affect directly sperm motility or acrosome reaction. In the present work, six modulators were used in order to clarify the intercommunication between CatSper channels and intracellular Ca^{2+} stores (especially the RNE) and its effects on human sperm motility. Progesterone - a general inducer of $[Ca^{2+}]_i$, Mibefradil dihydrochloride hydrate and NNC 55-0396 dihydrochloride - inhibitors of CatSper and thus Ca^{2+} influx, thimerosal and 4-aminopyridine - mobilisers of stored Ca^{2+} and inducers of Ca^{2+} influx and trimethylamine hydrochloride – an alkaline inducer of Ca^{2+} influx.

With this work, it was possible to conclude that TMA efficiently induces Ca^{2+} influx through CatSper whilst Mibefradil and NNC act negatively on them hence interfering with the influx and also with the progesterone-induced response; moreover, thimerosal and 4-aminopyridine cause a rise of intracellular Ca^{2+} which appears to be partially mediated by intracellular Ca^{2+} stores, namely RNE. With the motility studies, TMA, Mibefradil and NNC-treated cells presented a change in swimming pattern: increased velocity when stimulated with TMA and Mibefradil and decreased velocity when with NNC. No statistical significance was attributed to the differences seen between thimerosal and 4-aminopyridine treatment the control (with sEBSS), accordingly to test t of Student. Therefore, there is a relevant

intercommunication between CatSper and ICS that prevents the decrease of intracellular Ca^{2+} to abnormal levels and also affects sperm motility, when interrupted.

Key words: human sperm; Ca^{2+} signalling; CatSper; intracellular Ca^{2+} stores; motility.

Index

CHAPTER I INTRODUCTION 1

I.1 OVERVIEW OF REPRODUCTION OF A LIVING ORGANISM 2

I.1.1 Mammalian reproduce sexually through specific cells 3

I.2 MAMMALIAN SPERMATOZOA 4

I.2.1 Sperm morphology varies with the species but maintains a similar segmentation in all 4

I.2.2 Meiosis and spermatozoa production begin in puberty and pursue uninterrupted throughout life 6

I.2.3 Spermatozoa acquires motility and thus ability to fertilise the egg through the process of capacitation 7

I.2.4 When approaching the oocyte site, a particular movement pattern is observed in spermatozoa: hyperactivation 8

I.3 HUMAN SPERMATOZOA 10

I.4 CA^{2+} SIGNALLING IN HUMAN / MAMMALIAN SPERMATOZOA 11

I.4.1 Plasma membrane channels 11

I.4.1.1 Proteins in the CatSper family form selective channels responsible for the flagellar influx of Ca^{2+} 12

I.4.1.2 Voltage-operated Ca^{2+} channels play a role in the induction of acrosome reaction whilst cyclic nucleotide-gated Ca^{2+} channels take part on the control of chemotactic activity 13

I.4.1.3 Empty intracellular stores signal store-operated Ca^{2+} channels to open leading to a rise of intracellular Ca^{2+} 14

I.4.2 Intracellular stores and ligand-gated channels 14

I.4.2.1 Acrosome reaction requires the depletion of the acrosomal Ca^{2+} store 15

I.4.2.2 Hyperactivation is regulated by a Ca^{2+} store in the neck/midpiece region probably the redundant nuclear envelope 16

I.4.3 Ca^{2+} ATPases and Na^{+}-Ca^{2+} exchangers 19

I.4.3.1 Ca^{2+} ATPases: PMCAs are important in sperm motility, SERCAs presence in sperm is yet uncertain and SPCAs refill the redundant nuclear envelope 20

I.4.3.2 Na^{+}-Ca^{2+} exchangers are less efficient than Ca^{2+} ATPases 21

I.4.4 Pharmacological modulators 22

I.4.4.1 Progesterone, a biological agonist of human sperm 22

I.4.4.2 Mibefradil, a T-type Ca^{2+} channel antagonist and NNC 55-0396, a nonhydrolyzable analog of Mibefradil 23

I.4.4.3 Thimerosal, an agonist of IP_3Rs 25

I.4.4.4 4-aminopyridine, the most potent inducer of hyperactivation 26

I.4.4.5 Trimethylamine, a pH modulator 26

I.5 OBJECTIVES 27

CHAPTER II MATERIALS AND METHODS 28

II.1 REAGENTS 29

II.2 BIOLOGICAL MATERIAL 29

II.2.1 Sample preparation 29

II.3 IMAGING STUDIES 30

II.3.1 Cells treatment 31

II.3.2 Imaging chamber assembly 31

II.3.3 Imaging 32

II.3.3.1 Protocol for single-compound testing 33

II.3.3.2 Protocol for multiple-compound testing 36

II.3.4 Data analysis 38

II.4 MOBILITY STUDIES 39
II.4.1 Cells treatment *39*
II.4.2 Protocol for single/multiple-compound testing *40*
II.4.3 Data analysis *41*

CHAPTER III RESULTS AND DISCUSSION 43

III.1 IMAGING STUDIES 44
III.1.1 Single-compound testing *44*
III.1.1.1 TMA studies 44
III.1.1.2 4-AP studies 48
III.1.1.3 Thimerosal studies 51
III.1.1.4 Mibefradil studies 52
III.1.1.5 NNC studies 55
III.1.2 Multiple-compound testing *59*
III.1.2.1 TMS & 4-AP studies 59
III.1.2.2 TMS & TMA studies 61
III.1.2.3 M & 4-AP studies 62
III.1.2.4 M & TMA studies 65
III.1.2.5 NNC & 4-AP studies 65
III.1.2.6 NNC & TMA studies 69
III.2 MOTILITY STUDIES 71
III.2.1 TMA's effect *71*
III.2.2 4-AP's effect *73*
III.2.3 Thimerosal's effect *75*
III.2.4 Mibefradil's effect *77*
III.2.5 NNC's effect *79*

CHAPTER IV CONCLUSIONS AND FUTURE PROJECTS 82

CHAPTER V REFERENCES 86

Chapter I

Introduction

I.1 Overview of reproduction of a living organism

The survival of a species relies on its ability to reproduce and transmit its genetic information to the next generation. This can be achieved by two kinds of reproduction: asexual and sexual.

Asexual reproduction originates offspring genetically identical to its progenitor and is performed by all Prokaryotes (a unicellular, nucleus-free group of organisms that includes bacterias and archaeas) and some Eukaryotes (a unicellular or multicellular group, with nucleus and several other membrane-bound organelles) such as many plants, fungi and protists. On the other hand, sexual reproduction is embraced by the majority of plants and animals producing offspring with a genetical mixture of both progenitors, thus creating variability within the species. One of the great advantages of this type of reproduction is the increasing of a species' rate of adaptability in an unstable environment and as Charles Darwin stated "It is not the strongest of the species that survives, nor the most intelligent that survives. It is the one that is the most adaptable to change."

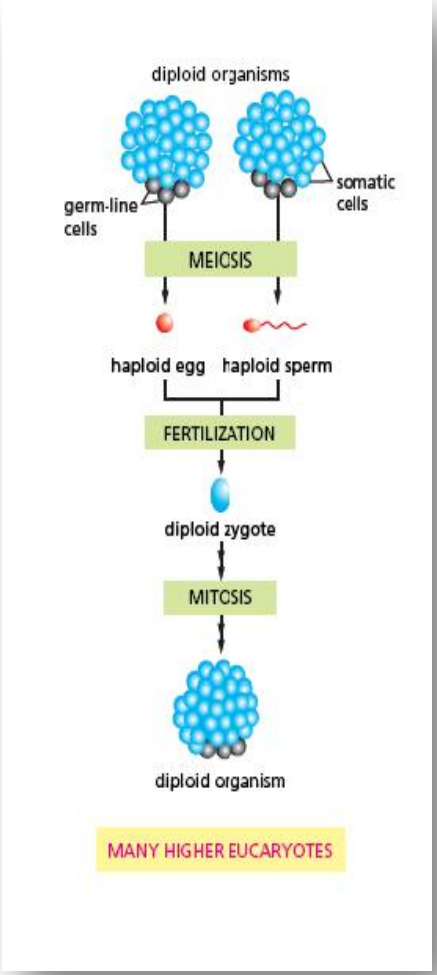

Figure 1 - Life cycle of many higher eucaryotes including mammals (adapted from Alberts *et al.*, 2007).

Some protists, fungi and insects can even adopt both reproductive modes choosing one accordingly to the surrounding environment and factors like access to nutrients, photoperiod, temperature, etc (Alberts *et al.*, 2007b).

I.1.1 Mammalian reproduce sexually through specific cells

In mammalian reproduction, an encounter between two specialised haploid cells of each progenitor needs to be arranged so as to form a new diploid organism. Therefore, a male gamete (spermatozoon; plural sperm) and a female gamete (oocyte or egg) of the same species must find each other within the female reproductive tract and fuse in the process of fertilisation (Figure 1).

According to the current model of mammalian fertilisation, when sperm reach the egg it passes through a matrix of cumulus cells and performs an exocytotic reaction on the surface of the zona pellucida (ZP). This structure, which acts as a thick coat of the egg protecting it from mechanical damage and preventing the entry of non-species-specific sperm, is degraded by the exocyted components, allowing the penetration of the sperm into the perivitelline space and subsequent fusion with the egg (Kirkman-Brown *et al.*, 2002; Alberts *et al.*, 2007b; Figure 2).

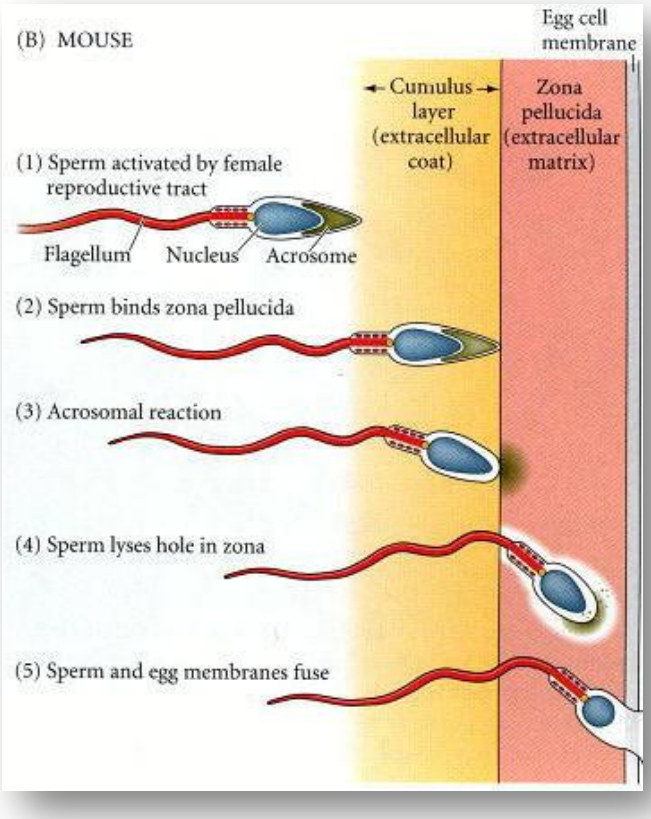

Figure 2 - Illustration of the current model of mammalian fertilisation using mouse sperm as an example (adapted from Gilbert, 2000).

I.2 Mammalian spermatozoa

Sperm are small, polarised, highly motile and haploid cells responsible for carrying the male genetic information of a species. The major role of the male gamete is to reach the female gamete and fertilise it to form a zygote, a diploid cell which will develop into an embryo. Depending on the chromosome borne by the sperm (Y or X), the embryo will evolve into a male offspring (XY) or a female offspring (XX) (Alberts *et al.*, 2007b).

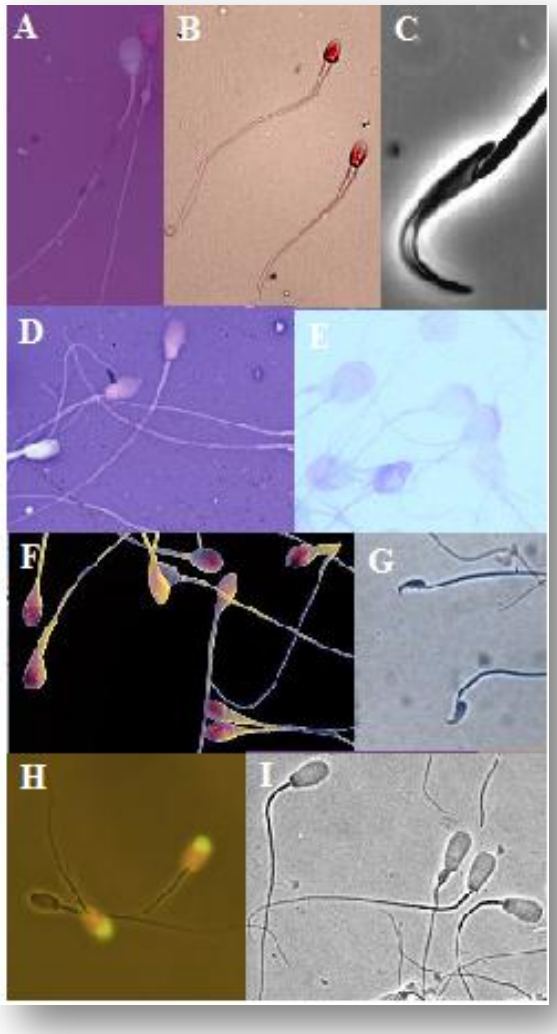

Figure 3 - Sperm of several species showing its morphological differences. (A) Dog - *Canis familiaris*. (B) Lion – *Panthera leo*. (C) Rat – *Rattus novergicus.* (D) Horse - *Equus caballus*. (E) Guinea pig - *Cavia porcellus*. (F) Human – *Homo sapiens*. (G) Mouse – *Mus musculus*. (H) Domestic goat - *Capra hircus*. (I) Bull – *Bos taurus* (adapted from http://www.um.es/grupo-fisiovet/Im-espermatozoides.htm)

I.2.1 Sperm morphology varies with the species but maintains a similar segmentation in all

Despite being very variable, displaying different shapes, formats and sizes characteristic of each species (Figure 3), a normal mammalian sperm can be basically divided into three regions: a head, a midpiece/neck and a tail or flagellum.

The head accommodates the highly condensed nucleus and the acrosome, a double-membraned vesicle located in the anterior portion of the head. This vesicle is responsible for providing the hydrolytic enzymes necessary to penetrate the female gamete in an exocytotic process named acrosome reaction.

As for the mid piece, it yields two essential organelles: a set of mitochondria to supply the cell with sufficient ATP for it to be able to move and the centriole. In most mammalians, the centriole is accountable for arranging and maintaining the microtubule system of the zygote.

The third and longest section of the cell is responsible for its motility, propelling the sperm through the female reproductive tract and helping in the perforation of the ovum's ZP (Figure 4). The core of the flagellum is composed of an axoneme with a 9+2 structure consisted of two central singlet microtubules surrounded by nine microtubules doublets each with a pair of dyneins arms. The active sliding between these doublets on alterning sides of the axoneme is accountable for the driving force of the flagellar wave-like beating (Alberts *et al.*, 2007b; Figure 4).

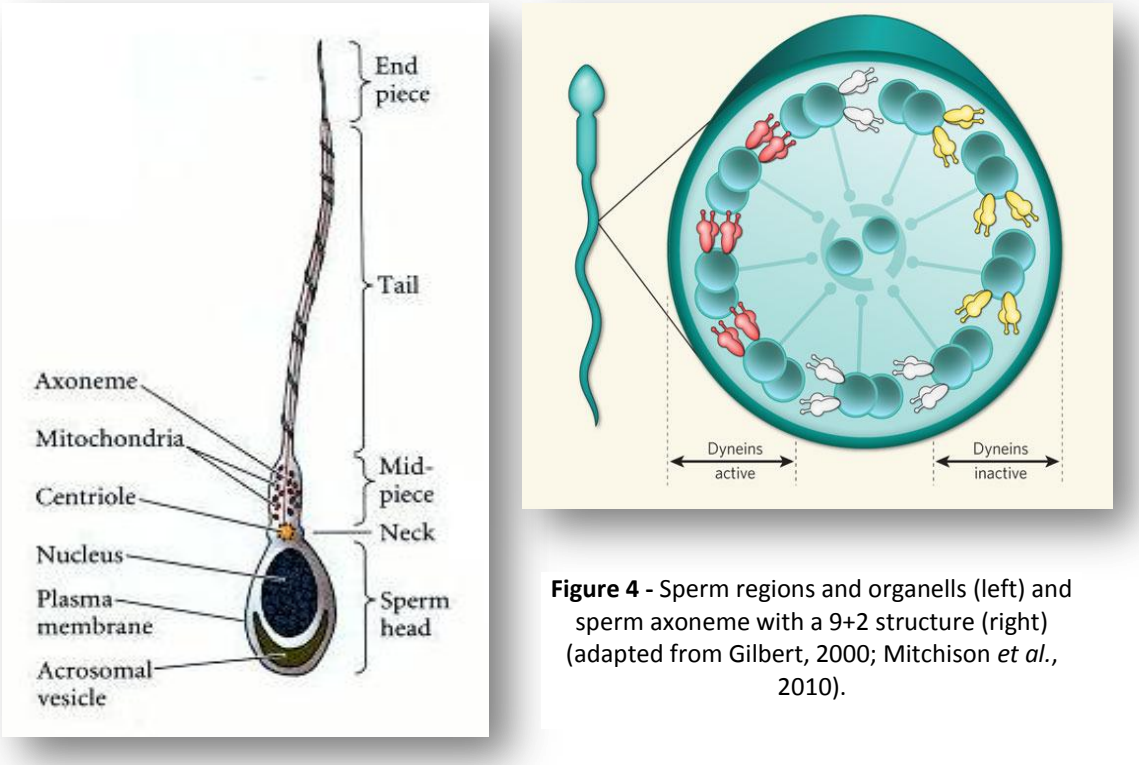

Figure 4 - Sperm regions and organells (left) and sperm axoneme with a 9+2 structure (right) (adapted from Gilbert, 2000; Mitchison *et al.*, 2010).

I.2.2 Meiosis and spermatozoa production begin in puberty and pursue uninterrupted throughout life

Spermatogenesis initiates in mammalian testis, specifically in the seminiferous tubules, at puberty with the proliferation of germ cells called spermatogonia. With the completion of the second division of meiosis, spermatids are produced and will undergo morphological changes as they differentiate into mature male gametes or sperm. These anatomical changes, known as spermiogenesis, include the growth of a tail, packaging of DNA, transcriptional arrest, gathering of mitochondria in a median region, removal of unnecessary elements such as cytoplasm and organelles so as to make the cell lighter, etc (Figure 5).

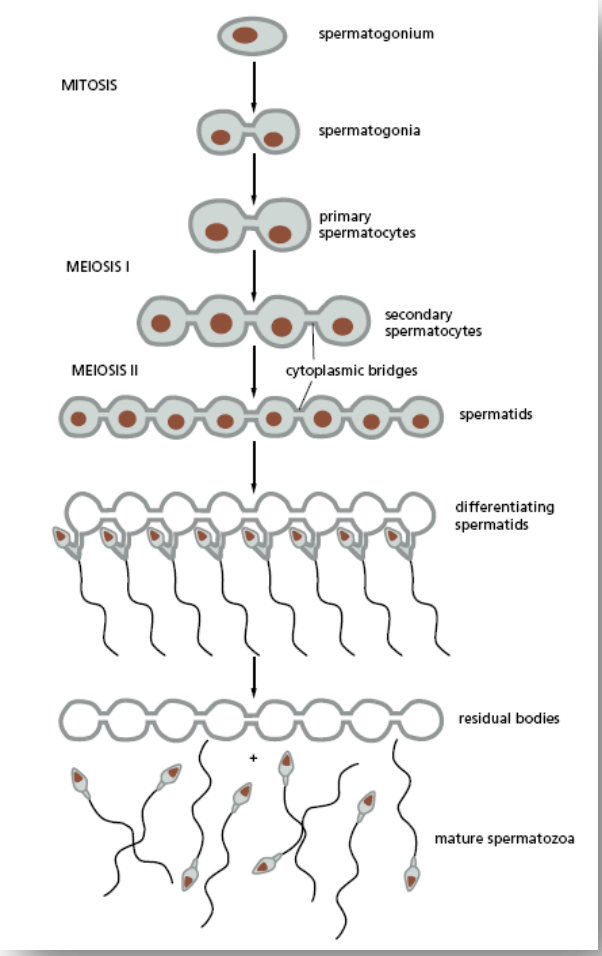

Figure 5 - Schematic spermatogenesis showing the different cells in the germ line (adapted from Alberts *et al.*, 2007).

A particular feature of spermatogenesis is its synchrony which allows a collective differentiation of all the immature cells through the sharing of cytoplasm via cytoplasmic bridges. This excess of cytoplasm - the residual bodies – is phagocytosed by Sertoli cells at the end of the process, releasing the mature cells into the lumen of the tubules which will later on be stored in the epididymis to undergo further maturation in order to gain motility (Alberts *et al.*, 2007b).

I.2.3 Spermatozoa acquires motility and thus ability to fertilise the egg through the process of capacitation

Capacitation is an essential step of the maturation of mammalian sperm responsible for the acquisition of motility by the male gamete. It comprises a combination of physiological changes that occur in sperm within the female reproductive tract and is associated with cholesterol efflux from the sperm plasma membrane, membrane hyperpolarization, variations in intracellular ion concentrations and enhanced phosphorilation of proteins in tyrosine residues (Visconti *et al.*, 2002; Figure 6).

Cholesterol efflux is accountable for an increase in the plasma membrane's fluidity and for alterations in membrane proteins and ion channels changing mainly Ca^{2+} and HCO_3^- fluxes. These ions, along with Cl^- and Na^+, are present in high concentrations in the female tract whilst others such K^+ are present in lower amounts and tend to escape to the extracellular medium generating a hyperpolarized state. Although the identity of the cholesterol acceptor in vivo is not clarified, the removal of this steroid in vitro is facilitated by serum albumin. Regarding the modulations on ion channels of the plasma membrane, they result in an intracellular increment of Ca^{2+} and HCO_3^- that will activate an adenylate cyclase (AC) causing a rise in the cyclic adenosine monophosphate (cAMP) and subsequent upregulation of protein tyrosine phosphorilation (Visconti *et al.*, 2002; Buffone *et al.*, 2005; Alberts *et al.*, 2007b).

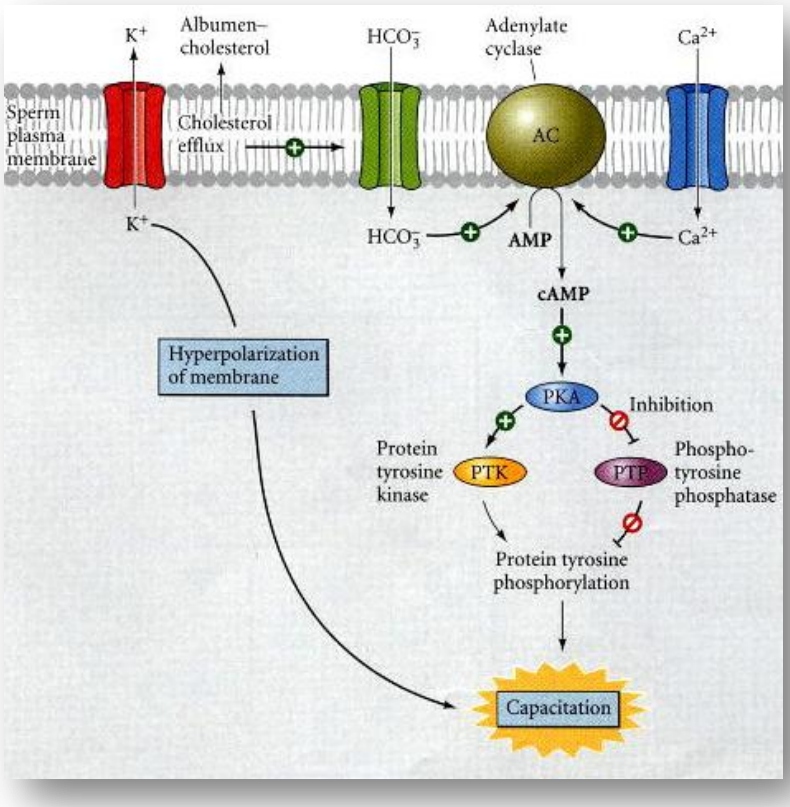

Figure 6 - Mechanisms leading to sperm capacitation. cAMP, cyclic adenosine monophosphate; AMP, adenosine monophosphate; PKA, protein kinase A (adapted from Gilbert, 2000).

I.2.4 When approaching the oocyte site, a particular movement pattern is observed in spermatozoa: hyperactivation

After activation upon ejaculation, sperm become motile and activated, enhancing its chances of fertilising the egg. This type of motility, characterized by a slight bend in the proximal midpiece and high beat frequency which allows a straight-path swimming, is not sufficient to propel the sperm through viscoelastic secretions within the female reproductive tract so a change in flagellar beating is in order. Therefore, hyperactivation takes place with hyperactivated sperm exhibiting a high amplitude bending in the proximal flagellum and midpiece, asymmetrical flagellar bending and low beat frequency which enables a more efficient penetration of the feminine mucous substances and ultimately the zona pellucida of the egg (Ho and Suarez, 2001b, Suarez, 2008; Figure 7). The cause of this change is not due to an

increase in the velocity of sliding microtubules but instead to the amount of microtubule sliding at a nearly straight region between bends of the flagellum; in other words, the microtubule sliding lasts longer leading probably to the reduction of the beat frequency (Ohmuro and Ishijima, 2006).

What specifically triggers hyperactivation in vivo and how it is regulated is not completely understood but there is evidence that three components – ATP, cAMP and Ca^{2+} - and an alkaline environment (pH of 7.9 – 8.5) are involved in the signal transduction cascade that induces hyperactivation, the latter being the most critical. Calcium ions, which can be brought in extracellularly through plasma membrane channels (PMC) or from Ca^{2+} stores, must enter the axoneme of the flagellum ergo generating a sudden rise of intracellular levels that is responsible for enhacing flagellar asymmetry and higher bending on one side of the flagellum (Ho *et al.*, 2002). As far as cAMP is concerned, it is undoubtly important to support motility in general being essential to initiate/maintain flagellar beat and to enhance beat frequency; however, it does not increase flagellar bend amplitude which is characteristic of hyperactivation (Suarez, 2008). So, in a sense, it can be seen as a prerequisite for hyperactivation since it mediates the activation of sperm motility (capacitation). As for ATP, it must be provided in higher quantities than those in activated sperm (Ho and Suarez, 2001b).

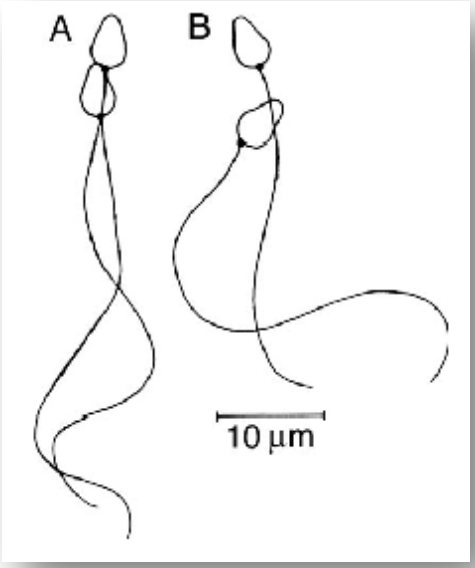

Figure 7 - Sperm flagellar beating. (A) Activated/capacitated sperm. (B) Hyperactivated sperm (adapted from Suarez, 2008).

It is important to stress that there are slight differences in the sperm dynamics inherent to each species.

I.3 Human spermatozoa

The head in normal human sperm is 4-5 µm by 2.5-3.5 µm, oval-shaped and with the acrosome usually occupying 40-70 % of the its surface area; the midpiece is 7-8 µm long, wider than the tail and may possess residual cytoplasm - cytoplasmic droplets - provided that its area is less than half the head's area whilst the flagellum is approximately 45 µm long and should be straight, uniform and uncoiled (WHO, 2010). However, most sperm in a sample is abnormal with some of the most common morphological abnormalities including alterations on the shape of the head, length of the flagellum, overall size, etc (Figure 8).

Like any other mammalian spermatozoa, human sperm also need to be activated by capacitation and undergo hyperactivation and acrosome reaction to be able to efficiently fertilise the human female gamete (the oocyte) and as seen above, Ca^{2+} signalling in sperm is crucial to accomplish these. Ca^{2+} can be attained from the surrounding medium through PMCs or from Ca^{2+} stores through ligand-gated channels and when present in excessive quantities can be cleared by Ca^{2+} pumps or Na^{+}-Ca^{2+} exchangers hence refilling the stores or extruding Ca^{2+} to the medium (Jimenez-Gonzalez *et al.*, 2006).

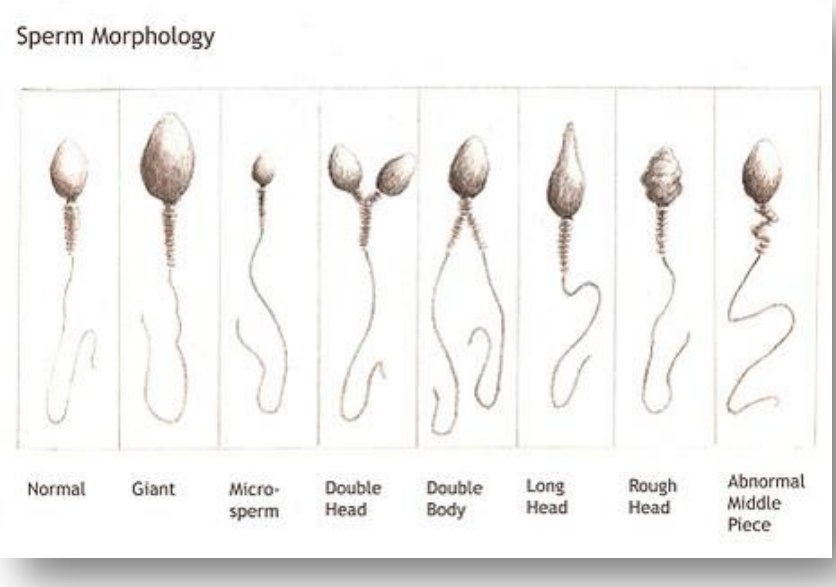

Figure 8 - Some examples of abnormal sperm morphology (adapted from www.cincinnatifertility.com/).

I.4 Ca^{2+} signalling in human / mammalian spermatozoa

I.4.1 Plasma membrane channels

Plasma membrane channels (PMC) are widely distributed in sperm and essential to allow extracellular Ca^{2+} entry which will be used to supplement $[Ca^{2+}]_i$ in the regulation of sperm capacitation, hyperactivation, acrosome reaction and even chemotaxis.

Four types of channels will be addressed - CatSpers, Store-operated, Voltage-operated and Cyclic nucleotide-gated – as well as its location, mode of action and effects on sperm activity (Figure 9)

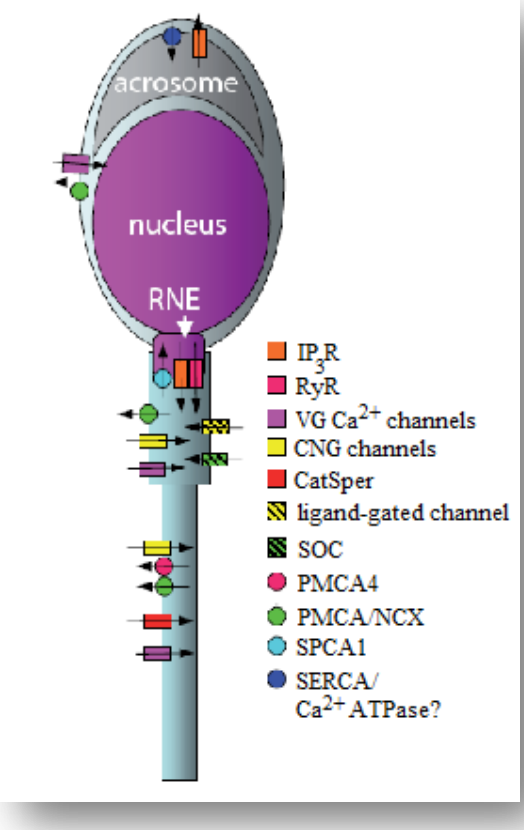

Figure 9 - Ca^{2+} channels (shown by rectangles) and pumps (shown by circles) present in sperm and its probable location. IP_3R, inositol 1,4,5-triphosphate receptor; RyR, ryanodine receptor; VG Ca^{2+} channels, voltage-gated; CNG channels, cyclic nucleotide-regulated; SOC, store-operated channels; PMCA, plasma membrane Ca^{2+}-ATPase; NCX, Na^{+}-Ca^{2+} exchanger; SPCA, secretory pathway Ca^{2+}-ATPase; SERCA, sarcoplasmic-endoplasmic reticulum Ca^{2+}-ATPase. RNE, redundant nuclear envelope (adapted from Bedu-Addo *et al.*, 2008).

I.4.1.1 Proteins in the CatSper family form selective channels responsible for the flagellar influx of Ca^{2+}

CatSper family, so far constituted by four members, is alkaline-sensitive, voltage-gated cation-channel like proteins found exclusively in sperm in the principal piece of the flagellum. CatSper1 and CatSper2, the most studied members of the family, are thought to form a homo- or heterotetrameric Ca^{2+} selective channel that requires an alkaline intracellular pH to be activated. When active, the channel opens allowing Ca^{2+} entry to the cell thus generating the intracellular rise necessary for prompting and sustaining hyperactivated motility (Carlson *et al.*, 2005; Harper and Publicover, 2005; Suarez, 2008).

Studies with CatSper null mice sperm revealed no changes in sperm production, protein tyrosine phosphorilation, induction of acrosome reaction and forward motility but fertility was severely affected with failure of fertilisation due to an inability to penetrate the matrix of cumulus cells surrounding the oocyte (Quill *et al.*, 2003; Carlson *et al.*, 2005). In sperm from male mice, $[Ca^{2+}]_i$ was found to be in basal concentrations which resulted in a high flagellar beat and low bend amplitude phenotype with no hyperactivated form of motility. Although hyperactivation usually occurs during capacitation, these two events are separately regulated thus explaining why the former was harmed but the latter remained unaffected (Quill *et al.*, 2003; Carlson *et al.*, 2005; Marquez *et al.*, 2007).

CatSper studies rely on compounds such as procaine and HC-056456 to modulate its activity (Figure 10). Procaine (PRC), a natural ester anesthetic, is reported to act on sperm motility by increasing beat asymmetry if in presence of extracellular Ca^{2+} (Carlson *et al.*, 2005) whilst HC-056456 acts as a blocker and is able to selectively and reversibly affect the Ca^{2+} influx mediated by these channels, by causing loss of flagellar asymmetry in hyperactivated sperm (Carlson *et al.*, 2009).

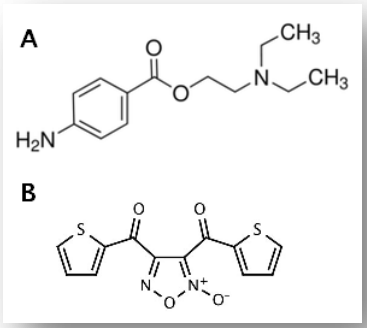

Figure 10 - Chemical structure of procaine (A) and HC-056456 (B) (adapted from http://www.sigmaaldrich.com and Carlson *et al.*, 2009).

Since the majority of Ca^{2+} necessary for hyperactivation comes from the extracellular medium, by enabling the entry of this Ca^{2+}, CatSpers play an important role on the regulation of sperm motility. Therefore, its detailed characterisation and further studies can present some solutions for patients with motility-related sub-fertility.

I.4.1.2 Voltage-operated Ca^{2+} channels play a role in the induction of acrosome reaction whilst cyclic nucleotide-gated Ca^{2+} channels take part on the control of chemotactic activity

Voltage-operated calcium channels (VOCC) are a family of transmembrane proteins that assemble in channels permeable to Ca^{2+} and are present in the head, midpiece and flagellum (Figure 9). Initially classified into L, N, P/Q, R and T-types, these channels are currenty grouped into three subfamilies – Ca_v1, Ca_v2 and Ca_v3 types – the first two forming high-voltage activated channels and the last low-voltage activated channels (Catterall *et al.*, 2003). When active, VOCCs act in a similar way to CatSpers, allowing Ca^{2+} entry to the cell thus inducing a rise of $[Ca^{2+}]_i$ and some are thought to cause the activation of a phospholipase C (PLC) hence generating inositol 1,4,5-triphosphate (IP_3) important for the induction of acrosome reaction (De Blas et al., 2002; Jimenez-Gonzalez et al., 2006).

The existence of cyclic nucleotide-gated channels (CNG) in human sperm is quite controversial. To the ones who acknowledge their presence in sperm, CNG are a family of Ca^{2+}-permeable membrane proteins located in the midpiece and flagellum (Figure 9) which, when stimulated by cAMP or cyclic guanosine monophosphate (cGMP), can mediate Ca^{2+} influx that will contribute to hyperactivation. In the head, olfactory receptors and its agonists (such as the cytokine Rantes and the floral odorant bourgeonal) are also activators of CNG channels, playing a role in the control of chemotaxis towards elements of the female fluids by affecting flagellar beat and bending waves in a chemotactic-like manner (Ho and Suarez, 2001b; Jimenez-Gonzalez et al., 2006; Suarez, 2008). On the other hand, a recent study by Brenker *et al.* (2012), denied the existence of these channels and attributed its effects to CatSper.

I.4.1.3 Empty intracellular stores signal store-operated Ca^{2+} channels to open leading to a rise of intracellular Ca^{2+}

Besides an extracellular source, Ca^{2+} can be obtained from intracellular organelles which are emptied through the opening of ligand-gated channels thus contributing with Ca^{2+} for several important events such as hyperactivation and acrosome reaction. As mentioned above, acrosome reaction requires one first transient Ca^{2+} influx provided by the opening of VOCC which generates IP_3 that will bind to IP_3 receptors located in the membrane of these stores, hence causing its emptying (De Blas *et al.*, 2002; Kirkman-Brown *et al.*, 2002). The second sustained Ca^{2+} influx is mediated by Ca^{2+}-permeable PMCs named store-operated channels (SOC) which are believed to be activated by the depletion of intracellular stores through the production of a gating-signal. This process of Ca^{2+} entering through SOC after the stores' evacuation is known as capacitative calcium entry (CCE) (De Blas *et al.*, 2002, Herrick *et al.*, 2005; Putney 1990).

The most likely candidates for SOC are a family of canonical transient receptor potential channels (TRPC) that in mouse can be found in the sperm head (TRPC2) to promote acrosome reaction (Herrick *et al.*, 2005; Costello *et al.*, 2009), in the midpiece (TRPC1) and in the flagellum (TRPC3) to assist hyperactivation (Marquez *et al.*, 2007). As for human sperm, TRPC1, TRPC3 (showed to interact with IP_3 receptors as direct coupling for CCE), TRPC4 and TRPC6 were identified in the flagellum (Kirkman-Brown *et al.*, 2002; Suarez, 2008). Other possible families proposed to participate in human CCE are a sensor for detection of Ca^{2+} store status (stromal interaction molecule 1, STIM1) and a Ca^{2+}-permeable membrane channel (ORAI calcium release-activated calcium modulator 1, ORAI1) located mostly on the sperm neck and midpiece but also on the acrosomal region. These are thought to interact with TRPC to form and regulate SOC (Costello *et al.*, 2009).

I.4.2 Intracellular stores and ligand-gated channels

Intracellular Ca^{2+} stores (ICS) are reservoirs that are emptied through ligand-gated channels therefore generating complex Ca^{2+} signals which will regulate many

sperm activities accordingly to the cell's necessity. These stores can also be used to sequester Ca^{2+} through pumps and exchangers when it is present in high quantities in the cytoplasm thus reducing or inhibiting its signalling. Usually, ICS contain enough Ca^{2+} to initiate the activity whether it is acrosome reaction or hyperactivation; however, extracellular Ca^{2+} is required to enhance or sustain it (Ho and Suarez, 2001b; Herrick *et al.*, 2005; Marquez *et al.*, 2007).

Two ICS - acrosome and redundant nuclear envelope - and two ligand-gated channels – IP_3 receptors and ryanodine receptors - will be addressed (see Figure 9).

I.4.2.1 Acrosome reaction requires the depletion of the acrosomal Ca^{2+} store

After the penetration of the cumulus cells matrix, hyperactivated sperm encounter the outer coat of the oocyte – the zona pellucida – the last barrier between the two gametes. To be able to pierce through it, sperm need to undergo the acrosome reaction on its surface thus fusing the outer membrane of the acrosome with the ZP. This fusion exposes the inner membrane of the acrosome and allows the release of hydrolytic enzymes such as acrosin and hyaluronidase that will account for the degradation of the barrier and consequently for full penetration of the sperm into the oocyte (Kirkman-Brown *et al.*, 2002). As mentioned above, acrosome reaction (which takes 15 to 60 minutes in the human) involves a rise of $[Ca^{2+}]_i$ in the sperm which can be achieved by the entry of extracellular Ca^{2+} followed by release from an ICS in response to ZP binding. The acrosome itself is most probably the ICS in question and its Ca^{2+} is mobilised via IP_3 pathway mediated by extracellular Ca^{2+} (Herrick *et al.*, 2001; Kirkman-Brown *et al.*, 2002).

IP_3 receptors (IP_3R) are a family of tetrameric ligand-gated channel receptors with three members described - IP_3R1, IP_3R2 and IP_3R3 - that is present in the membrane of IP_3-gated Ca^{2+} stores. Although IP_3R2 cannot be found in human sperm, IP_3R1 is highly expressed in the outer membrane of the acrosomal store thus justifying its reduced expression in acrosome-reacted sperm whilst IP_3R3 possesses a wider location in the posterior portion of the sperm head, midpiece and flagellum and no altered expression after acrosome reaction (Kuroda *et al.*, 1999; Kirkman-Brown *et al.*, 2002; Jimenez-Gonzalez *et al.*, 2006; Costello *et al.*, 2009; Figure 11).

Due to the first transient influx of Ca^{2+} through VOCCs, a PLC is activated originating IP_3 which diffuses through the cytoplasm towards the acrosomal store. Upon its membrane, IP_3 binds to IP_3R thus causing its opening, subsequent release of Ca^{2+} and depletion of the store which will activate SOCs (De Blas *et al.*, 2002). This IP_3-IP_3R binding and therefore Ca^{2+} release is enhanced by alkaline intracellular pH and will contribute to acrosome reaction (Kuroda *et al.*, 1999).

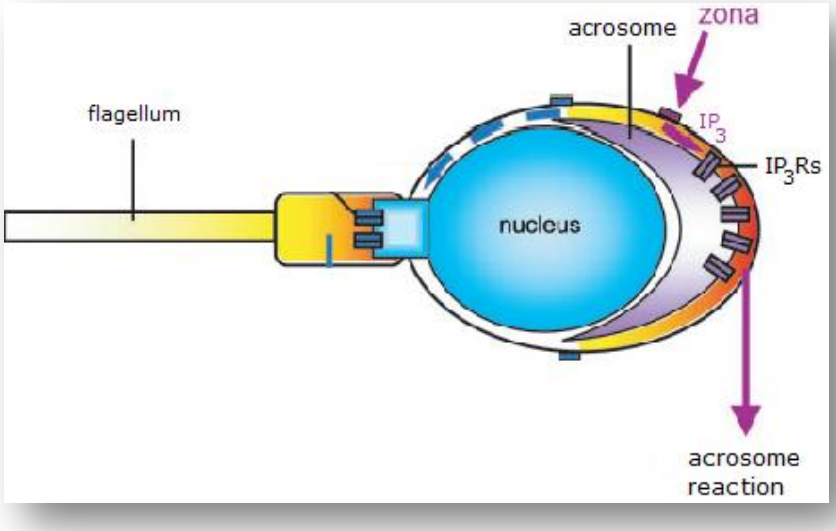

Figure 11 - Schematic human spermatozoa showing one Ca^{2+} store, its ligand-gated channels and effects on the spermatozoa activity. IP_3, inositol 1,4,5-triphosphate; IP_3R, IP_3 receptors; zona, zona pellucida (adapted from Harper *et al.*, 2005).

I.4.2.2 Hyperactivation is regulated by a Ca^{2+} store in the neck/midpiece region probably the redundant nuclear envelope

During spermiogenesis, an important event occurs in the nucleus of the differentiating spermatid – the condensation of chromatin – and, as result of it, a membrane-bounded organelle known as redundant nuclear envelope (RNE) evolves and clusters in the neck/midpiece region. RNE consists on layers of membranes continuous with the nuclear envelope and is associated with long tubular mitochondria, surrounding the axoneme at the flagellar base. Its irregular distribution along the base of the flagellum suggests that this structure is involved in the regulation of sperm motility providing Ca^{2+} to one side of the axoneme thus generating asymmetrical beating (Ho and Suarez, 2001a; Ho and Suarez, 2003; Suarez, 2008).

RNE in bull sperm is thought to possess two sub-compartments: one filled with nuclear pores and a second with vesicles and enlarged cisternae but few pores. During nucleus condensation, nuclear pores are transferred to the RNE being positioned on a narrow band on the neck whilst the vesicles and cisternae are situated on a central region (Figure 12). These vesicles were shown to include an important Ca^{2+}-binding protein abundant in Ca^{2+} stores of somatic cells – calreticulin – thus ascribing the role of ICS in the sperm neck/midpiece to the RNE and in particular to the central region with the vesicles and cisternae (Ho and Suarez, 2003). Human sperm also present two types of these calreticulin-containing vesicles in the cytoplasmic droplet of the neck region, one enclosing denser amorphous material (dCCV) than the other (lCCV) (Naaby-Hansen *et al.*, 2001; Figure 13).

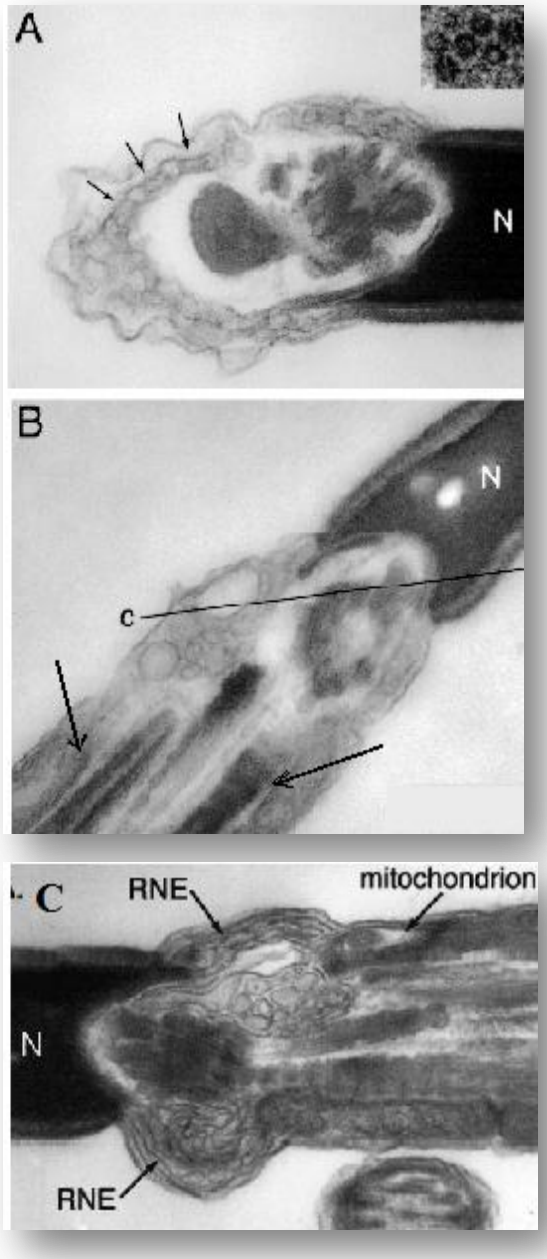

Figure 12 - Transmission electron micrograph of the bull sperm neck/midpiece region. (A) Arrows point at nuclear pores. (B) Arrows point at enlarged cisternae. (C) Assymetric distribution of the redundant nuclear envelope (RNE) (adapted from Ho *et al.*, 2001).

IP_3 receptors, namely human IP_3R3, were also discovered in the vesicular structures on the central region of the neck/midpiece (Naaby-Hansen *et al.*, 2001; Ho *et al.,* 2001).

Other kind of receptors that have been linked with this ICS in some species but its presence in others is not clear are ryanodine receptors (RyR). RyRs are, like IP_3R, a family of ligand-gated channel receptors with also three members described - RyR1,

RyR2 and RyR3 - that may or may be not present in the membrane of ICS (Jimenez-Gonzalez *et al.*, 2006). In human sperm, RyR1 and RyR2 were found (Harper *et al.*, 2004; Costello *et al.*, 2009).

This family of receptors is the major mediator of Ca^{2+} release from the ICS in a positive feedback mechanism, when activated by cytoplasmic Ca^{2+} binding or under conditions of increased Ca^{2+} loading into the store. This process is known as Ca^{2+}-induced Ca^{2+} release (CICR) and it appears to mobilise RNE, causing Ca^{2+} oscillations and conducing to its depletion (Chiarella *et al.*, 2004; Bedu-Addo *et al.*, 2008). IP_3R may also play a role in CICR by releasing Ca^{2+} to the cytoplasm that will activate RyR leading to a further increase of Ca^{2+} (Alberts *et al.*, 2007a; Costello *et al.*, 2009). Regarding the degree of affinity with RyR, ryanodine (Ry) has the highest one, acting as an agonist or antagonist in a dose-dependent manner: whilst at low concentrations Ry promotes CICR, at higher doses Ry behaves like an antagonist of these channels thus suppressing stored Ca^{2+} release (Walensky and Snyder, 1995; Chiarella *et al.*, 2004).

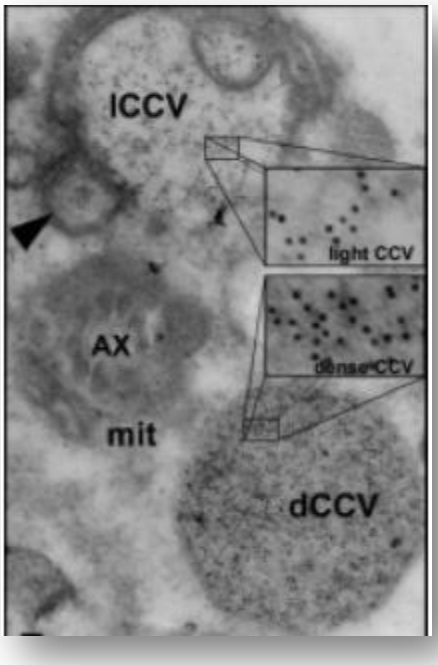

Figure 13 - Transmission electron micrograph of the human sperm cytoplasmic droplet on the neck/midpiece region (cross-section). AX, axoneme; mit, mitochondrial sheat; dCCV, dense calreticulin-containing vesicle; lCCV, light calreticulin-containing vesicle (adapted from Naaby-Hansen *et al.*, 2001).

In summary, RNE is able to respond directly to IP_3 and by CICR through both IP_3R and RyR (Bedu-Addo *et al.*, 2008). Furthermore, it is believed to affect the axoneme thus initiating and regulating hyperactivation whilst the responsibility of maximising and sustaining this type of motility falls on extracellular Ca^{2+} (Ho and Suarez, 2001b; Marquez *et al.*, 2007; Figure 14).

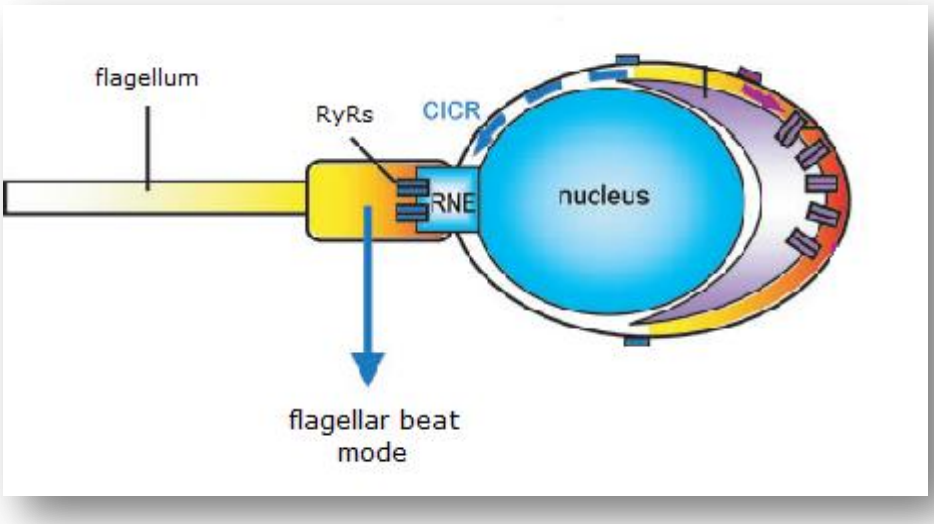

Figure 14 - Schematic human spermatozoa showing one Ca^{2+} store, one kind of ligand-gated channels and its effects on motility. RyRs, ryanodine receptors; RNE, redundant nuclear envelope; CICR, Ca^{2+}-induced Ca^{2+} release (adapted from Harper *et al.*, 2005).

I.4.3 Ca^{2+} ATPases and Na^{+}-Ca^{2+} exchangers

As mentioned above, two sets of channels accountable for increasing intracellular Ca^{2+}: PMCs are essential for extracellular Ca^{2+} influx whilst ligand-gated channels mediate Ca^{2+} efflux from ICS. However, there is a need to maintain appropriate intracellular levels of this ion, balancing this rise either by extruding Ca^{2+} from the cell and/or uptaking into ICS. This role is played by Ca^{2+} ATPases, the greatest intervenient in Ca^{2+} efflux which are stimulated by a Ca^{2+} binding protein - calmodulin - and Na^{+}-Ca^{2+} exchangers which are thought to be regulated by a seminal plasma protein released during capacitation known as caltrin (see Figure 9). Comparing its efficiencies, Ca^{2+} ATPases remove Ca^{2+} three times faster than Na^{+}-Ca^{2+} exchangers (Wennemuth *et al.*, 2003; Bedu-Addo et al, 2008; Suarez, 2008).

I.4.3.1 Ca^{2+} ATPases: PMCAs are important in sperm motility, SERCAs presence in sperm is yet uncertain and SPCAs refill the redundant nuclear envelope

Plasma membrane Ca^{2+} ATPases (PMCAs), widely distributed in sperm, are the fastest Ca^{2+} removal mechanism in sperm, extruding it when present in excessive concentrations (Jimenez-Gonzalez *et al.*, 2006; Figure 15). PMCA4, the most studied member of the family, is located in the flagellum and is thought to mediate sperm motility since its inhibiton causes loss of flagellar activity and affects the control of $[Ca^{2+}]_i$ (Bedu-Addo et al, 2008; Schuh *et al.*, 2003).

Although the absence of sarcoplasmic-endoplasmic reticulum Ca^{2+} ATPases (SERCAs) in non-mammalian sperm is proven, its presence in human sperm is still controversial (Gunaratne and Vacquier, 2006; Bedu-Addo et al, 2008). There is some evidence that SERCA may be located in the outer membrane of the acrosomal store or, at least, some kind of SERCA-like pumps; however, it is not believed to contribute in a significant manner to the uptake of Ca^{2+} into the ICS, since acrosome reaction can still occur during its inhibition (Naaby-Hansen *et al.*, 2004; Harper *et al.*, 2004; Harper and Publicover, 2005; Rossato *et al.*, 2001; Figure 15).

The third Ca^{2+} ATPase is a secretory pathway Ca^{2+} ATPase (SPCA) which shares structural similarities and mechanisms of action with the previously mentioned two others (Gunteski-Hamblin *et al.*, 1992). One variant – SPCA1 – is located in the posterior head and midpiece of human sperm, being thought to play a significant role in Ca^{2+} storage, specifically in regulating Ca^{2+} uptake into the redundant nuclear envelope in the neck/midpiece region (Harper and Publicover, 2005; Harper *et al.*, 2005; Suarez, 2008; Figure 15).

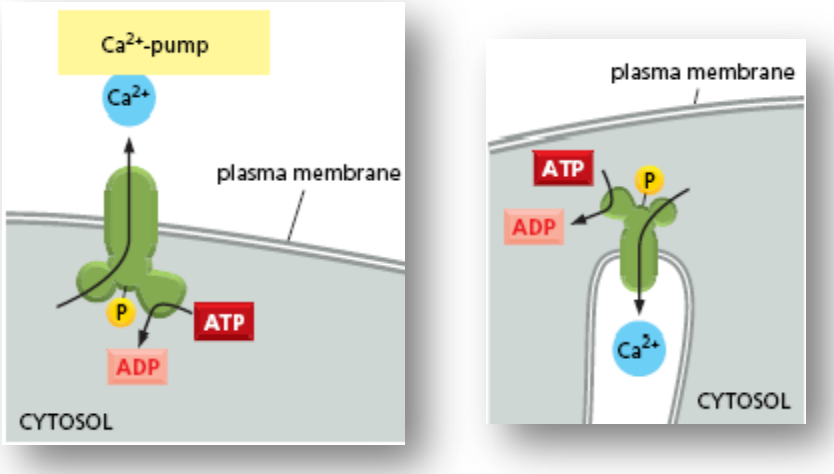

Figure 15 - Mode of action of a plasma membrane Ca^{2+} ATPase (PMCA) (left) and of a sarcoplasmic-endoplasmic reticulum Ca^{2+} ATPase (SERCA) or a secretory pathway Ca^{2+} ATPase (SPCA) (right) (adapted from Alberts *et al.*, 2007a).

I.4.3.2 Na^{+}-Ca^{2+} exchangers are less efficient than Ca^{2+} ATPases

Exchangers or antiporters are coupled transporters, transferring simultaneously two solutes in opposite directions. Initially inhibited by caltrin (a seminal protein), Na^{+}-Ca^{2+} exchangers (NCX) are located in the plasma membrane on the post-acrosomal and midpiece region of human sperm and operate by exporting one Ca^{2+} molecule whilst importing three Na^{+} molecules, thus keeping the cytosolic Ca^{2+} concentration low (Jimenez-Gonzalez *et al.*, 2006; Alberts *et al.*, 2007a; Figure 16). One particularity about these exchangers is that they can also contribute to Ca^{2+} influx by functioning in reverse mode (Michelangeli *et al.*, 2005).

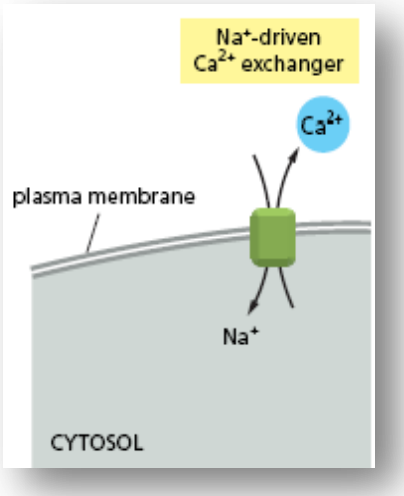

Figure 16 - Mode of action of a Na^{+}-Ca^{2+} exchanger (NCX) (adapted from Alberts *et al.*, 2007a).

I.4.4 Pharmacological modulators

Studies of Ca^{2+} stores, channels, pumps and exchangers as well as its internal interactions and effects on sperm activities require the use of pharmacological modulators either to inhibit or induce Ca^{2+} transportation or simply affect directly sperm motility or acrosome reaction. Some examples of channel regulators are progesterone, caffeine (RyR) and procaine (hyperactivation), which act as agonists and HC-056456 (CatSper), nifedipine (VOCC), heparin (IP_3R) and tetracaine (RyR) which are antagonists. Ca^{2+} pumps can also be indirectely regulated by thapsigargin (SERCA), carboxyeosin (PMCA and bis-phenol (SERCA & SPCA) (Carlson *et al.*, 2005; Carlson *et al.*, 2009; Chiarella *et al.*, 2004; Harper *et al.*, 2004; Harper *et al.*, 2005; Kirkman-Brown *et al.*, 2003; Lishko *et al.*, 2011; Schuh *et al.*, 2003; Walensky and Snyder, 1995).

In this work, six modulators were used either alone or combined: progesterone (P4), Mibefradil dihydrochloride hydrate (M), NNC 55-0396 dihydrochloride (NNC), Thimerosal (TMS), 4-aminopyridine (4-AP) and trimethylamine hydrochloride (TMA).

I.4.4.1 Progesterone, a biological agonist of human sperm

Progesterone is a hydrophobic female hormone that is produced during ovulation at micromolar levels by the layers of cumulus cells surrounding the oocyte. It is then released as a gradient and believed to induce sperm capacitation, hyperactivation, acrosome reaction and even chemotaxis by acting upon Ca^{2+} channels and producing a specific response (Kirkman-Brown *et al.*, 2002; Figure 17).

In both capacitated and non-capacitated sperm, P4 causes a biphasic response, starting with a rapid and transient (1-2 min) rise of $[Ca^{2+}]_i$ which is initiated in the postacrosomal head region and succeeded by a sustained Ca^{2+} response in the form of a plateau (Kirkman-Brown *et al.*, 2000; Kirkman-Brown *et al.*, 2002; Bedu-Addo *et al.*, 2008). The first increment is thought to be mediated by plasma membrane Ca^{2+} channels to which P4 binds extracellularly such as CatSpers (Lishko *et al.*, 2011; Strunker *et al.*, 2011) and/or VOCCs since it is abolished with the removal of extracellular Ca^{2+}, whilst the second is maybe due to Ca^{2+} mobilisation through to the depletion of ICS, which cyclical emptying/refilling plays an essential role in the

generation of Ca^{2+} oscillations (Kirkman-Brown *et al.*, 2000; Kirkman-Brown *et al.*, 2002).

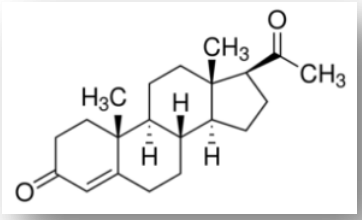

Figure 17 - Chemical structure of progesterone (adapted from http://www.sigmaaldrich.com).

In the follicular fluid, when in high concentrations, P4 was shown to have a broader effect on sperm, not only enhancing acrosome reaction but also hyperactivation, ZP-penetration and oocyte perforation. Therefore, sperm responsiveness to P4 is closely related to its fertilisation capacity, being this response a precious diagnostic tool for IVF treatments (Krausz *et al.*, 1996). Moreover, the reaction to P4 is thought to differ from the one observed in vitro, as studies with a gradient stimulation (representing the gradient surrounding the oocyte in the female reproductive tract) revealed no transient Ca^{2+} rise. Instead, it was detected a slow increase at which large Ca^{2+} oscillations, which are resistant to the reduction of extracellular Ca^{2+}, overlayed. Flagellar beat mode was also alternated in synchrony with the oscillations cycle, especially during its Ca^{2+} peaks in which flagellar bending and lateral movement head were observed (Harper *et al.*, 2004; Harper and Publicover, 2005; Bedu-Addo *et al.*, 2008). As for induction of acrosome reaction it is likely to be caused by P4 during the initial brief Ca^{2+} influx (Walensky and Snyder, 1995; Kirkman-Brown *et al.*, 2002; Harper and Publicover, 2005; Harper *et al.*, 2006).

Due to its well characterised Ca^{2+} response in sperm, P4 is usually constituted a control in imaging experiments, to verify the physiological state of the cells.

I.4.4.2 Mibefradil, a T-type Ca^{2+} channel antagonist and NNC 55-0396, a nonhydrolyzable analog of Mibefradil

T-type channels, also known as Ca_v3, are low voltage-activated, fast-inactivating channels that are widely distributed in sperm (in the flagellum, midpiece and back of the head) and contribute to the increase of $[Ca^{2+}]_i$ by mediating its influx (De Blas et al., 2002; Kirkman-Brown et al., 2002). Mibefradil is a tetralol derivative Ca^{2+} channel antagonist which is known to directly inhibit these channels in mouse spermatogenic cells (Arnoult *et al.*, 1998). This compound was also found to have an inhibitory effect

on P4-activated Ca^{2+} influx, P4-initiated acrosome reaction and to decrease the % of motile sperm (Garcia and Meizel, 1999).

Although Mibefradil's direct effects on T-type Ca^{2+} channels are quite clear, there are still some disagreements between authors: Bonaccorsi *et al.* (2001) reported no effect of the compound on P4-induced acrosome reaction even though a delay in P4 maximum response was observed; Treviño *et al.* (2004) detected no significant alterations on basal motility but noticed a change in the velocity parameters leading to a less progressive trajectory. Furthermore, an indirect inhibition of high voltage-activated, long lasting-inactivating channels was achieved in a rat insulin-secreting cell line, questioning its selectivity on T-type Ca^{2+} channels (Wu *et al.*, 2000).

Since Mibefradil was shown to affect T-type and high-voltage Ca^{2+} channels, NNC was developed by modifying its structure, in order to achieve a selective inhibitory effect on T-type channels (Figure 18). In a rat insulin-secreting cell line, even at high concentrations (100 μM), high-voltage channels were not inhibited by NNC since the metabolite responsible was not being produced due to the non-hydrolysis of the compound. Hence, NNC appeared to be more selective to T-type Ca^{2+} channels than Mibefradil (Huang *et al.*, 2004).

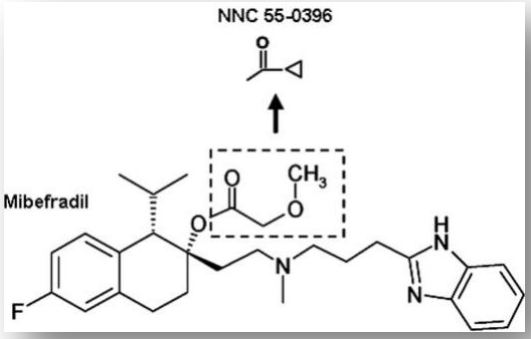

Figure 18 – Chemical structure of Mibefradil and its analog NNC 55-0396. In the latter, the content of the dashed box is substituted by the new structure indicated by the arrow (adapted from Huang *et al.*, 2004).

In human sperm, both compounds were found to inhibit the rapid Ca^{2+} influx evoked by alkaline pH and P4 through the blockade of voltage-gated Ca^{2+} channels (Lishko *et al.*, 2011; Strünker *et al.*, 2011). These channels are thought to be CatSper (see Chapter I.4.1.1), which are pH sensitive and can be activated by lipophilic

compounds such as P4 (nM concentrations), mediating its induced Ca^{2+} entry. Whilst 30 µM of M are necessary to block P4/alkaline-induced Ca^{2+} signals, only 2 µM of NNC are needed to block P4-induced currents. (Lishko *et al.*, 2011; Strünker *et al.*, 2011).

I.4.4.3 Thimerosal, an agonist of IP_3Rs

Thimerosal is a sulfhydryl agent mainly used as an antiseptic agent that binds to IP_3Rs, triggering Ca^{2+} release from the IP_3R-gated stores and hence, initiating events such as acrosome reaction and hyperactivation (Herrick *et al.*, 2005; Figure 19).

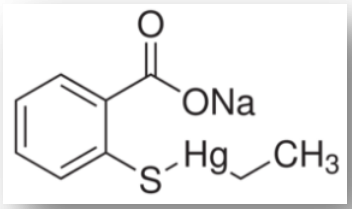

Figure 19 - Chemical structure of thimerosal (adapted from http://www.sigmaaldrich.com).

Thimerosal does not depend on extracellular Ca^{2+} influx in order to increase flagellar bend amplitude and asymmetry, characteristics of hyperactivation, although its presence is essential to sustain this type of motility (Marquez *et al.*, 2007). In bull sperm, depending on the dose, two types of trajectories can be detected: at lower concentrations (25 µM), sperm exhibit a circular trajectory whilst at higher concentrations (100 µM) a figure-of-eight movement (high amplitude bending in the proximal midpiece) can be observed (Ho and Suarez, 2001a). In mouse sperm, Thimerosal triggered a Ca^{2+} rise at the base of the flagellum by inducing Ca^{2+} release from the ICS in this region and thus hyperactivation. In uncapacitated sperm, Thimerosal was shown to induce high-amplitude anti-hook bends (in the opposite direction of the hook of the head), a dominant flagellar bend (Chang and Suarez, 2011).

Acrosome reaction in mouse sperm can also be prompt with high doses of Thimerosal (100 µM); yet, to do so, the presence of extracellular Ca^{2+} is required to mobilise the Ca^{2+} in the acrosomal ICS through IP_3 pathway. This Ca^{2+} will then activate SOC (Herrick *et al.*, 2005).

I.4.4.4 4-aminopyridine, the most potent inducer of hyperactivation

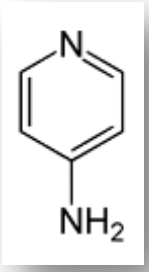

Figure 20 – Chemical structure of 4-aminopyridine (adapted from http://www.sigmaaldrich.com).

4-aminopyridine is an organic compound primarily used as a research tool that instigates Ca^{2+} signals in the posterior portion of sperm head and the neck, leading to a change in flagellar activity while having no effect on acrosome reaction (Bedu-Addo *et al.*, 2008; Figure 20).

It is believed that 4-AP mobilizes stored Ca^{2+} in the midpiece region (possibly from RNE) which results in an increase of asymmetric bending of the proximal flagellum, thus initiating hyperactivation. However, to maximize and sustain hyperactivated motility, extracellular Ca^{2+} influx is required. Studies show that 2mM of 4-AP are sufficient to raise $[Ca^{2+}]_i$ in the neck/midpiece region and in the flagellum through activation of CatSper and other channels (Bedu-Addo *et al.*, 2008; Gu *et al.*, 2004, Ho and Suarez, 2001b).

In mouse sperm, 4-AP induced high-amplitude pro-hook bends (in the direction of the hook of the head) in uncapacitated sperm, by triggering Ca^{2+} influx and a pH rise in the proximal principal piece due to the activation of CatSper (Chang and Suarez, 2011).

I.4.4.5 Trimethylamine, a pH modulator

Trimethylamine hydrochloride is an alkalinizing agent that promotes a raise in intracellular pH, which will activate the pH-sensitive CatSper channels and thus, induce Ca^{2+} influx (Figure 21). In human sperm, no direct induction of acrosome reaction was observed, suggesting that TMA does not act on ICSs (Cross and Razy-Faulkner, 1997).

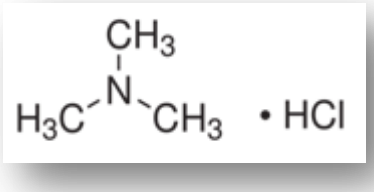

Figure 21 - Chemical structure of trimethylamine hydrochloride (adapted from http://www.sigmaaldrich.com).

I.5 Objectives

Regarding the knowledge so far of Ca^{2+} signalling, the main aim of this project is to clarify the intercommunication between CatSper channels and the ICS (especially the RNE) and its effects on human sperm motility.

In order to better understand this cooperation, two approaches will be used both in attached and free swimming cells. In the first part of this work, Ca^{2+} mobilisation will be evaluated through fluorescence imaging, using six pharmacological modulators which will induce/inhibit Ca^{2+} influx and/or promote release of stored Ca^{2+}. On the second part, the same modulators will be used to assess the effects of Ca^{2+} influx and store mobilisation on flagellar motility.

This work will hopefully add some valuable content to the current knowledge on sperm motility and shed some light on the mechanisms responsible for the acquisition of fertilising capacity by human sperm.

Chapter II

Materials and Methods

II.1 Reagents

Cells were exposed to five compounds known to affect Ca^{2+} mobilisation into and within the cell: Thimerosal (TMS), trimethylamine hydrochloride (TMA), 4-aminopyridine (4-AP), NNC 55-0396 hydrate (NNC; Tocris Bioscience) and Mibefradil dihydrochloride hydrate (M). Combinations of these chemicals were also tested.

All reagents and chemical compounds are from Sigma, unless otherwise stated.

II.2 Biological material

The human seminal samples were provided by anonymous donors to the Publicover's Lab Group for research purposes under the University of Birmingham Ethical Committee (ERC 07-009). All donors went through a preliminary analysis in order to check for seminal parameters such as motility, concentration and sperm morphology, according to the OMS standards (WHO, 2010). The donors used in this work presented above average parameters.

II.2.1 Sample preparation

Each sample was collected after 2 to 5 days of abstinence and its concentration (millions cells/ml) and progressive motility (%) was assessed (table annexe). Sperm concentration was determined in a Neubauer chamber using a 1:50 and 1:10 dilutions with distilled water (in order to immobilize the cells) for before and after swim up counting, respectively. All cells, despite its final concentration, were left capacitating at 6 millions/ml.

Sperm cells were isolated from the seminal plasma by direct swim up technique into Earle's balanced salt solution (sEBSS; pH 7.35; 285-295 mOsm; mM: 1.8 $CaCl.2H_2O$, 5.5 D-Glucose, 15 Hepes, 5.4 KCl, 0.811 $MgSO_4.7H_2O$, 118.4 NaCl, 52.4 $NaHCO_3$, 1.01 NaH_2PO_4, 19.0 Na lactate, 2.5 Na pyruvate) supplemented with 0,3% (w/v) fatty acid free bovine serum albumin (BSA; US Biological). To each 5 ml loosely-capped polystyrene tube, 1 ml of sEBSS was under-layered with 0.2 ml of semen. The tubes

were then incubated at a 45º angle for one hour (37ºC, 6% CO_2) after which 0.75 ml of the supernatant (containing highly motile cells) were recovered to a 15 ml falcon tube and left resting for another three hours in the incubator to allow capacitation of the cells.

II.3 Imaging Studies

For these studies an inverted microscope Nikon Eclipse TE 300 connected to a computer with imaging software (Andor IQ version 2.5.1) was used to observe the cells. The gravity perfusion system was constituted by 6 syringes filled with the compounds to be tested and controlled by a VC-6 Six Channel Valve Controller Controller (Warner Scientific, UK) (Figure 22).

The aim was to observe the effect of the compounds on Ca^{2+} mobilisation through fluorescence microscopy. Hence, the experiments were conducted in a dark room in order to prevent false results due to daylight and at a stable 25 ºC (or 30 ºC when Thimerosal was tested) since fluctuations in temperature may affect the mobilisation.

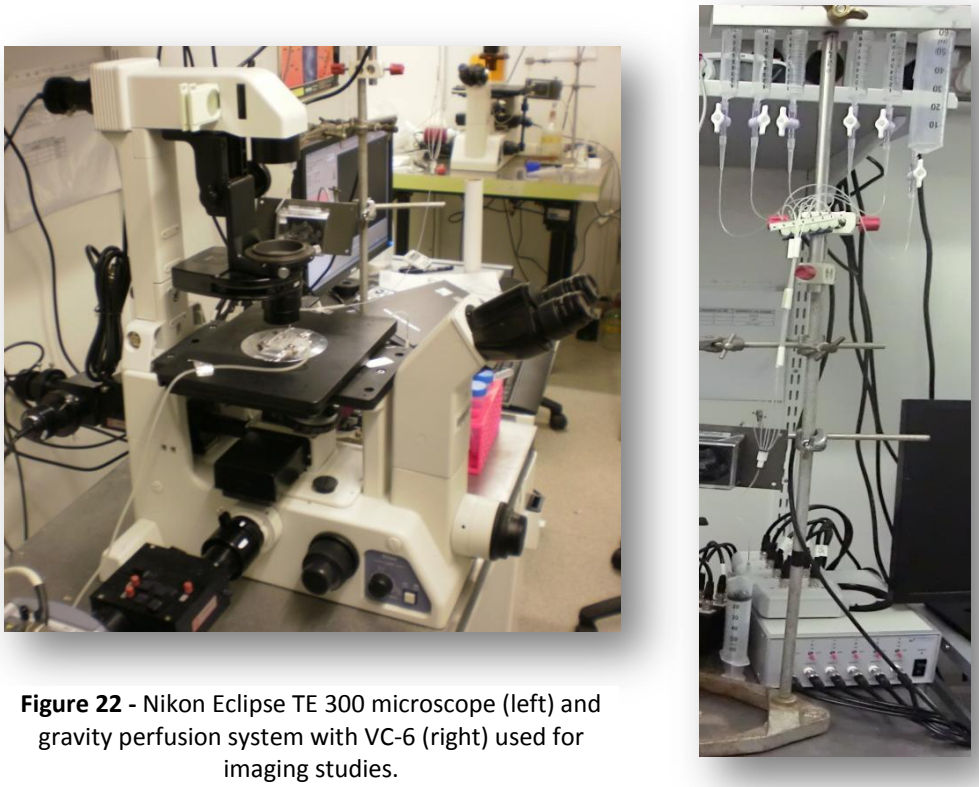

Figure 22 - Nikon Eclipse TE 300 microscope (left) and gravity perfusion system with VC-6 (right) used for imaging studies.

II.3.1 Cells treatment

Calcium Green-1 AM, a fluorescent dye with an excitation/emission of 506/531 nm (blue/green light), was used to label the cells. A stock solution of 860 µM was prepared in the laboratory by adding a 20% pluronic solution in DMSO (Invitrogen) so as to enhance dye solubility, and stored frozen for future use.

Cells were incubated for 45 minutes (37ºC, 6% CO_2) using a 1:100 dilution of the dye (8.6 µM), in order to observe potential changes in the intracellular Ca^{2+} concentration when exposed to the compounds being tested. Afterwards, a centrifugation at 300 rpm for 5 minutes took place, with subsequent discard of the supernatant (~ 550 µl) and resuspension of the cell pellet in dye-free sEBSS. The cells were then left resting for 30 minutes in the incubator to allow full de-esterification of the dye.

II.3.2 Imaging chamber assembly

To allow perfusion, partial immobilization of the cells was necessary. For that purpose, a 10 µl drop of poly-D-lysine solution (0.001%) was pipetted onto the center of a coverslip (22 mm x 50 mm; VWR International) which was then left to dry on a heated stage until a uniform coating of the glass surface was achieved.

To assemble the polycarbonate imaging chambers (mm: 22 x 35 x 6 ; 120 µl; Figure 23), vacuum grease (Dow Corning®) was used to attach the poly-D-lysine coated coverslip to the bottom and a circular coverslip (12 mm; VWR International) to the top, securing the area of observation and preventing leakage from the chamber. After assembly, cells were gently loaded into the chamber through the inflow port, becoming adherent to the coated area mainly by the head.

The chamber was then ready to be mounted on the microscope stage with the inflow port attached to the perfusion system and the outflow port coupled to a suction pump in order to retrieve the overflow from the chamber (Figure 23).

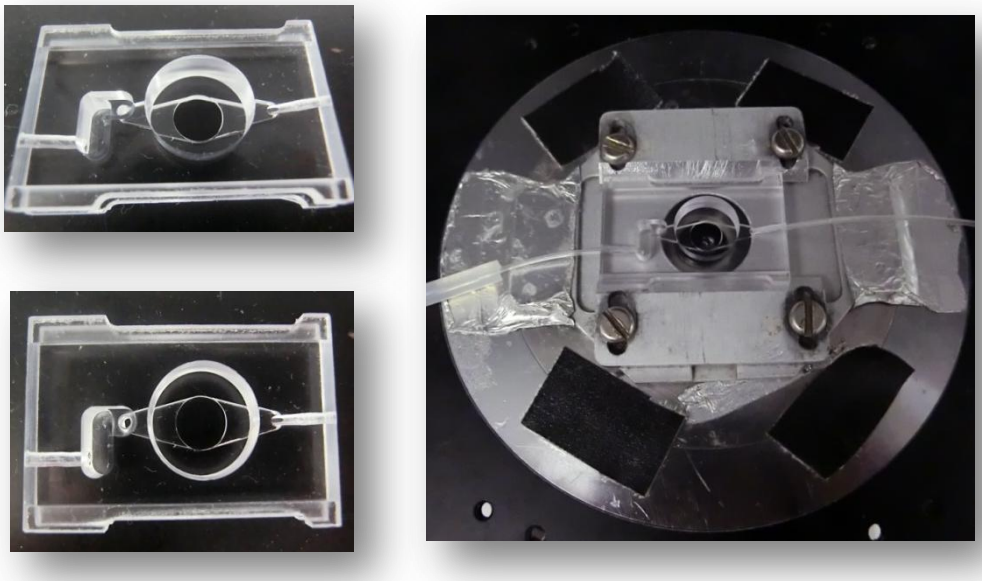

Figure 23 – Polycarbonate imaging chambers (side and up views; left) and chamber mounted on the microscope stage (right) connected to the suction pump on the left port and to perfusion system on the right port.

II.3.3 Imaging

For the whole length of the experiments, cells were continuously perfused with flow rate adjusted to approx 0.75 ml/min. Perfusion with sEBSS was carried out for about 3 minutes before recording, so as to remove loose cells and any remaining extracellular dye. To select the field of view, cells were observed under a phase contrast 40x/0.60 air ph2 DM objective and preference was given to regions with some flagellar activity and medium cell density to ensure the integrity of the signal.

Experiments were conducted with a blue light-emitting diode (LED) as a source of illumination and 14 bit grey/pseudo, 512 (0.4) x 512 (0.4) 3D fluorescence images were acquired using an image acquisition software - Andor IQ (Figure 24). In order to minimize photo-damage of the cells, a short exposure time (75 ms each frame), long acquisition interval (typically 2 seconds) and minimum light intensity were applied.

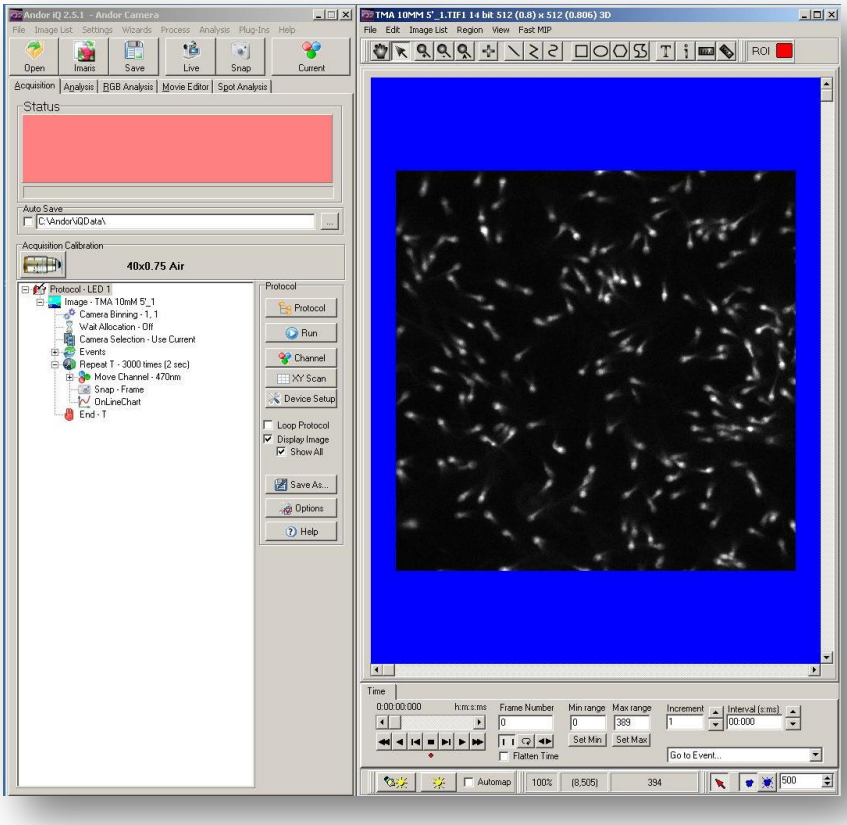

Figure 24 - Example of a fluorescence image obtained with Andor IQ.

II.3.3.1 Protocol for single-compound testing

A typical experiment of this kind began with the cells being perfused with sEBSS for several minutes, followed by addition of the compound to be tested, progesterone (P4) and again sEBSS at the end. sEBSS and P4 constituted two control periods, the first one to establish the baseline of the experiment and the latter, to verify the physiological state of the cells. Stimulation periods were intercalated with wash-off periods in order to retrieve the $[Ca^{2+}]_i$ baseline and allow a clearer observation of the chemical's effect on cells.

A single concentration of Thimerosal, NNC and Mibefradil was tested whereas two concentrations of TMA and three of 4-AP were assessed (Bedu-Addo et al., 2008; Cross and Razy-Faulkner, 1997; Strünker *et al.*, 2011). Mibefradil and NNC concentrations were chosen accordingly to Strünker *et al*. (2011) which states that higher concentrations than the ones used in this work were shown to evoke Ca^{2+}

responses due to the compounds themselves. Cross and Razy-Faulkner (1997) report that 50 mM of TMA along with P4 increase the number of dead cells, so lower concentrations were chosen for this work. All solutions were made by diluting the chemical into sEBSS and exposure times varied between 4 to 15 minutes (Table 1).

Table 1 - Concentrations (mM) and exposure times (min) of the compounds tested. 4-AP – 4-aminopyridine, M – Mibefradil, TMA – trimethylamine, TMS – Thimerosal, P4 - Progesterone

	4-AP	M	NNC	TMA	TMS	P4
Concentration (mM)	2, 3, 4	0.04	0.01	10, 20	0.001	0.003
Exposure time (min)	5	4	4	5, 10, 15	10	0.30-1

Since TMA and 4-AP act upon sperm in a similar way (see chapter I.4) the same protocol was applied (Figure 25).

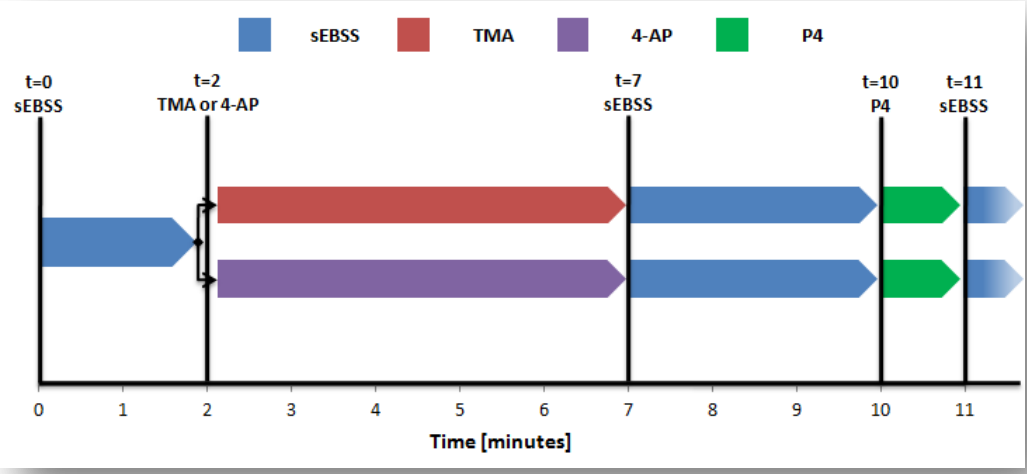

Figure 25 – Example of a typical experiment of a 5-minute perfusion with TMA / 4-AP, with a total duration of at least 11 minutes. Times should be corrected for a 10 and 15-minute perfusion with TMA. P4 was added for about 30-60 seconds until peak was observed. t=x marks the beginning of perfusion with the chemical(s)

The protocol used for Thimerosal testing was identical to the previous one with the difference that a longer perfusion with sEBSS in the beginning of the experiments was applied (Figure 26). This was to allow further data comparisons with a set of multiple-compound testing (see Chapter II.3.3.1)

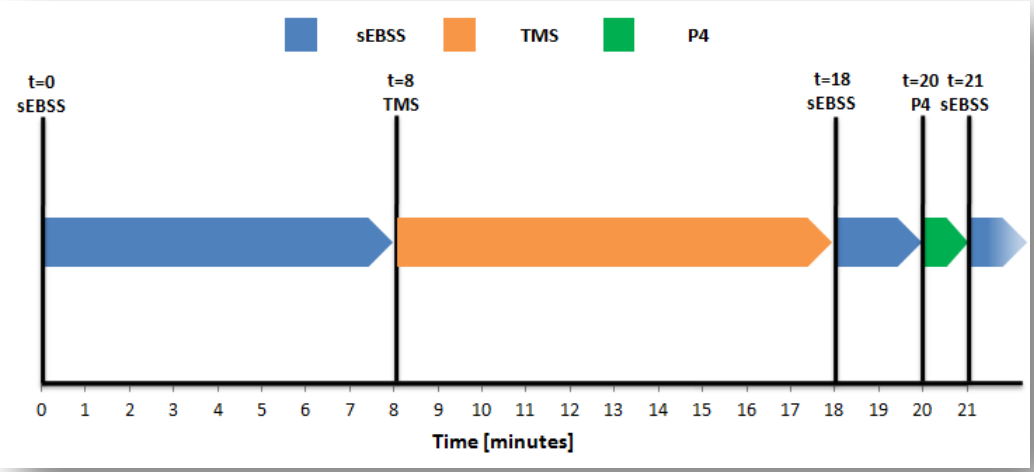

Figure 26 - Example of a typical experiment of a 10-minute perfusion with TMS, with a total duration of at least 21 minutes. t=x marks the beginning of perfusion with the chemical(s).

In order to test Mibefradil and NNC, two CatSper inhibitors, two protocols were set both without perfusion of sEBSS before P4: in one, P4 was perfused alone (Figure 27a) whilst in the other, it was combined with Mibefradil or NNC (Figure 27b). The aim of the second protocol was to observe the cells' response to P4 when these compounds were present.

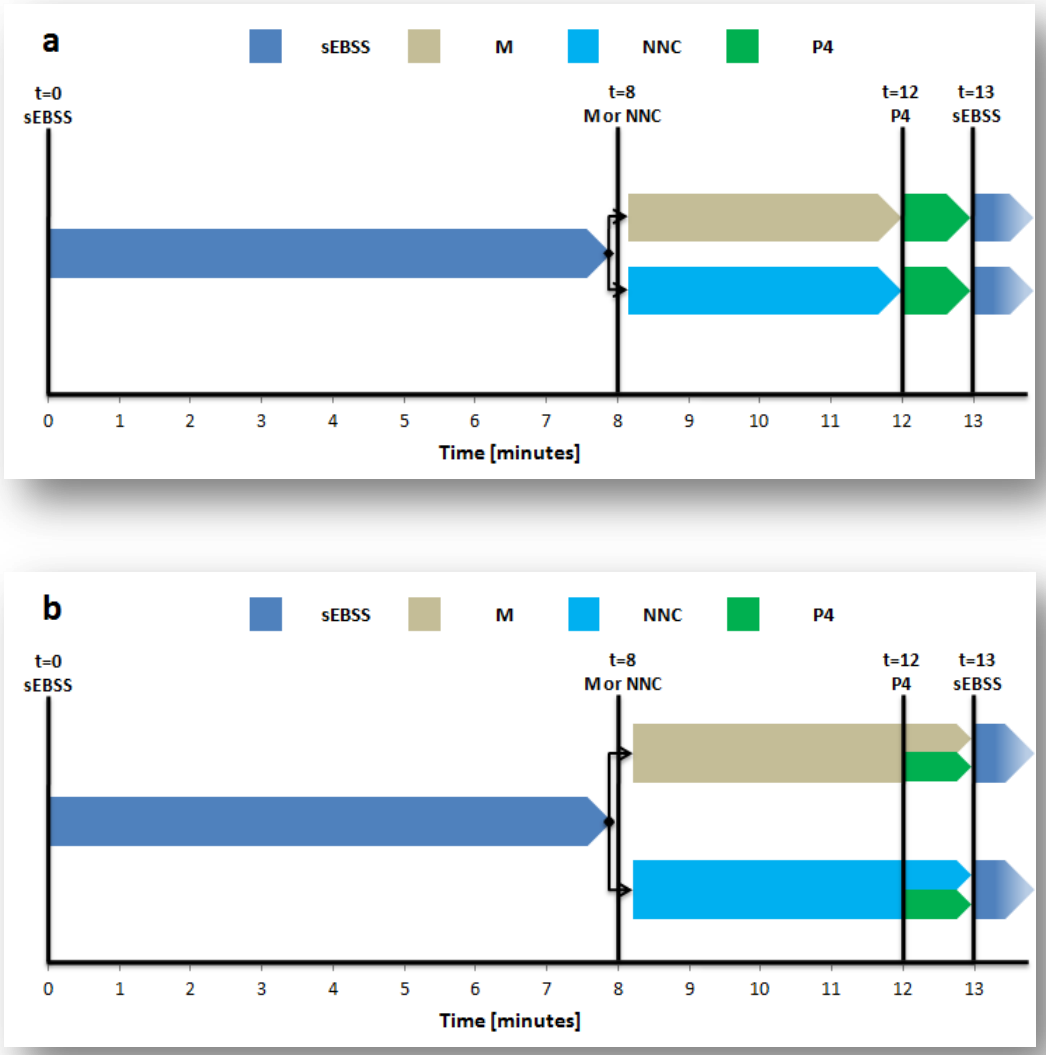

Figure 27 - Example of a typical experiment of a 4-minute perfusion with M / NNC, with a total duration of at least 13 minutes. a) P4 added alone; b) P4 added with M / NNC. t=x marks the beginning of perfusion with the chemical(s).

II.3.3.2 Protocol for multiple-compound testing

In this case and similarly to the previous set, a typical experiment began with sEBSS being perfused into the cells for several minutes, followed by addition of:

- the compound to be tested
- a combination of two compounds
- the previous combination with P4, a solution with three compounds (in some experiments)
- sEBSS at the end

A single concentration of Thimerosal, NNC and Mibefradil was tested whereas two concentrations of TMA and three of 4-AP were assessed (see Table 1). Exposure time to the chemicals was 4 or 5 minutes.

Whilst TMA and 4-AP were perfused onto the cells during the whole experiment, Mibefradil, NNC and Thimerosal were only applied in the middle and at end of the test (Figure 28). The aim of the longer application of TMA/4-AP was to enhance the response to the other chemicals for a better observation of their effects. sEBSS and P4 constituted the two control periods (see Chapter I.3.3.1).

To achieve multiple-compound perfusion, mixed solutions with [TMA/4-AP and M/NNC/TMS] were made, as well as [TMA/4-AP, M/NNC/TMS and P4] solutions.

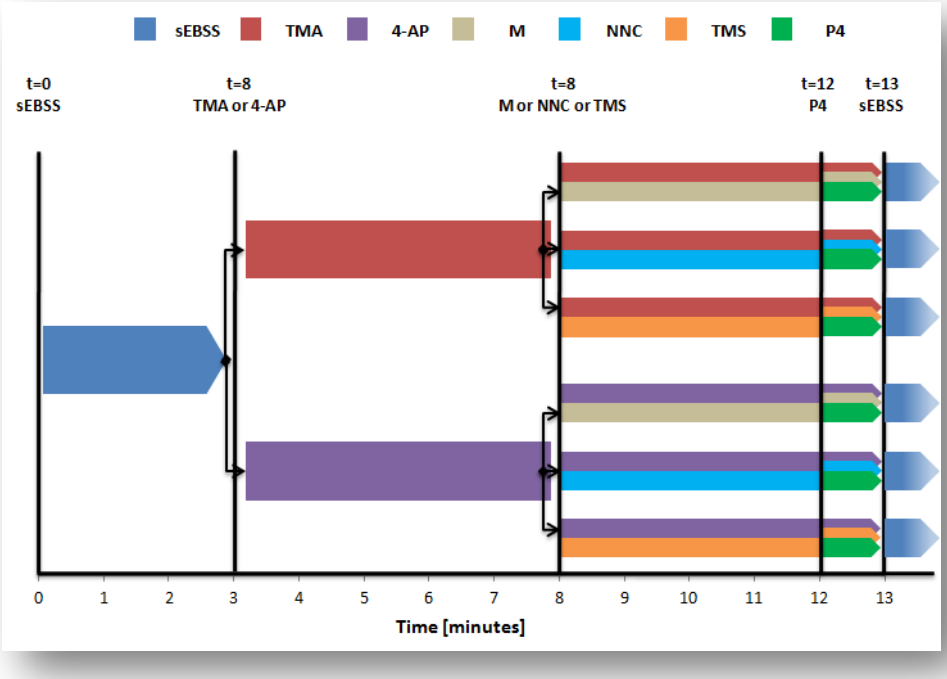

Figure 28 - Example of a typical experiment of a multiple-compound testing, with a total duration of at least 13 minutes. t=x marks the beginning of perfusion with the chemical(s).

II.3.4 Data analysis

Fluorescence images were analysed with the acquisition software used to run the experiments (Andor IQ) by delineating the cells head, where the signal is more intense (Figure 29).

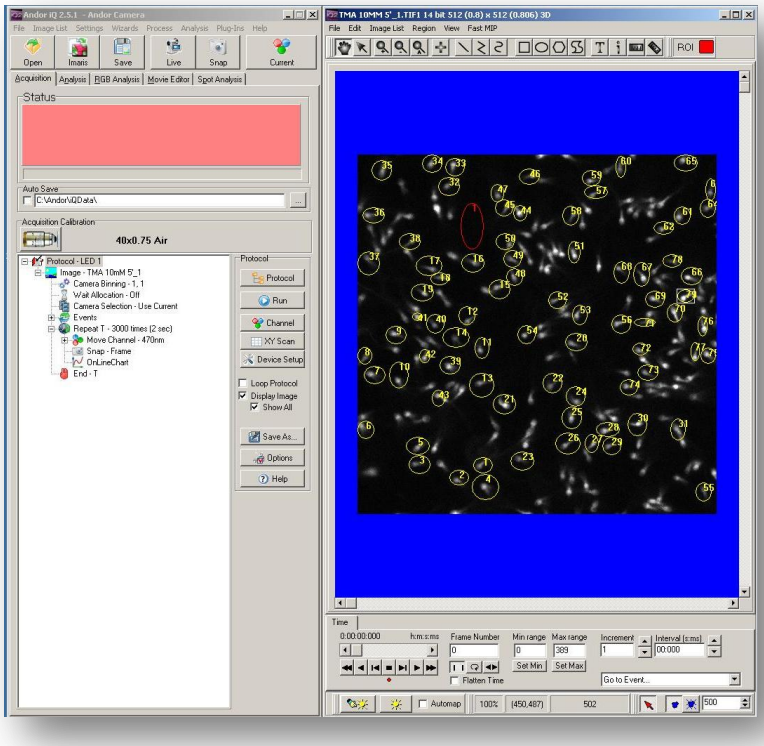

Figure 29 - Example of a fluorescence image analysis with Andor IQ. Yellow circles are the regions of interest (heads) and the red circle is the region used for background correction.

Background-corrected intensity values were imported to Microsoft Excell version 2007 and normalised to the control period (baseline; before stimulation with any chemical) using the equation $R = [(F - F_{rest})/F_{rest}] \times 100\%$, where *R* is normalised fluorescence intensity, *F* is fluorescence intensity at time *t* (sec) and F_{rest} is the average of at least 20 determinations of *F* taken during the control period (Kirkman-Brown *et al*., 2004).

With the normalised data, two kinds of graphs could be obtained: one showing the Ca^{2+} response (as a % change in fluorescence) over time and a second one presenting the % of cells with a peak in fluorescence during stimulation period. For this, both the average and standard deviation of the five highest values of the control

period (A_c; SD_c; data right before stimulation) was compared to the analogous average and standard deviation of the stimulation period (A_s; SD_s; data right at the end of stimulation). An intensity peak was assumed to occur in the cell during a specific period, when the statement ((A_s-SD_s) > (A_c+SD_c)) was true. Similarly, a decrease in fluorescence was assessed with the statement ((A_s+SD_s) < (Ac-SDc)).

II.4 Mobility Studies

The aim of these studies was to observe the swimming pattern of the cells when exposed to a single compound or combinations of two. To achieve this, an inverted microscope Nikon Eclipse TE 300 was used, being the experiments conducted in a dark room at a stable temperature of 30 ºC, to more closely mimic the physiological temperatures sperm would experience in the female reproductive tract.

II.4.1 Cells treatment

250 µl of cell suspension (capacitated sperm, at 6 millions/ml) were centrifuged at 300 rpm for 5 minutes. The cell pellet was then resuspended in a solution of the compound(s) to be tested, at the desired concentration (~ 200 µl) and a digital stopwatch was set, marking the beginning of incubation.

All compounds were tested for a single concentration and a control with sEBSS was also included, for further comparisons. Effects on motility were assessed with several samplings during the 5 minutes of incubation with the compound to be tested (Table 2).

Table 2 - Concentrations (mM) of the compounds tested. 4-AP – 4-aminopyridine, M – Mibefradil, TMA – trimethylamine, TMS - Thimerosal

	4-AP	M	NNC	TMA	TMS	sEBSS
Concentration (mM)	2	0.04	0.01	10	0.001	

II.4.2 Protocol for single/multiple-compound testing

Experiments were conducted in a bright field (white light) mode with streaming acquisition of images, made possible by the constant aperture of the camera's (iXon X-4605) shutter during the whole experiment. The 14 bit grey/pseudo, 512 (1.6) x 512 (1.6) 3D images were acquired every 75 ms using the image acquisition software Andor IQ and the total duration of the experiment was typically 15 seconds.

Cells were observed under a phase contrast 10x/0.30 ph1 DL objective, so as to allow a longer tracking and a higher number of cells in the field (Figure 30).

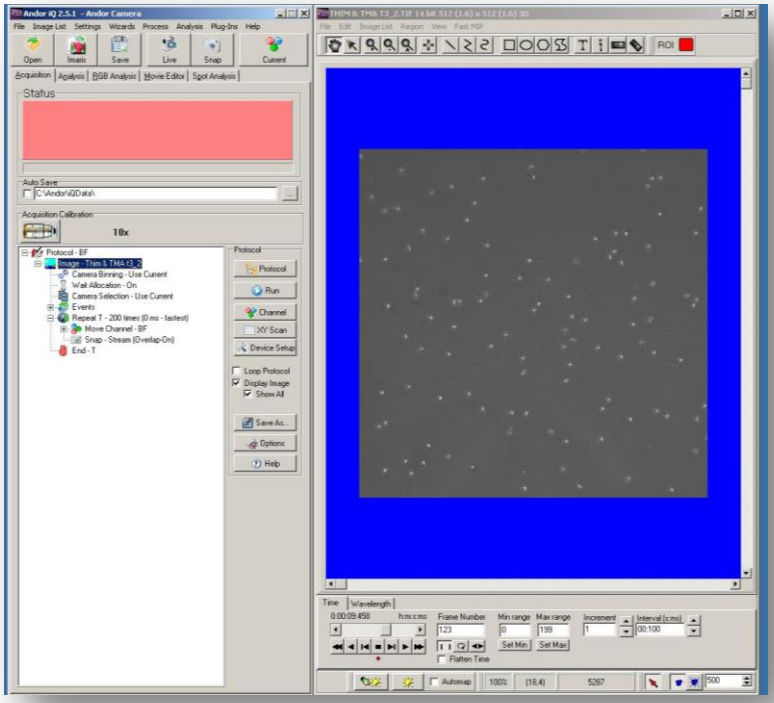

Figure 30 – Example of a bright field image acquired with Andor IQ.

For each sampling, a 10 µl drop of cell suspension was pippetted on the center of a slide (mm: 76 x 26 x 1.0-1.2; Thermo Scientific) and a cover glass (mm: 22 x 22; VWR International) was placed on top. The whole set was then carefully placed facing down on the microscope stage and recording was initiated only after no flow was observed.

II.4.3 Data analysis

Image sequences were analysed with the software Image Pro-Analyser version 7.00.591 by firstly performing an automatic tracking of the cells' movement within the field of view and secondly, manually checking the integrity of the tracks obtained. Non-motile cells, impurities and extra tracks in a single cell were deleted as well as data collected after the interchange of tracks after the shock of two or more cells (Figure 31).

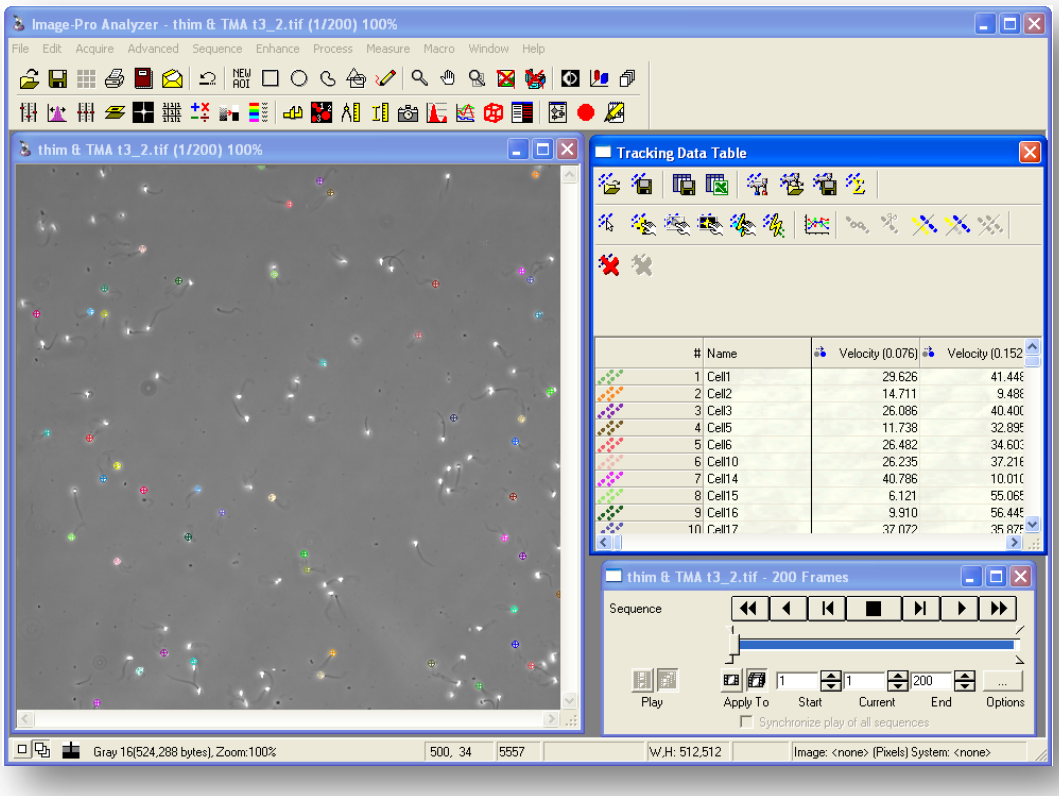

Figure 31 - Example of a bright image analysis with Image Pro-Analyzer. Each colour corresponds to one cell and thus one track.

One parameter – velocity - was obtained from the tracking and processed on Microsoft Excell version 2007 in order to create graphs that allowed comparisons between the compound tested and the control (with sEBSS) (Figure 32). Samplings of the compound from distinct experiments (different days) were concatenated and compared with samplings of the control from the same days (statistical test t of Student was applied). This procedure was necessary in order to obtain a higher number of cells to analyse and also to verify the consistency of the results.

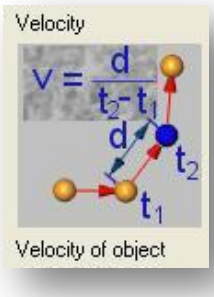

Figure 32 - Description of the variable "velocity" retrieved from the analysis of the tracking with Image Pro-Analyser.

Chapter III

Results and Discussion

III.1 Imaging Studies

Sperm populations are extremely heterogeneous either between donors or within the same donor. Thus, it is possible that cells from the same ejaculate respond differently to the same stimulus and even more probable to find differences in separate donors. These results try to give a general idea of what is happening when a typical sperm population contacts with these compounds.

III.1.1 Single-compound testing

III.1.1.1 TMA studies

When TMA is perfused into the cells, the typical response was a relatively fast increase on the fluorescence intensity, followed by a plateau that remains until the end of stimulation period. With the removal of TMA, fluorescence decreases back to baseline levels whilst perfusion with P4 induced a classic transient response (Figure 33). Since TMA is an alkalinising agent (see Chapter I.4.4.5), the fluorescence rise could be explained by the activation of pH-sensitive plasma membrane channels such as CatSper that would lead to an increase of $[Ca^{2+}]_i$, and the plateau formation could be due to the saturation of these channels. TMA's effect seems to be reversible since after its removal, a decline of Ca^{2+} levels can be seen possibly because these channels are not being over-stimulated.

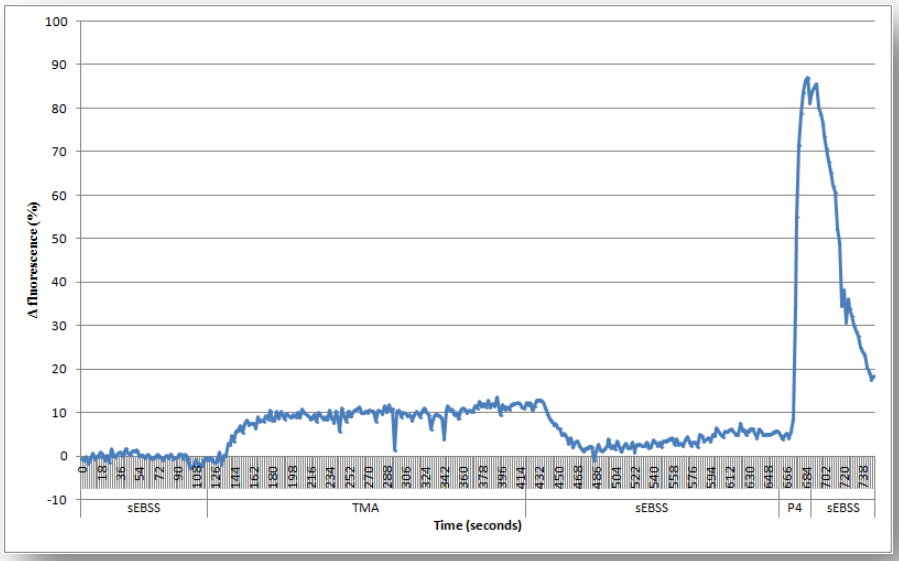

Figure 33 - Mean of % change in fluorescence in capacitated sperm in TMA studies. [TMA] = 10 mM; stimulation period = 5 min. n = 4, 79 cells.

At 10 mM, TMA response is quite similar between 5, 10 and 15 minutes of stimulation, although it seems that the settling of the plateau is not yet complete within 5 minutes, since there is still a slight increase of fluorescence until the end (Figure 34).

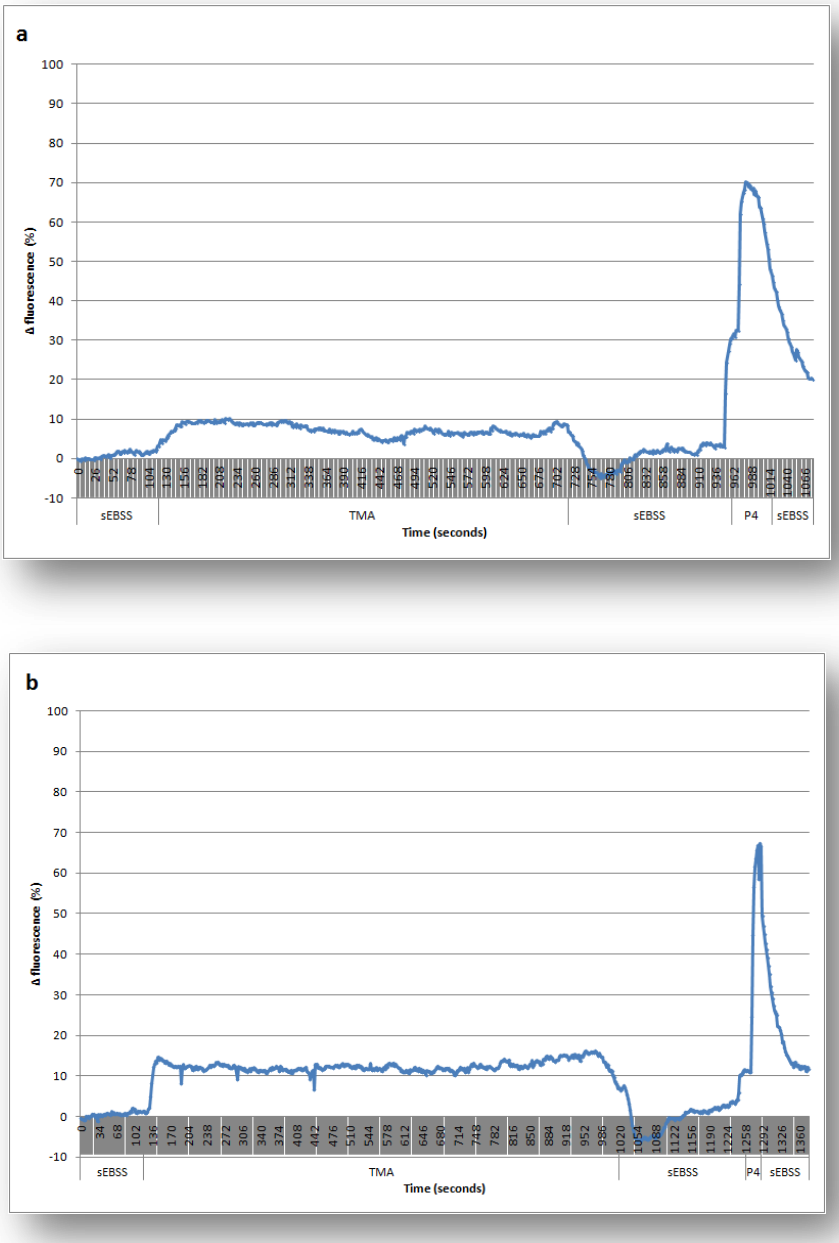

Figure 34 - Mean of % change of fluorescence in capacitated sperm in TMA studies. a) [TMA] = 10 mM; stimulation period = 10 min; n = 52 cells; 4 experiments. b) [TMA] = 10 mM; stimulation period = 15 min; n = 75 cells; 5 experiments.

At 20 mM, TMA was only tested for 10 minutes since stimulation time did not seem to have an influence on the response to the compound. However, with this concentration, no plateau was observed as the fluorescence kept rising until the end of the stimulation period (Figure 35).

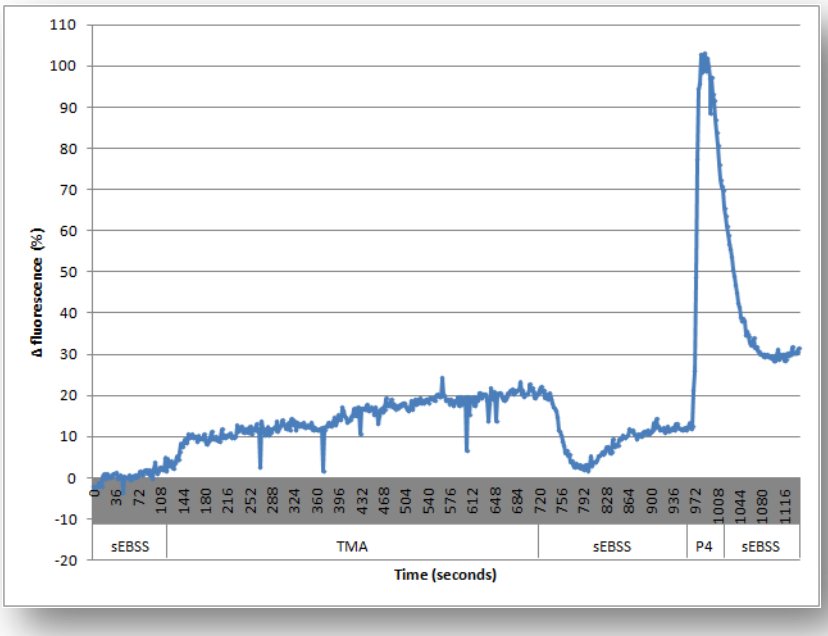

Figure 35 - Mean of % change in fluorescence in capacitated sperm in TMA studies. [TMA] = 20 mM; stimulation period = 10 min; n = 77 cells; 4 experiments.

Possible response differences between the three times within the same concentration (10 mM) revealed to be non-significant ($p > 0.05$) with mean values (%) of 58.3 ± 12.13 (n = 5), 56.2 ± 12 (n = 4) and 70.9 ± 11.8 (n = 5) for 5, 10 and 15 minutes, respectively (Figure 36).

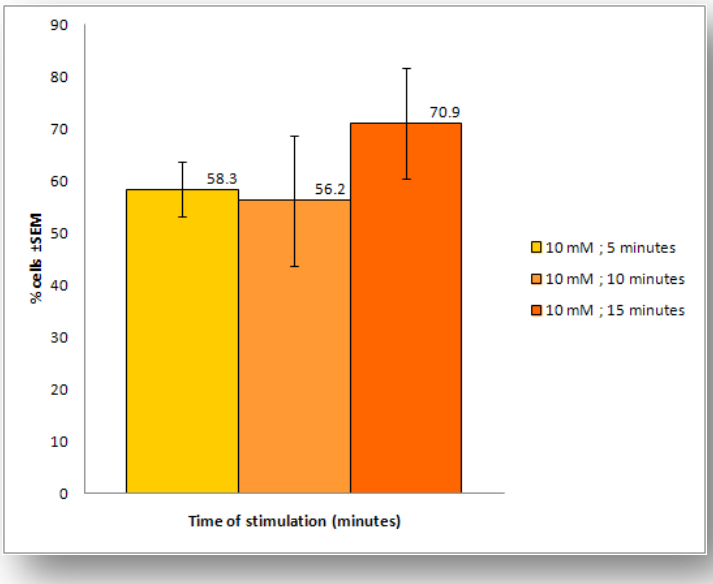

Figure 36 – Mean values (%) ± standard error of the mean of capacitated sperm responding to stimulation with TMA for 5, 10 and 15 minutes. 5 min: n = 5, 152 cells; 10 min: n = 4, 119 cells and 15 min: n = 5, 75 cells. $p > 0.05$ between times.

Although % change in fluorescence graphs of 10 and 20 mM appear to be slightly different (no plateau at 20 mM) no statistical significance was found between them (n = 4 ; p > 0.05) with mean values (%) of 56.2 ± 12 and 64.9 ± 11.8 for 10 and 20 mM, respectively (Figure 37).

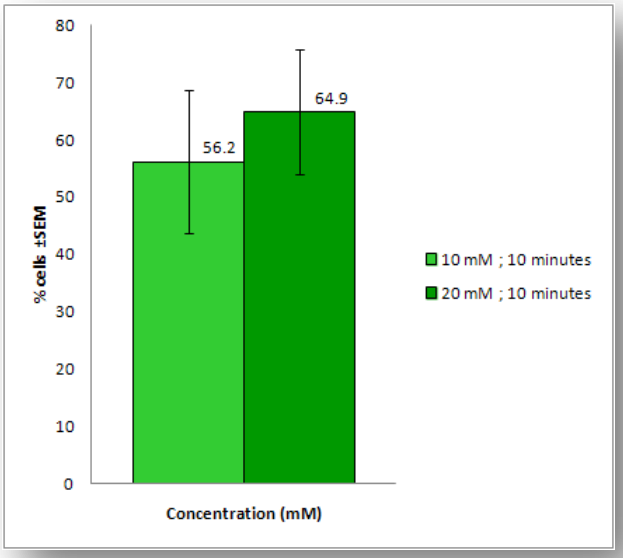

Figure 37 - Mean values (%) ± standard error of the mean of capacitated sperm responding to stimulation for 10 minutes with TMA at 10 and 20 mM. 10 mM: n = 4, 163 cells and 20 mM: n = 4, 85 cells. p > 0.05.

III.1.1.2 4-AP studies

The typical response of human sperm to 4-AP is similar to the TMA one: a quite fast increase of fluorescence, followed by a plateau. Fluorescence decreases with the removal of 4-AP and a normal response to P4 can be seen (Figure 38). Comparing both compounds, it seems as if the cells respond more slowly to the presence of 4-AP entering the plateau later, which could be explained by 4-AP initially mobilising intracellular calcium stores (that presumably takes longer than promoting Ca^{2+} influx through plasma membrane channels) (see Chapter I.4.4.4). Moreover, the P4 peak on 4-AP cells appears to be smaller, probably due to the filling of the ICSs after its depletion with extracellular Ca^{2+}. This Ca^{2+} would not be allowed to accumulate inside the cell, being immediately stored thus explaining the lower fluorescence.

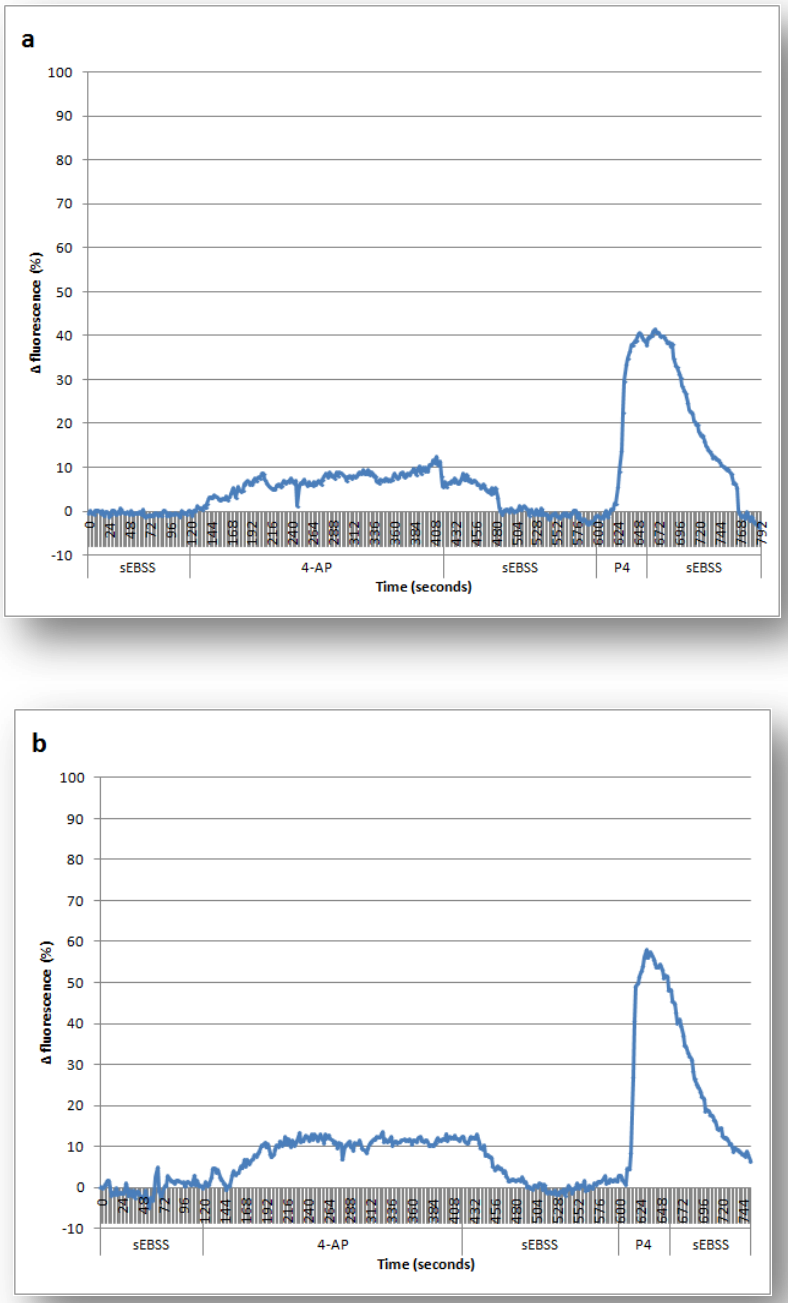

Figure 38 - Mean of % change in fluorescence in capacitated sperm in 4-AP studies. a) [4-AP] = 2 mM; stimulation period = 5 min; n = 102 cells; 4 experiments. b) [4-AP] = 3 mM; stimulation period = 5 min. n = 3, 111 cells.

Although responses to [4-AP] 2 and 3 mM appear to be similar, with 4 mM the cells seem to respond differently. Shortly after addition of 4-AP, there is a peak that resembles P4 response followed by a slow decrease and a new moderate rise much like the ones seen for lower concentrations (Figure 39). One hypothesis to explain this phenomenon could be that higher concentrations of 4-AP act on both ICS and plasma

membrane channels at the same time, inducing a rapid and great increase of $[Ca^{2+}]_i$. SOC channels and Ca^{2+} ATPases / NXCs would be then activated and start to extrude and uptake Ca^{2+} (thus the decrease in fluorescence) whilst the channels continue to internalise Ca^{2+}, maintaining increased intracellular Ca^{2+}.

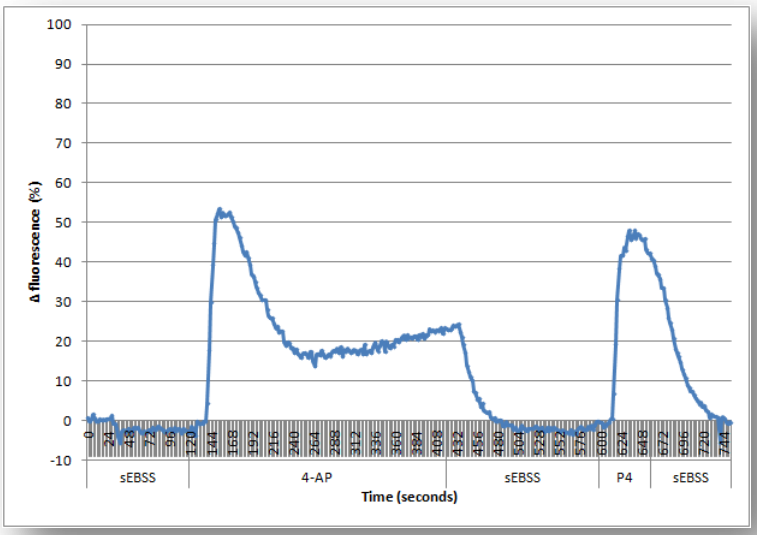

Figure 39 - Mean of % change in fluorescence in capacitated sperm in 4-AP studies. [4-AP] = 4 mM; stimulation period = 5 min. n = 3, 102 cells.

Comparing the mean values (%) for the three concentrations, 4 mM presents in fact a higher value with 73.5 ± 9.2 (n = 3) against 67.5 ± 12.9 (n = 4) and 62 ± 12.2 (n = 3) for 2 and 3 mM, respectively. However, these differences are non-significant since p values between concentrations came out higher than 0.05 (Figure 40).

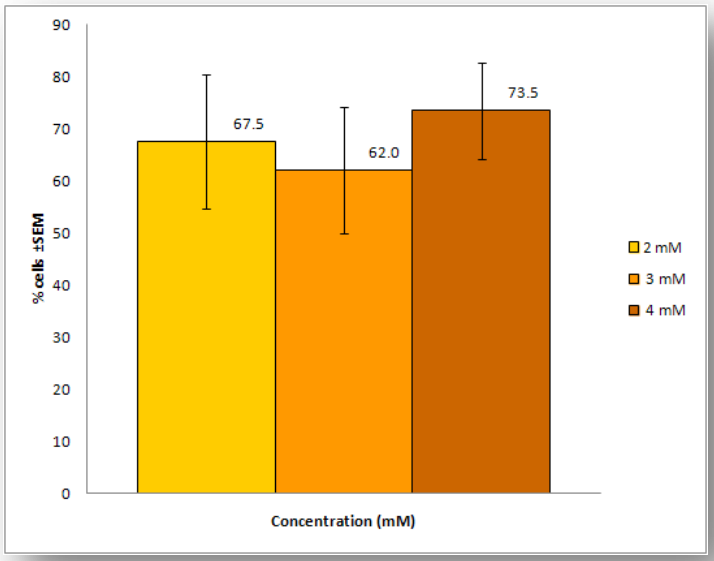

Figure 40 - Mean values (%) ± standard error of the mean of capacitated sperm responding to stimulation for 5 minutes with 4-AP at 2, 3 and 4 mM. 2 mM: n = 4, 103 cells; 3 mM: n = 3, 111 cells and 4 mM: n = 3, 105 cells. $p > 0.05$ between concentrations.

III.1.1.3 Thimerosal studies

When sperm cells are exposed to Thimerosal, a short rise in fluorescence followed by a decrease and later establishment of a plateau can be observed (mean value (%) of cells responding to Thimerosal stimulation was 49 ± 9.4, n = 6, 151 cells). Although an initial peak is not very obvious, the ensuing plateau settles at a higher intensity comparing to the baseline with sEBSS (Figure 41). Thimerosal's capacity to bind to IP_3Rs and thus release Ca^{2+} from IP_3-gated stores could explain the small rise and the plateau could be due to the equilibrium achieved by Ca^{2+} uptake into the stores and some Ca^{2+} influx by plasma membrane channels (as Thimerosal was shown to act on in order to sustain a response) (see Chapter I.4.4.3).

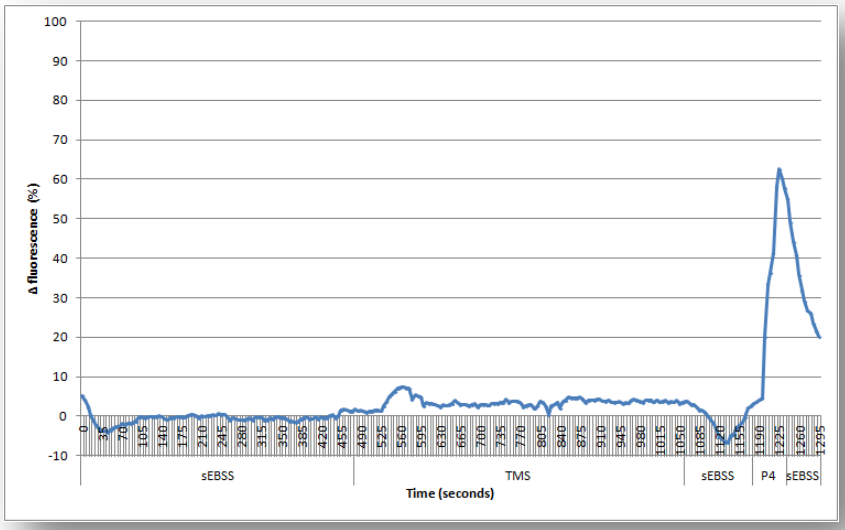

Figure 41 - Mean of % change in fluorescence in capacitated sperm in TMS studies. [TMS] = 1 µM; stimulation period = 10 min. n = 5, 143 cells.

III.1.1.4 Mibefradil studies

When exposed to Mibefradil, cells' Ca^{2+} dynamics are quite different from the ones previously observed. After a short peak in the beginning of the stimulation, Ca^{2+} levels start to decrease below baseline levels into negative values. When P4 is added, a normal response with a rapid and high peak can be seen (Figure 42). As Mibefradil is known to inhibit CatSper and T-type channels (see Chapter I.4.4.2), it is possible that some of these channels are involved in maintaining baseline Ca^{2+} levels and this is abolished when cells are exposed to Mibefradil (thus the noticeable decrease in fluorescence). After the removal of this blocker and with the stimulation with P4, these channels are activated, leading to the great increase shown.

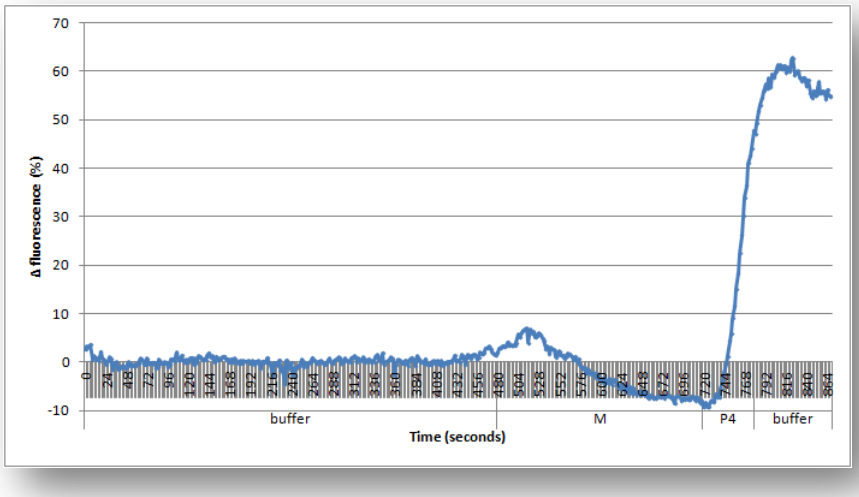

Figure 42 - Mean of % change in fluorescence in capacitated sperm in M studies. [M] = 40 µM; stimulation period = 4 min. n = 4, 174 cells.

However, when P4 is perfused along with Mibefradil, cells' response is different from the characteristic P4 steep increase (Figure 43). At least three hypotheses for this kind of dynamic can be formulated:

1. P4 could be inducing Ca^{2+} influx through plasma membrane channels before Mibefradil (which seems to have a slow action) can act on them; hence, the intermediate level characterized by a gradual increase might be the beginning of Mibefradil's blocking effect.
2. Mibefradil does not completely inhibit Ca^{2+} influx, allowing P4 to act on other Mibefradil-insensitive plasma membrane channels and still instigate Ca^{2+} influx though at a minor scale.
3. Mibefradil binds to the channel or an associate protein and prevents P4 disconnection from its receptor by, for example, changing the channel's conformation.

If #1 or #2 are taken into account, the first increase would be due to P4 action, the intermediate one to Mibefradil action and the continuing rise until the end could be the intake of Ca^{2+} (that is present on sEBSS) through re-activated plasma membrane channels along with some P4 that was not properly washed off. Considering #3, the final rise would be cells' response to the "trapped" P4 after wash off of Mibefradil with

sEBSS. However, this hypothesis is refuted by Strünker *et al.* (2011) work that claims Mibefradil reversibly blocks P4-induced Ca^{2+} transients.

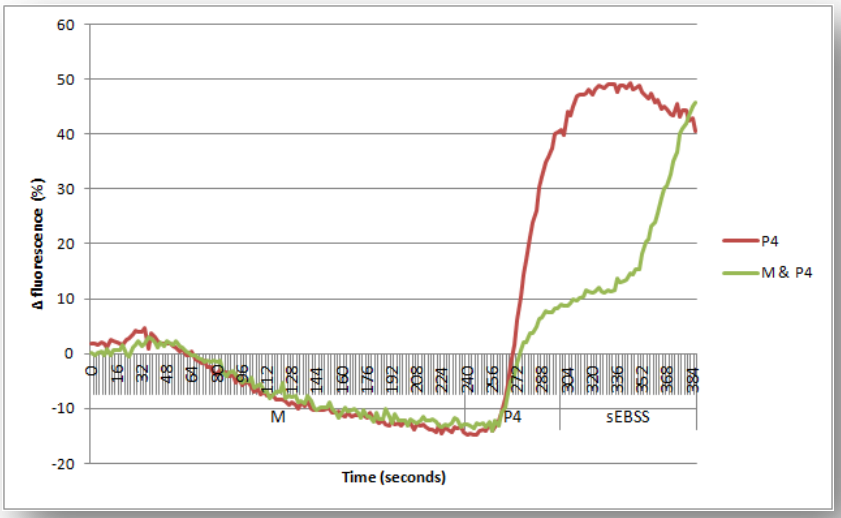

Figure 43 - Mean of % change in fluorescence in capacitated sperm in M studies. [M] = 40 µM. M stimulation period = 4 min; P4 alone / M & P4 stimulation period = 1 min. P4: n = 4, 122 cells; M & P4: n = 5, 116 cells.

In one experiment, perfusion with sEBSS at the end was extended in order to understand better the kinetics of M & P4 response. After the peak was reached, a decrease in fluorescence was observed, followed by a second rise leading to another peak (Figure 44). Assuming hypothesis #3 is the most likely, the second peak could be due to the imprisonment of P4 on the receptor even after wash off of Mibefradil and the formation of what it seems like P4-induced Ca^{2+} oscillations. Perhaps more experiments with a longer perfusion with sEBSS could confirm or refute this hypothesis.

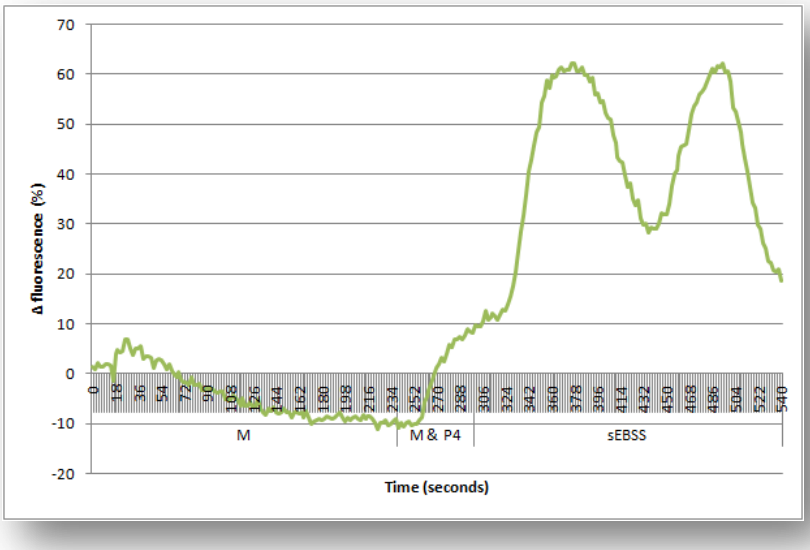

Figure 44 - Mean of % change in fluorescence in capacitated sperm in M studies. [M] = 40 µM. M stimulation period = 4 min; M & P4 stimulation period = 1 min. M & P4: n = 1, 15 cells.

III.1.1.5 NNC studies

With NNC, cells' Ca^{2+} dynamics are quite variable: three types of reactions to the compound can be seen. One is somewhat similar to the Mibefradil one, showing a decrease until negative values with the difference that the initial peak in fluorescence is higher than the one in analogous studies with Mibefradil (49 %, n = 3, 98 cells). Furthermore, NNC seems to act faster than Mibefradil since the initial peak is steeper and the decrease is less gradual than the later (Figure 45). Since both act on CatSper and NNC is an analog of Mibefradil (see Chapter I.4.4.2), it is possible that NNC is more specific than Mibefradil inhibiting the main plasma membrane channels responsible for Ca^{2+} influx.

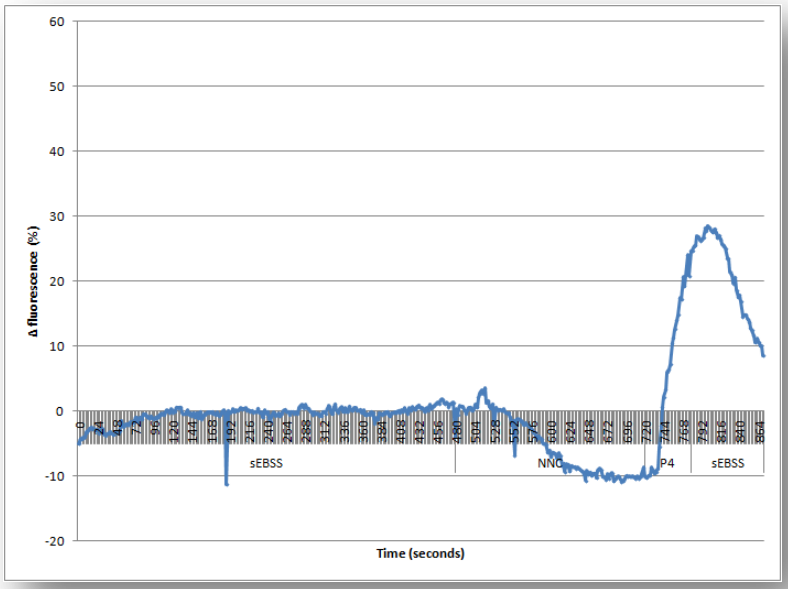

Figure 45 - Mean of % change in fluorescence in non-responding (inhibited) capacitated sperm in NNC studies. [NNC] = 10 µM. M stimulation period = 4 min. n = 3, 98 cells.

The other two reactions to NNC include a rise in fluorescence instead of a decrease, expected when an inhibitor of Ca^{2+} influx is added to the cells (19 %, n = 3, 98 cells) and a decrease until levels above the baseline (32 %, n = 3, 98 cells) (Figure 46). If NNC is a more specific blocker than Mibefradil, it is possible that in some cells, it binds to the channel on an activating area, inducing Ca^{2+} influx rather than preventing it. Another hypothesis could be that NNC would be activating a different channel or pathway (not directly through CatSper) to increase $[Ca^{2+}]_i$. However, there is no indication so far that any of these might happen.

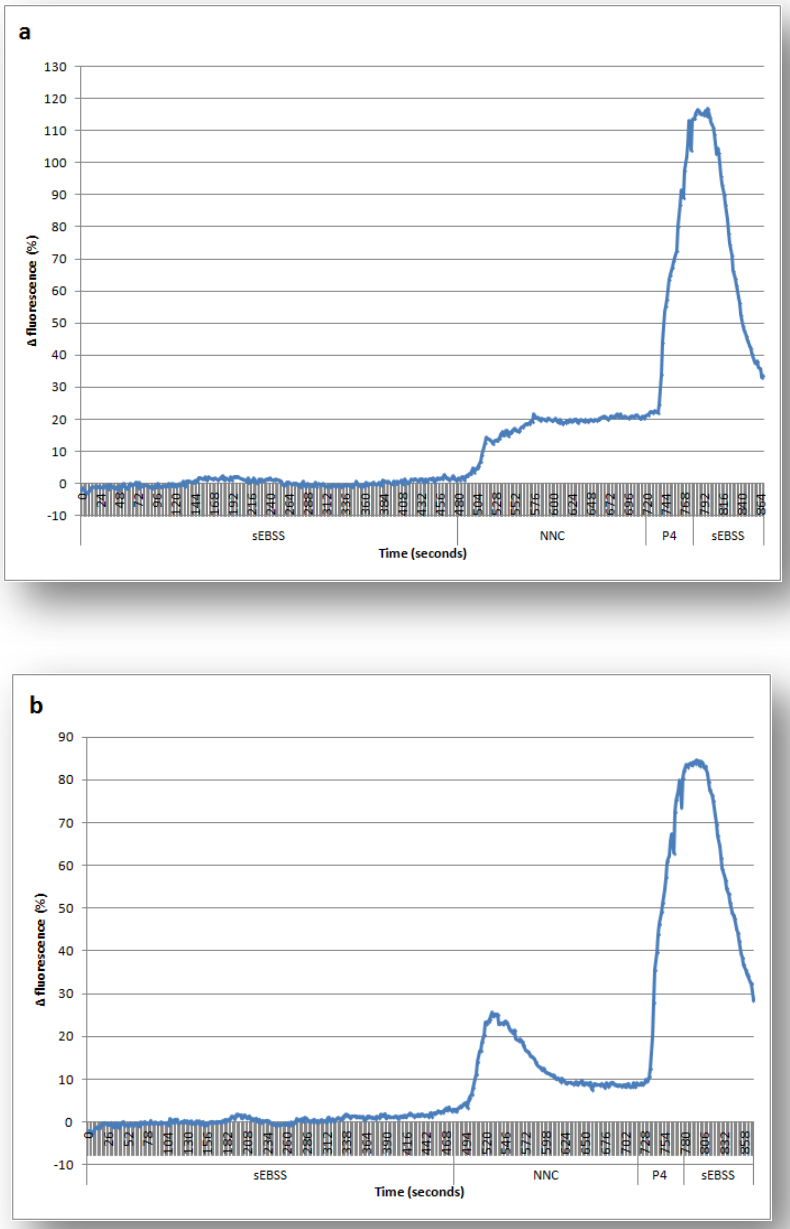

Figure 46 – Mean of % change in fluorescence in capacitated sperm in NNC studies. [NNC] = 10 µM. M stimulation period = 4 min. n = 3, 98 cells; a) cells responding to NNC; b) cells partially inhibited by NNC

When P4 is added along with NNC, a typical P4 response can be observed though the rise in fluorescence is not as high as the former. Moreover, there is no abrupt decrease after maximum amplitude is reached but instead, the formation of a plateau and the beginning of a slower decrease (Figure 47). Hence, it seems that NNC partially blocks P4-induced response by acting on CatSper and reducing Ca^{2+} influx.

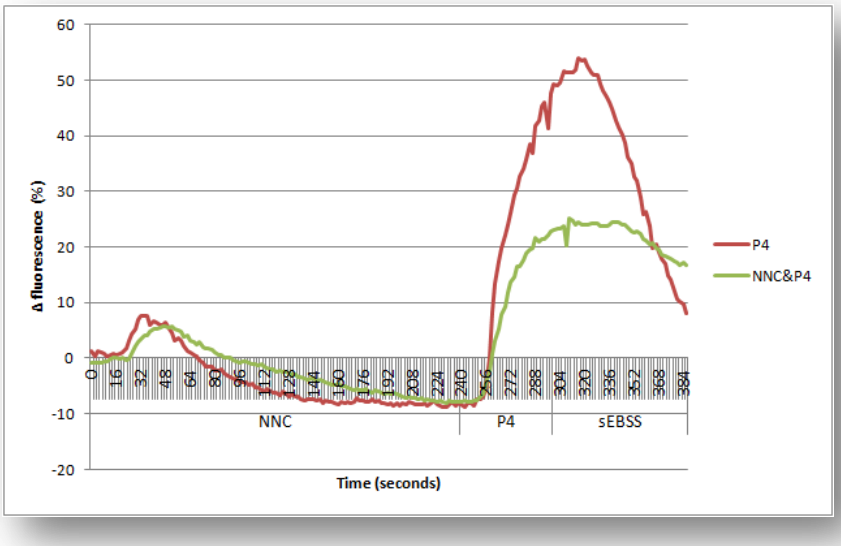

Figure 47 - Mean of % change in fluorescence in capacitated sperm in NNC studies. [NNC] = 10 µM. NNC stimulation period = 4 min; P4 alone / NNC & P4 stimulation period = 1 min. P4: n = 2, 28 cells; M & P4: n = 5, 51 cells.

Efficiency of NNC was also compared with the Mibefradil one, using the % cells which showed a decrease in fluorescence, when in contact with one of the Ca^{2+} influx blockers. Mibefradil proved to be more efficient by inducing this decrease in a bigger % cells than NNC with 81.8 ± 8 Vs 38.2 ± 0.9, respectively (Figure 48). This is probably due to the multiplicity of cells' reactions to NNC as reported above (see Figure 46).

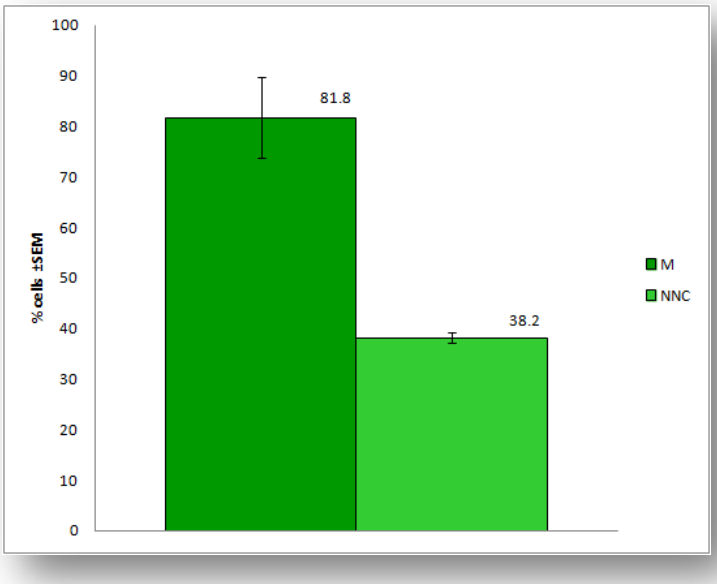

Figure 48 - Mean values (%) ± standard error of capacitated sperm non-responding (inhibited) with M and NNC at 40 and 10 µM, respectively. M: n = 3, 138 cells; NNC: n = 2, 74 cells. $p < 0.05$.

III.1.2 Multiple-compound testing

Cells used to calculate the statistical significance between concentrations and to create bar charts were all responsive to perfusion with the first compound (4-AP, TMA) and, afterwards, to the second (Thimerosal, NNC, Mibefradil).

III.1.2.1 TMS & 4-AP studies

When the two compounds are added at the same time, there is a sudden increase of fluorescence, a gradual decrease and a second, more stable rise (Figure 49). The rapid and great change of fluorescence could be due to both the promotion of Ca^{2+} influx and the release of Ca^{2+} from ICS through ligand-gated channels like IP_3R, since Thimerosal is an agonist of these channels and 4-AP is thought to act on plasma membrane channels in order to sustain the Ca^{2+} response (see Chapters I.4.4.3 and I.4.4.4). The subsequent decrease could be attributed to CCE, with the uptake of Ca^{2+} into the depleted stores through SOC channels. After the filling of the stores, Ca^{2+} influx is maintained by both compounds thus the slower rise; this influx would be roughly double the one instigated by 4-AP alone.

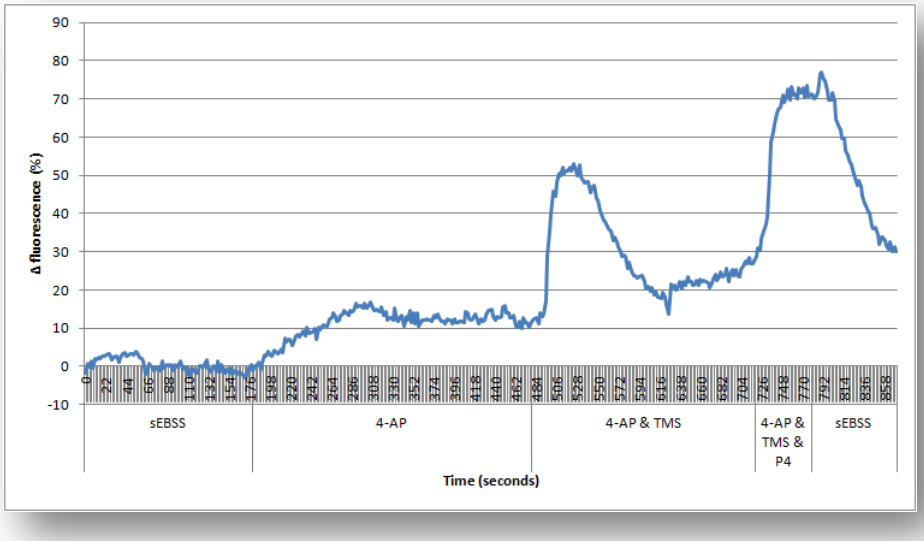

Figure 49 – Mean of % change in fluorescence in capacitated sperm in TMS & 4-AP studies. [4-AP] = 2 mM; [TMS] = 1 µM; stimulation period = 4 min. n = 6, 96 cells.

Comparing the three [4-AP]s, the initial rise after the addition of TMS & 4-AP appears to be similar in terms of amplitude at 2 and 3 mM but the decay seems faster at 3 and 4 mM (see Figure 49, Figure 50).

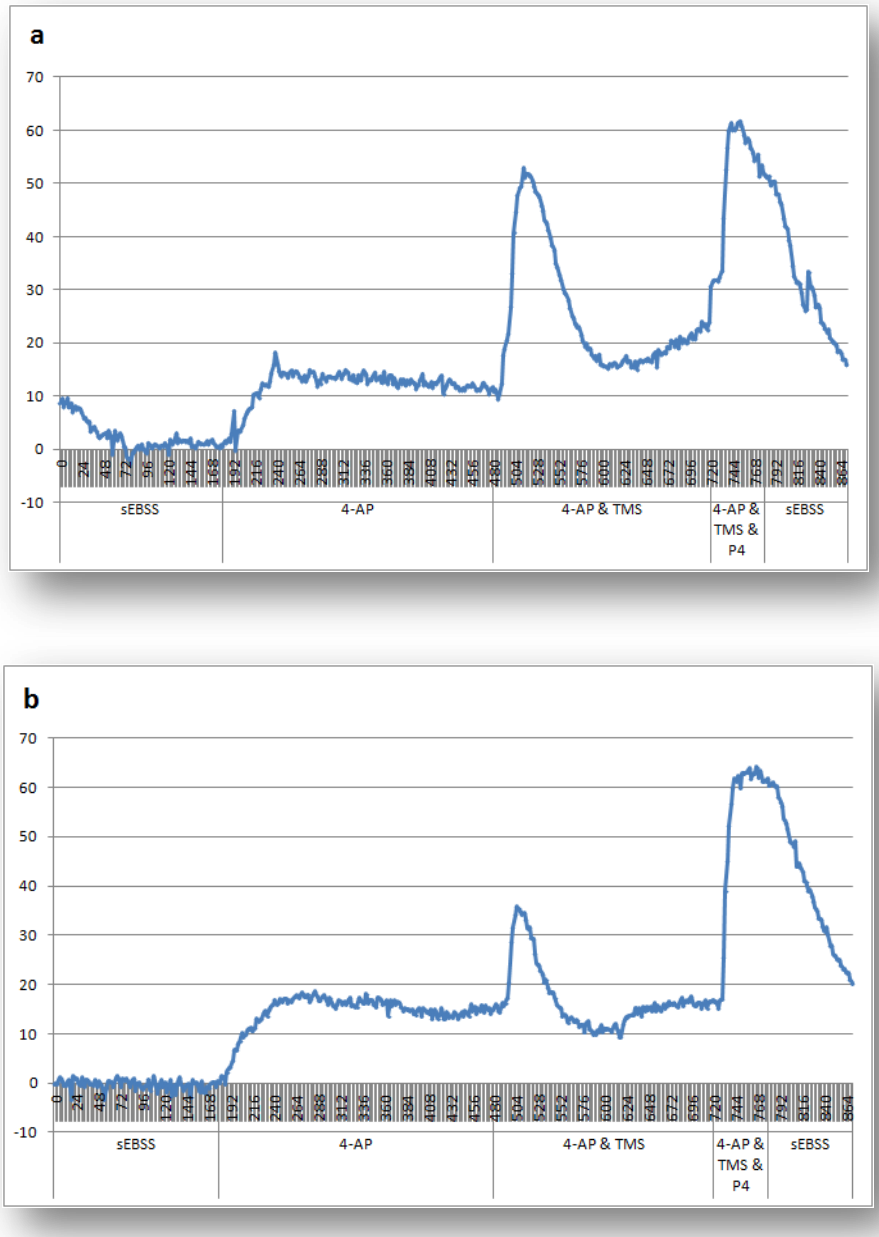

Figure 50 - Mean of % change in fluorescence in capacitated sperm in TMS & 4-AP studies. a) [4-AP] = 3 mM; [TMS] = 1 µM; stimulation period = 4 min; n = 95 cells; 6 experiments. b) [4-AP] = 4 mM; [TMS] = 1 µM; stimulation period = 4 min; n = 85 cells; 4 experiments.

Mean values (%) of response to both compounds at the three [4-AP]s were statistically non-significant ($p > 0.05$) between each other with 45.2 ± 20.6, 43.9 ± 11.9

and 34.2 ± 9.8 for 2, 3 and 4 mM, respectively (Figure 51). Even so, response to both compounds seems to decrease with higher [4-AP], contrarily to what was seen before (see Chapter III.1.1.4). This could be due to the high rate of Ca^{2+} efflux from the stores and influx through plasma membrane channels induced by both Thimerosal and high [4-AP] that might cause saturation of these channels (hence delaying influx) whilst Ca^{2+} is being pump into the stores, thus the decrease in fluorescence.

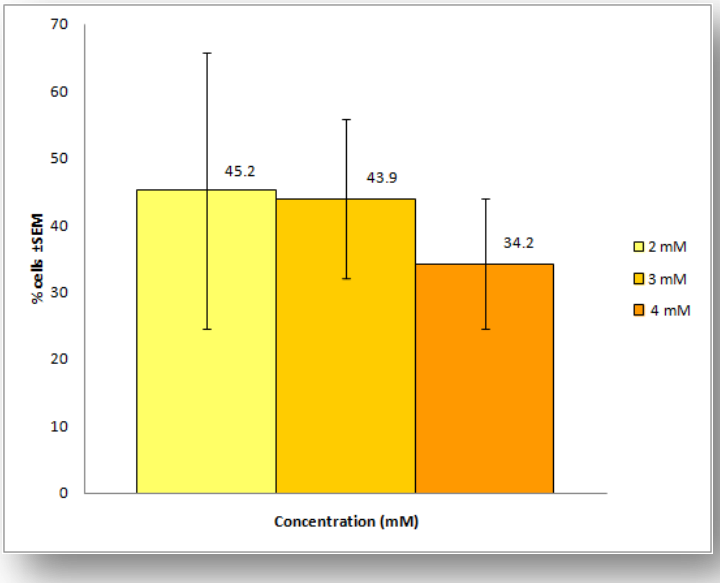

Figure 51 - Mean values (%) ± standard error of the mean of capacitated sperm responding to stimulation for 4 minutes with TMS & 4-AP with [4-AP] at 2, 3 and 4 mM. 2 mM: n = 3, 88 cells; 3 mM: n = 5, 93 cells and 4 mM: n = 4, 94 cells. $p > 0.05$ between concentrations.

III.1.2.2 TMS & TMA studies

When Thimerosal is added along with TMA, cells' response differs little from the 4-AP & TMS one: a smaller initial peak and faster further increase in fluorescence (mean value (%) of 85.5 ± 0.3; n=2) can be seen (Figure 52). Since TMA affects plasma membrane channels (see Chapter I.4.4.5), the second increase will be probably due to the instigation of Ca^{2+} influx both by TMA and Thimerosal (thus being faster).

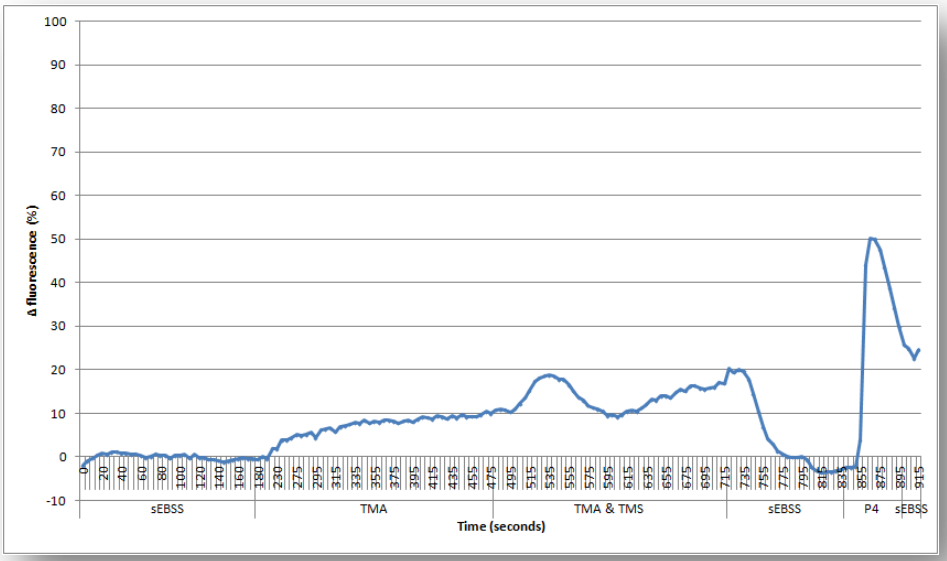

Figure 52 - Mean of % change in fluorescence in capacitated sperm in TMS & TMA studies. [TMA] = 10 mM; [TMS] = 1 µM; stimulation period = 4 min. n = 2, 43 cells.

III.1.2.3 M & 4-AP studies

When Mibefradil is added along with 4-AP, a short peak can be observed in the beginning of the stimulation, followed by a decrease in fluorescence below baseline levels (Figure 53). This fall could be explained by the inhibition of Ca^{2+} influx through plasma membrane channels, probably the ones 4-AP acts on since fluorescence falls below the rise induced by 4-AP (either CatSper or T-type) (see Chapters I.4.4.2 and I.4.4.4). Cells' response to the perfusion with the three compounds resembles the typical P4-induced one; however, at the end of the experiment, the beginning of a second peak like the one described above (see Chapter III.1.1.4 Mibefradil studies) can be seen at the three concentrations.

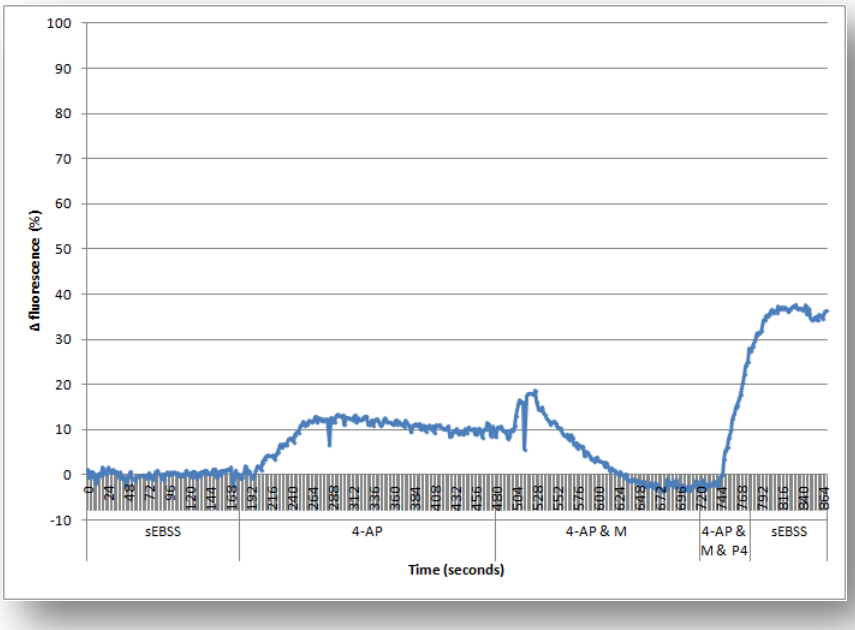

Figure 53 - Mean of % change in fluorescence in capacitated sperm in M & 4-AP studies. [4-AP] = 2 mM; [M] = 40 µM; stimulation period = 4 min. n = 3, 77 cells.

Cells' response to [4-AP]s at 3 mM and 4 mM present a similar pattern, that slightly differs from the 2 mM one: the initial peak after addition of M & 4-AP is much less noticeable and the following decrease does not fall below baseline levels. Adding M & 4-AP after perfusion with 4-AP alone seems to cause a greater fall at 3 mM than at 4 mM; also, the latter decrease appears to be more gradual than the former (Figure 54).

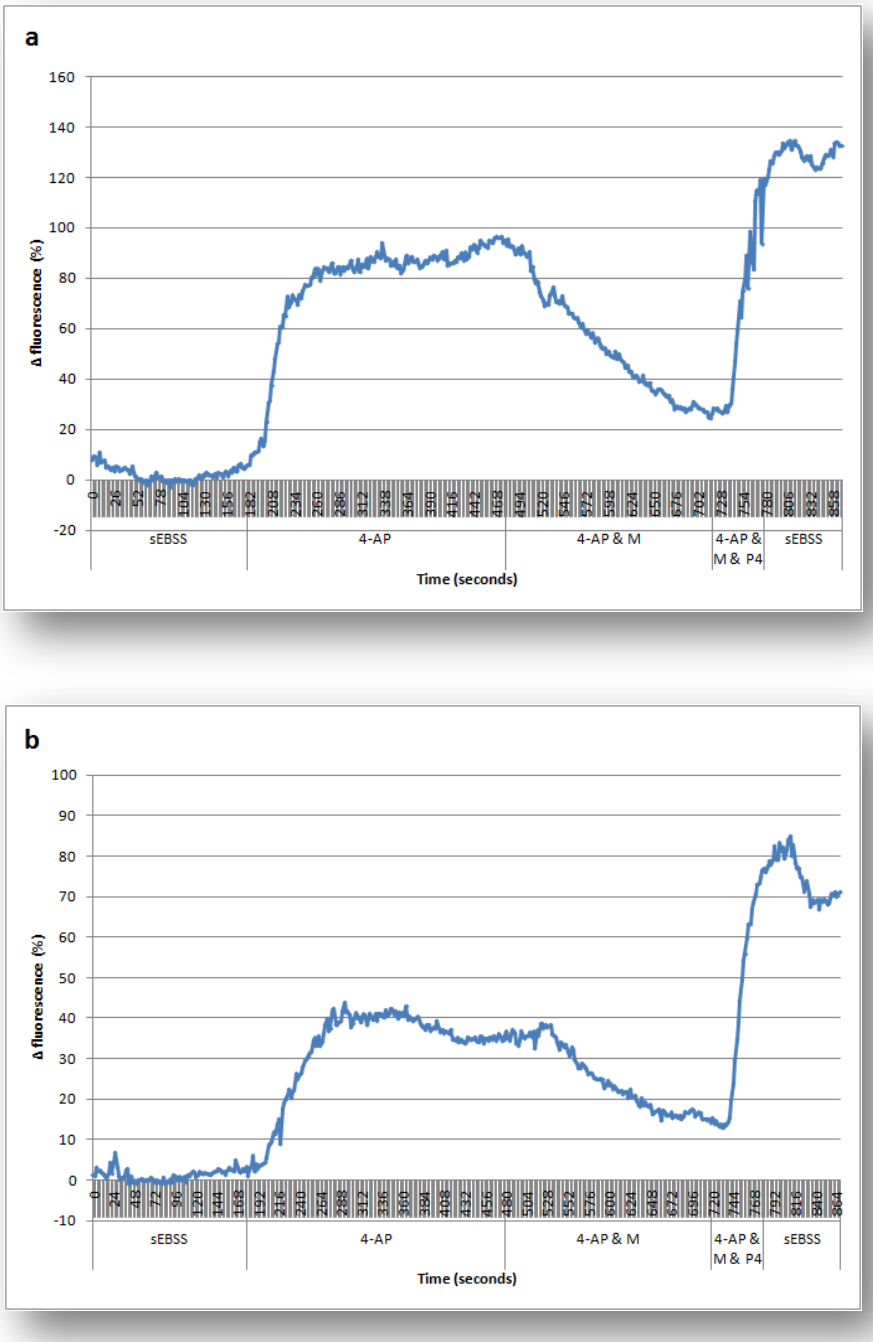

Figure 54 - Mean of % change in fluorescence in capacitated sperm in 4-AP & M studies. a) [4-AP] = 3 mM; [M] = 40 µM; stimulation period = 4 min; n = 77 cells; 4 experiments. b) [4-AP] = 4 mM; [M] = 40 µM; stimulation period = 4 min; n = 29 cells; 2 experiments.

Although the differences between concentrations were non-significant ($p > 0.05$) with mean values (%) of non-responding (inhibited) cells of 78.8 ± 11.6 (n = 3), 81 ± 4.5 (n = 4) and 57.5 ± 24.1 (n = 2) for 2, 3 and 4 mM respectively, apparently cells are less inhibited by Mibefradil when higher concentrations of 4-AP are applied along (Figure

55). Given that in the 2 mM response Mibefradil could inhibit CatSper sufficiently, so as to reduce $[Ca^{2+}]_i$ base levels, one explanation for its lack of ability to produce a similar response could be that higher [4-AP]s stimulate ligand-channels in intracellular stores to release Ca^{2+}. Hence, Mibefradil's inhibitory response would be mitigated by a Ca^{2+} efflux into the cytoplasm, which is more pronounced at 4 mM.

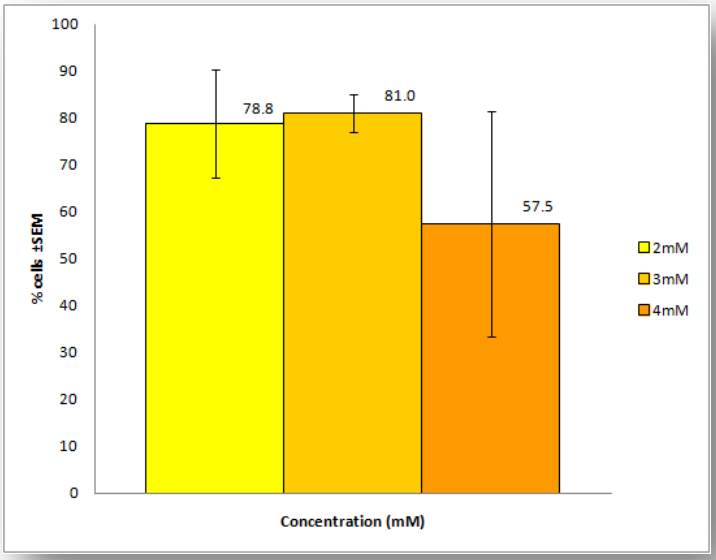

Figure 55 - Mean values (%) ± standard error of the mean of capacitated sperm non-responding (inhibited) to stimulation for 4 minutes with M & 4-AP with [4-AP] at 2, 3 and 4 mM. 2 mM: n = 3, 69 cells; 3 mM: n = 4, 106 cells and 4 mM: n = 2, 47 cells. $p > 0.05$ between concentrations.

III.1.2.4 NNC & 4-AP studies

Although being an analog of Mibefradil, NNC's effect on cells seems to be slightly different from the latter with the decrease caused by NNC & 4-AP appearing to be less steep. Also, it seems that there is a direct relationship between [4-AP] and % of NNC's inhibition, with higher rates of blockade being achieved with higher [4-AP]s (Figure 56).

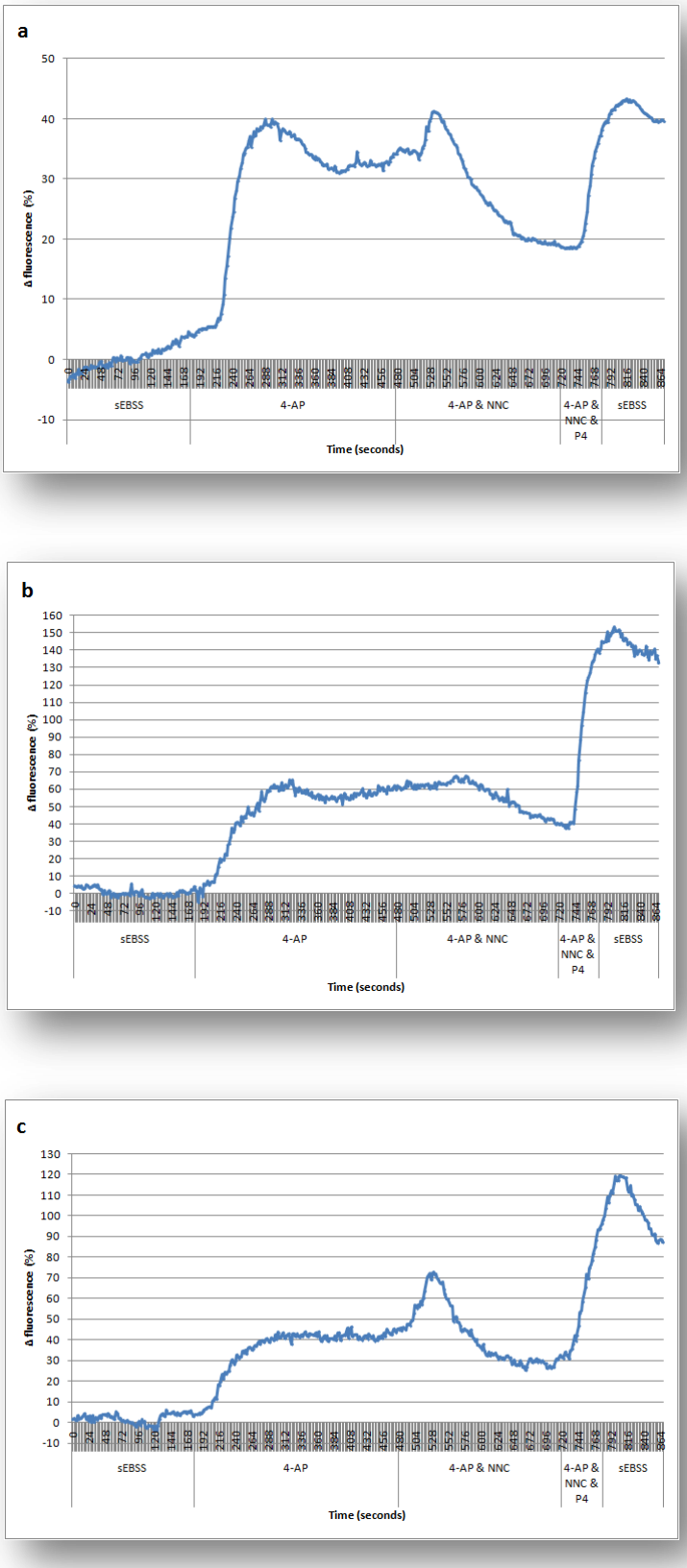

Figure 56 - Mean of % change in fluorescence in capacitated sperm in NNC & 4-AP studies. a) [4-AP] = 2 mM; [NNC] = 10 µM; stimulation period = 4 min; n = 83 cells; 5 experiments. b) [4-AP] = 3 mM; [NNC] = 10 µM; stimulation period = 4 min. n = 3, 73 cells. c) [4-AP] = 4 mM; [NNC] = 10 µM; stimulation period = 4 min; n = 22 cells; 2 experiments.

However, when the mean values (%) of inhibited cells of the three 4-AP concentrations are calculated, the opposite verifies with higher decreases in fluorescence being seen at lower [4-AP]s (70.4 ± 14.3, 48.1 ± 12.8 and 44.9 ± 3.6 at 2, 3 and 4 mM, respectively), albeit the differences are non-significant ($p > 0.05$; Figure 57). This ambiguity is probably due to the three possible reactions to NNC discussed above (Chapter III.1.1.5).

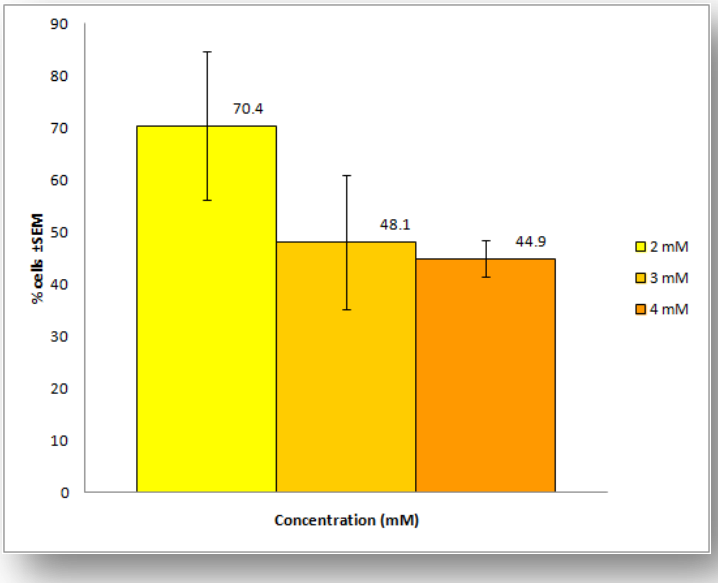

Figure 57 - Mean values (%) ± standard error of the mean of capacitated sperm non-responding (inhibited) to stimulation for 4 minutes with NNC & 4-AP with [4-AP] at 2, 3 and 4 mM. 2 mM: n = 5, 79 cells; 3 mM: n = 5, 138 cells and 4 mM: n = 3, 63 cells. $p > 0.05$ between concentrations.

III.1.2.5 M & TMA studies

When TMA is perfused with Mibefradil, two kinds of inhibition can be seen: at 10 mM the decrease appears clear and quite fast towards baseline levels whilst at 20 mM it seems steadier and not complete (Figure 58). Response to both compounds and P4 seems to be analogous to the one observed in M & 4-AP studies (see Chapter III.1.2.4).

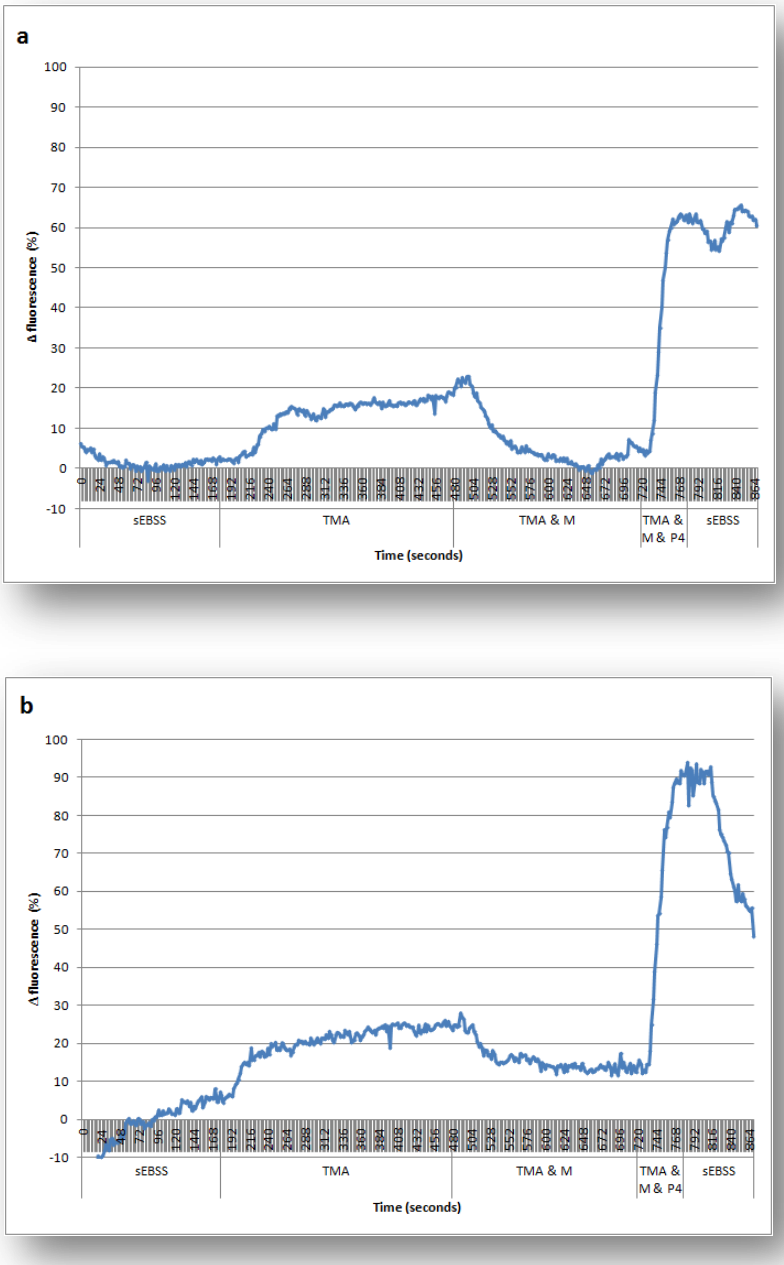

Figure 58 - Mean of % change in fluorescence in capacitated sperm in M & TMA.
a) [TMA] = 10 mM; [M] = 40 µM; stimulation period = 4 min. n = 3, 20 cells.
b) [TMA] = 20 mM; [M] = 40 µM; stimulation period = 4 min; n = 29 cells; 2 experiments.

Non-response (inhibition) differences between concentrations are non-significant (mean values (%) of 69.3 ± 15.1 and 55.8 ± 5.8; $p > 0.05$), albeit it appears that higher [TMA]s mitigate the Mibefradil inhibitory effect (Figure 59). Since TMA acts on pH-sensitive CatSper and Mibefradil is known to block them (see Chapters I.4.4.2 and I.4.45), it is likely that greater [TMA]s have a stronger effect on these channels

than Mibefradil or can induce Ca^{2+} influx from other channels that Mibefradil cannot block, thus counteracting the blockade.

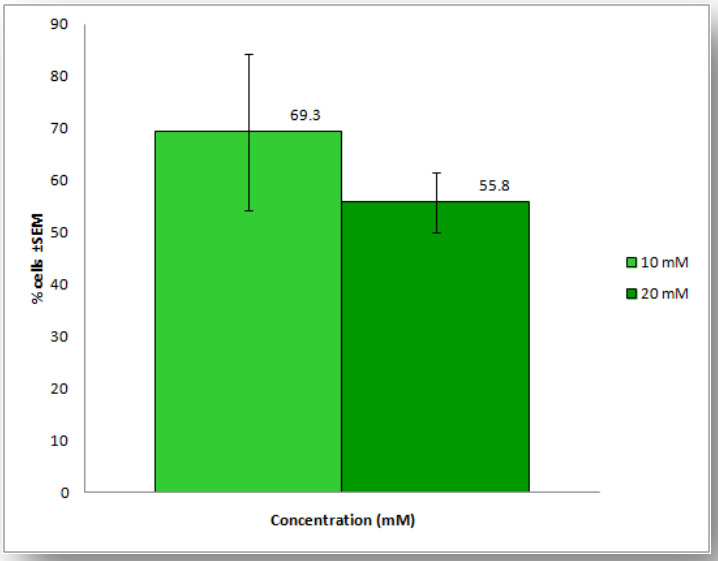

Figure 59 - Mean values (%) ± standard error of the mean of capacitated sperm non-responding (inhibited) to stimulation for 4 minutes with M & TMA with [TMA] at 10 and 20 mM. 10 mM: n = 3, 24 cells; 20 mM: n = 2, 37 cells. $p > 0.05$.

III.1.2.6 NNC & TMA studies

In NNC & TMA studies, cells' inhibition after addition of both compounds seems to be quite different depending on [TMA]. At 10 mM, after a sharp decrease, fluorescence rises until a plateau is achieved whilst at 20 mM, a rapid but small peak can be seen, followed by a slow decrease (Figure 60).

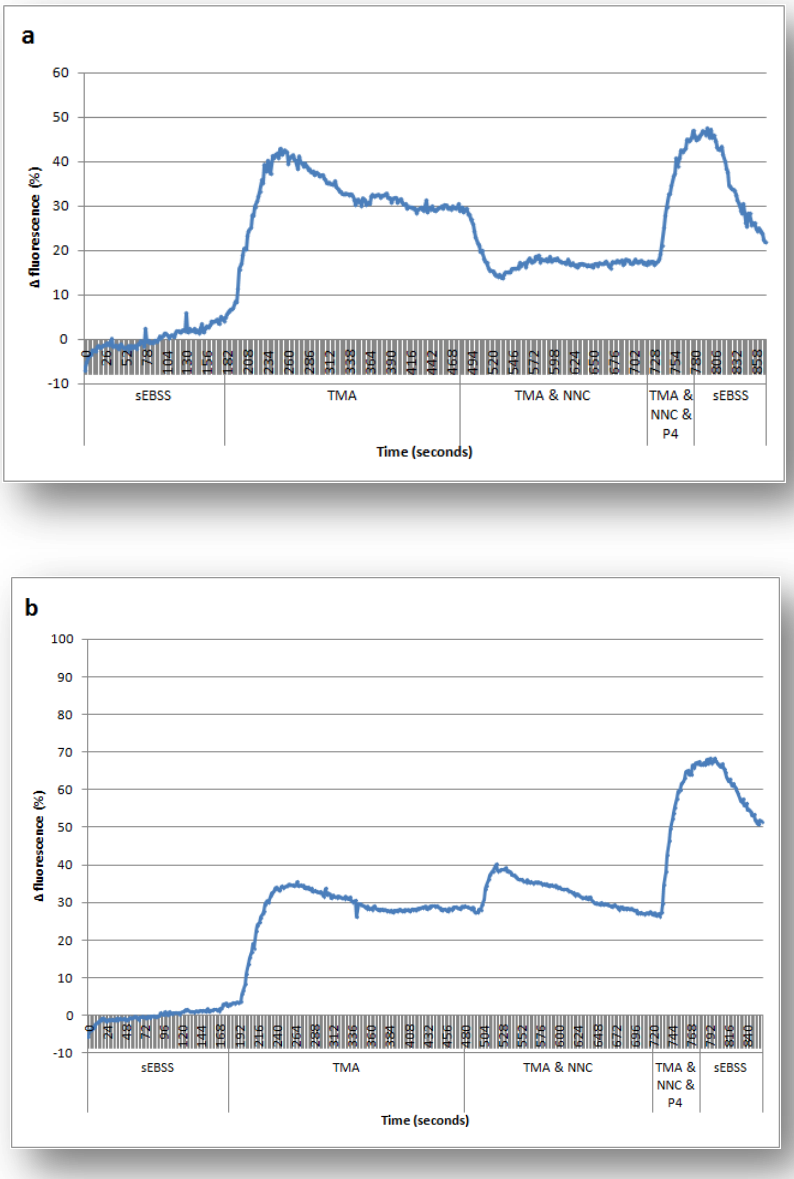

Figure 60 - Mean of % change in fluorescence in capacitated sperm in TMA & NNC studies. a) [TMA] = 10 mM; [NNC] = 10 µM; stimulation period = 4 min. n = 3, 31 cells. b) [TMA] = 20 mM; [NNC] = 10 µM; stimulation period = 4 min; n = 81 cells; 4 experiments.

Mean values (%) of inhibition were calculated to both concentrations but revealed to be non-significant ($p > 0.05$) between each other (62.4 ± 29.1 and 54.5 ± 12.1 for 10 and 20 mM, respectively. Nevertheless, TMA at 20 mM appears to prevent at some extent the decrease in fluorescence due to inhibition by NNC (Figure 61). Since TMA is known to act on pH-sensitive CatSper, which are also blocked by NNC (see Chapter I.4.4.5), it is possible that a higher [TMA] acts more efficiently on these

channels, maintaining Ca^{2+} influx (though at a smaller rate) or that other VOCC insensitive to NNC are involved in the basal Ca^{2+} level maintenance in the cell.

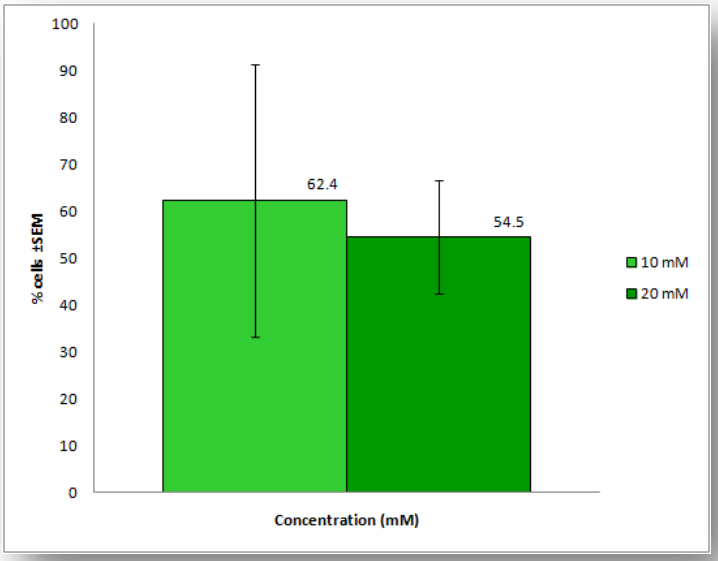

Figure 61 - Mean values (%) ± standard error of the mean of capacitated sperm non-responding (inhibited) to stimulation for 4 minutes with NNC & TMA with [TMA] at 10 and 20 mM. 10 mM: n = 2, 38 cells; 20 mM: n = 4, 90 cells. $p > 0.05$.

III.2 Motility Studies

III.2.1 TMA's effect

Five samples collected in two separate days from different donors were used to evaluate TMA's effect on free swimming cells and compared with their respective controls.

Close visual observation of cells' movement revealed a more linear trajectory with low amplitude bending due to reduced or even absent lateral head displacement. Moreover, an increase of flagellar beating was also evident. Software analysis of cells' tracks confirmed the visual examination, reporting a rise in velocity with a mean value

(µm/s) of 45.06 ± 0.94 for TMA Vs 42.22 ± 1.02 for sEBSS (control). A p value of 0.046 attributed statistical significance to the results (Figure 62).

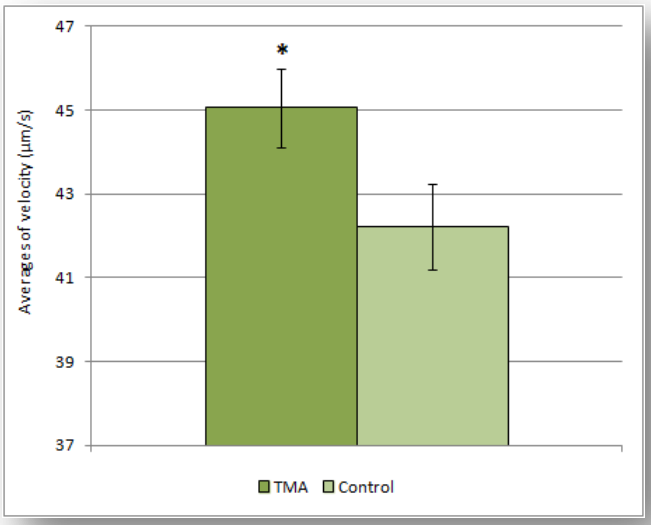

	TMA	Control
AVG	45.06	42.22
VAR	157.45	122.92
STDEV	12.55	11.09
SEM	0.94	1.02
MAX	74.58	89.48
MIN	11.04	17.51
n	2	2
# cells	179	119
p value	0.046	

Figure 62 –Averages of velocity (µm/s) for TMA-treated free swimming cells and sEBSS-treated cells (control) (left); Statistical parameters (µm/s) calculated for free swimming cells treated with TMA or sEBSS (control) (right). [TMA] = 10 mM. AVG – average; VAR – variance; STDEV – standard deviation; SEM – standard error of the mean; MAX – maximum value; MIN – minimum value.
P value significant.

To better understand the differences between the two cell types of experiment, mean values were grouped within intervals of 5 µm/s for both control and TMA groups, so as to build an histogram with the cells' frequencies (%) for each interval. Analysis of velocity distribution suggests that cells were swimming at 40 - 55 µm/s in the control, increased their velocities to 55 – 75 µm/s when exposed to TMA (Figure 63). One plausible explanation for this phenomenon could be the known influence of TMA on Ca^{2+} channels, responsible for Ca^{2+} influx into the cell. This influx of Ca^{2+} through CatSper, which are situated on the principal piece of the flagellum, could induce a higher beating frequency, thus enhancing the speed of the cell.

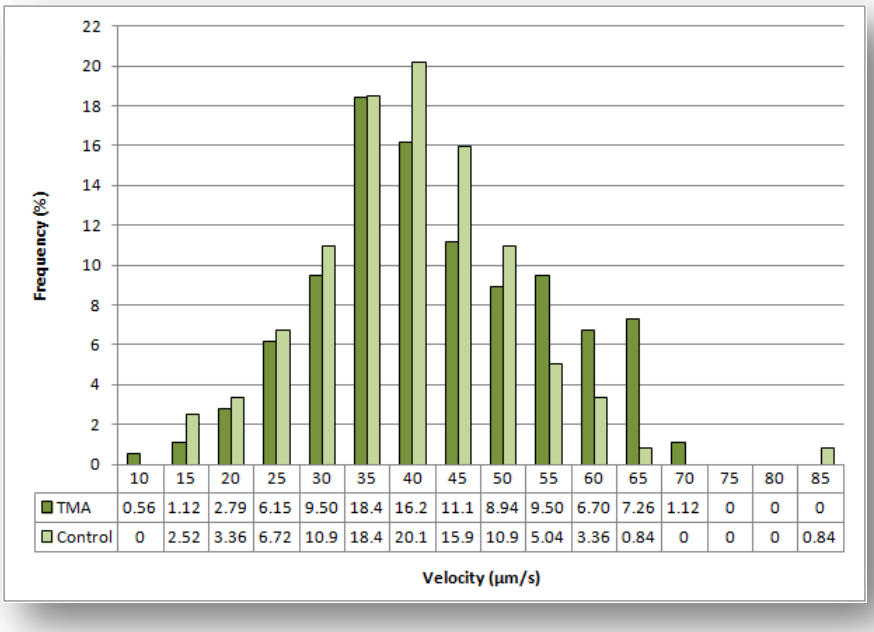

	10	15	20	25	30	35	40	45	50	55	60	65	70	75	80	85
TMA	0.56	1.12	2.79	6.15	9.50	18.4	16.2	11.1	8.94	9.50	6.70	7.26	1.12	0	0	0
Control	0	2.52	3.36	6.72	10.9	18.4	20.1	15.9	10.9	5.04	3.36	0.84	0	0	0	0.84

Figure 63 – Velocity (µm/s) distribution for sEBSS (control) or TMA-treated cells.

III.2.2 4-AP's effect

For the evaluation of 4-AP's effect on free swimming cells, three samples obtained in two separate days were used and compared with their respective controls.

Visual observation of 4-AP-treated spermatozoa revealed a relatively high number of hyperactivated cells (as it was expected since 4-AP induces hyperactivation) with enhanced flagellar asymmetry and increased bend amplitude when compared with control. Cells that were not hyperactived showed a sinuous and slow progressive trajectory, together with high lateral head displacement. Difference between mean velocity values (µm/s) were non-significant ($p > 0.05$) with 54.82 ± 1.08 and 56.15 ± 0.77 for cells in 4-AP and sEBSS, respectively (Figure 64). The small decrease in velocity in 4-AP could be explained by the high rate of hyperactivated cells some of which were non progressive, swimming in star-shaped pattern.

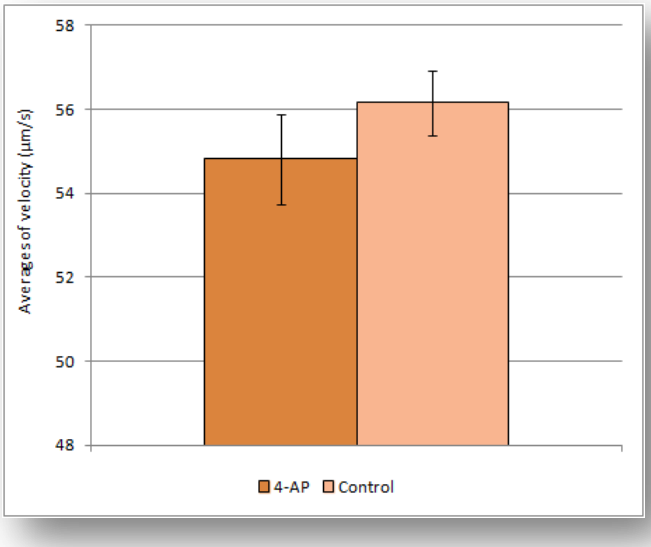

	4-AP	Control
AVG	54.82	56.15
VAR	200.59	251.41
STDEV	14.16	15.86
SEM	1.08	0.77
MAX	101.07	96.43
MIN	10.63	13.00
n	2	2
# cells	173	427
p value	0.337	

Figure 64 - Averages of velocity (µm/s) for 4-AP-treated free swimming cells and sEBSS-treated cells (control) (left); Statistical parameters (µm/s) calculated for free swimming cells treated with 4-AP or sEBSS (control) (right). [4-AP] = 2 mM. AVG – average; VAR – variance; STDEV – standard deviation; SEM – standard error of the mean; MAX – maximum value; MIN – minimum value. P value not significant.

The histogram of both frequencies (%) of cells' velocity (µm/s) when treated with 4-AP or sEBSS is very similar between the two compounds, with a bell-shaped distribution pointing towards a normal distribution of the data. Thus, the decrease of velocity reported 4-AP-treated cells does not present a statistical significance (Figure 65).

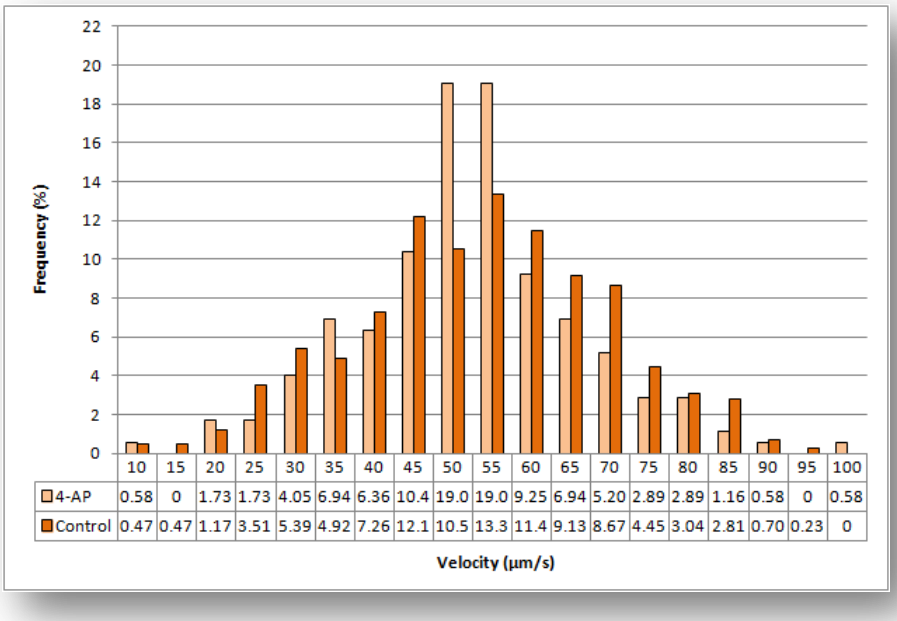

	10	15	20	25	30	35	40	45	50	55	60	65	70	75	80	85	90	95	100
4-AP	0.58	0	1.73	1.73	4.05	6.94	6.36	10.4	19.0	19.0	9.25	6.94	5.20	2.89	2.89	1.16	0.58	0	0.58
Control	0.47	0.47	1.17	3.51	5.39	4.92	7.26	12.1	10.5	13.3	11.4	9.13	8.67	4.45	3.04	2.81	0.70	0.23	0

Figure 65 - Velocity (µm/s) distribution for sEBSS (control) or 4-AP-treated cells.

III.2.3 Thimerosal's effect

Contrarily to the previous studies, the five samples used on this one were from the same donor, on the same day. Nevertheless, they were compared with the control ones from that day.

Although it is reported that Thimerosal, like 4-AP, induces hyperactivation (Chapter I.4.4.3) only a few cells were hyperactivated perhaps due to the low concentration of the compound (1 µM). However, it looks like a great number of cells were displaying increased lateral head displacement, one of hyperactivation's characteristics. Software analysis of cells' tracks showed a small rise of velocity, albeit non-significant ($p > 0.05$), with mean values (µm/s) of 54.21 ± 0.84 Vs 53.72 ± 1.85 for cells in Thimerosal and sEBSS, respectively (Figure 66).

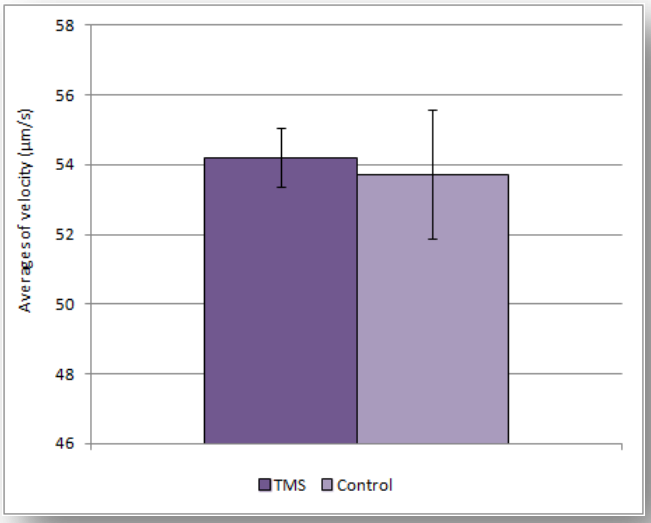

	TMS	Control
AVG	54.21	53.72
VAR	182.77	154.4
STDEV	13.52	12.43
SEM	0.84	1.85
MAX	84.3	86.22
MIN	6.97	25.81
n	1	1
# cells	261	45
p value	0.820	

Figure 66 - Averages of velocity (µm/s) for TMS-treated free swimming cells and sEBSS-treated cells (control) (left); Statistical parameters (µm/s) calculated for free swimming cells treated with TMS or sEBSS (control) (right). [TMS] = 1 µM. AVG – average; VAR – variance; STDEV – standard deviation; SEM – standard error of the mean; MAX – maximum value; MIN – minimum value. P value not significant.

The histogram confirmed the statistical non significance ($p > 0.05$) given by the statistical parameters. Also, it is noticeable an uncommon distribution of the control values, which would probably be closer to a normal distribution if a larger number of tracks were included (Figure 67).

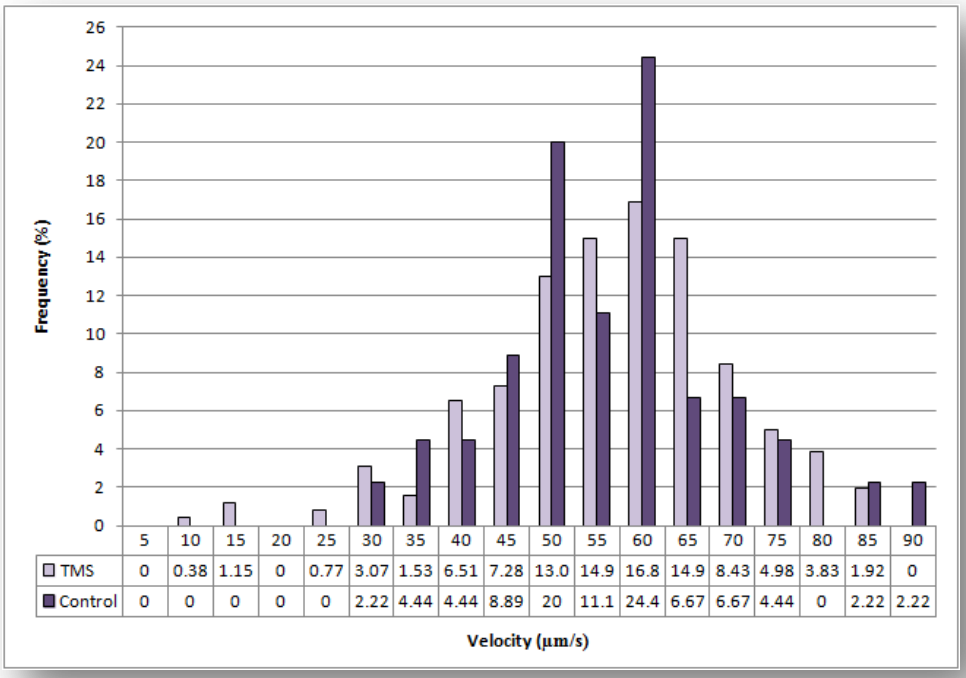

	5	10	15	20	25	30	35	40	45	50	55	60	65	70	75	80	85	90
TMS	0	0.38	1.15	0	0.77	3.07	1.53	6.51	7.28	13.0	14.9	16.8	14.9	8.43	4.98	3.83	1.92	0
Control	0	0	0	0	0	2.22	4.44	4.44	8.89	20	11.1	24.4	6.67	6.67	4.44	0	2.22	2.22

Figure 67 - Velocity (µm/s) distribution for sEBSS (control) or TMS-treated cells.

III.2.4 Mibefradil's effect

Mibefradil's effect on free swimming cells was evaluated using nine samples collected in two separate days from two donors and compared with the respective control samples.

Cells' examination revealed two kinds of dynamics:

1. increased flagellar beating with almost no lateral head displacement (as seen with TMA);
2. increased flagellar beating with some head displacement leading to a faster progression (though not as fast as the previous cells).

Software analysis of cells' tracks reported a big statistical significance ($p < 0.001$) between Mibefradil and sEBSS with Mibefradil's velocity mean values (µm/s) being much lower than the control ones: 51.16 ± 1.96 Vs 42.22 ± 8 for cells in Mibefradil and sEBSS, respectively (Figure 68).

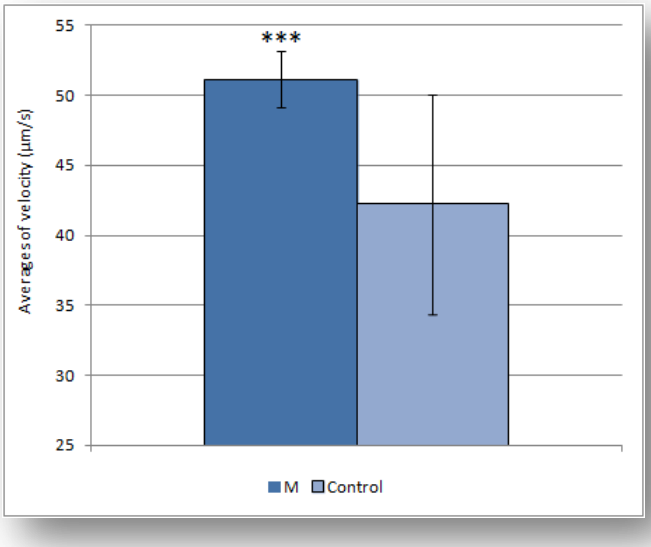

	M	Control
AVG	51.16	42.22
VAR	449.61	122.92
STDEV	21.20	11.09
SEM	1.97	8
MAX	112	89.48
MIN	5.06	17.51
n	2	2
# cells	116	119
p value	8.266E-05	

Figure 68 - Averages of velocity (µm/s) for M-treated free swimming cells and sEBSS-treated cells (control) (left); Statistical parameters (µm/s) calculated for free swimming cells treated with M or sEBSS (control) (right). [M] = 40 µM. AVG – average; VAR – variance; STDEV – standard deviation; SEM – standard error of the mean; MAX – maximum value; MIN – minimum value. P value significant (< 0.001).

Analysis of the correspondent histogram confirmed this double cells' dynamics when exposed to Mibefradil. Apparently, Mibefradil seems to be increasing cells' velocity from around 35 – 50 µm/s to higher intervals ranging from 55 to 110 µm/s, peaking at 70 – 75 µm/s (hence cells # 1) (Figure 69). The reason why it is changing cells' motility this way is not clear since there are no studies (so far) that relate intracellular Ca^{2+} levels to flagellar beating. However, it is possible that there is a connection between the two and if so, since Mibefradil is known to be an inhibitor of CatSper, a decrease of motility due to the blocking of Ca^{2+} influx through these channels would be expected. One hypothesis to explain this, assuming the previous statement about the relation between the two events is correct, is that a yet unknown pathway to raise $[Ca^{2+}]_i$ is being used by the cells which can lead to a rapid flagellar beating.

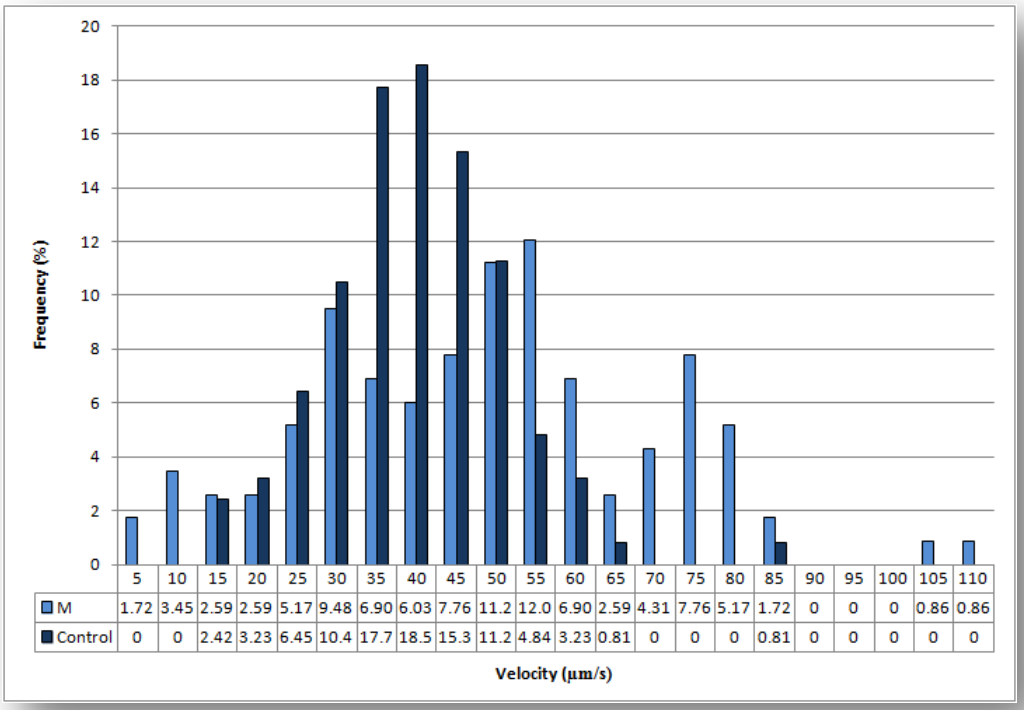

	5	10	15	20	25	30	35	40	45	50	55	60	65	70	75	80	85	90	95	100	105	110
M	1.72	3.45	2.59	2.59	5.17	9.48	6.90	6.03	7.76	11.2	12.0	6.90	2.59	4.31	7.76	5.17	1.72	0	0	0	0.86	0.86
Control	0	0	2.42	3.23	6.45	10.4	17.7	18.5	15.3	11.2	4.84	3.23	0.81	0	0	0	0.81	0	0	0	0	0

Figure 69 - Velocity (µm/s) distribution for sEBSS (control) or M-treated cells.

III.2.5 NNC's effect

For the evaluation of NNC's effects on cells, five samples collected on the same day were compared to its control ones.

Cells' visual observation revealed a quite surprising discovery: a great number of cells appeared to be hyperactivated, exhibiting high amplitude bendings and flagellar asymmetry. This result was intriguing since NNC is known to inhibit CatSper and thus Ca^{2+} influx that is necessary to sustain hyperactivation. The process itself requires an elevation of $[Ca^{2+}]_i$ (for example by addition of 4-AP) in order to be triggered. Software analysis of cells' tracks reported a great statistical significance ($p < 0.001$) for differences between cells in NNC and sEBSS. Mean values (µm/s) were clearly distinctive with 47.92 ± 0.76 and 56.78 ± 1.02 for cells in NNC and sEBSS, respectively (Figure 70).

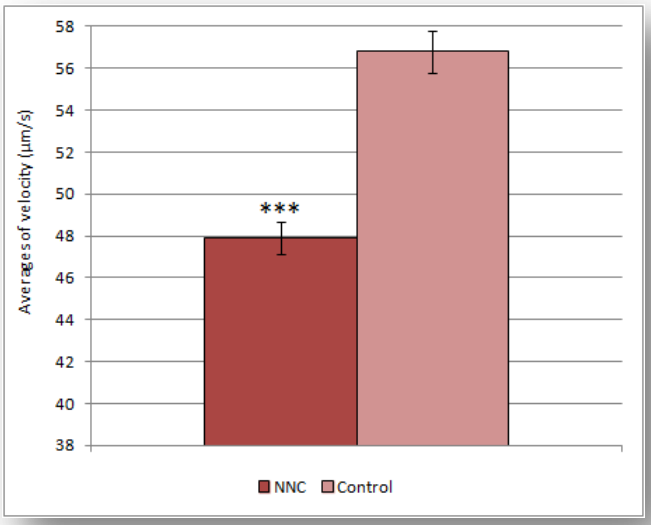

	NNC	Control
AVG	47.92	56.78
VAR	155.61	209.28
STDEV	12.47	14.47
SEM	0.76	1.02
MAX	86.18	96.43
MIN	12.27	13
n	1	1
# cells	270	200
p value	4.359E-12	

Figure 70 - Averages of velocity (µm/s) for NNC-treated free swimming cells and sEBSS-treated cells (control) (left); Statistical parameters (µm/s) calculated for free swimming cells treated with NNC or sEBSS (control) (right). [NNC] = 10 µM. AVG – average; VAR – variance; STDEV – standard deviation; SEM – standard error of the mean; MAX – maximum value; MIN – minimum value. P value significant (< 0.001).

A clear shift to left of the NNC histogram can be seen when compared to the sEBSS one, thus denoting a decrease in velocity (Figure 71). Since earlier on this work, the multiplicity of NNC effect's on $[Ca^{2+}]_i$ was reported, it is fair to say that NNC might be increasing intracellular Ca^{2+} sufficiently to liberate stored Ca^{2+} hence initiating hyperactivation or, by blocking CatSper and Ca^{2+} influx, activating a mechanism that will induce Ca^{2+} efflux from ICS and, consequently, hyperactivation.

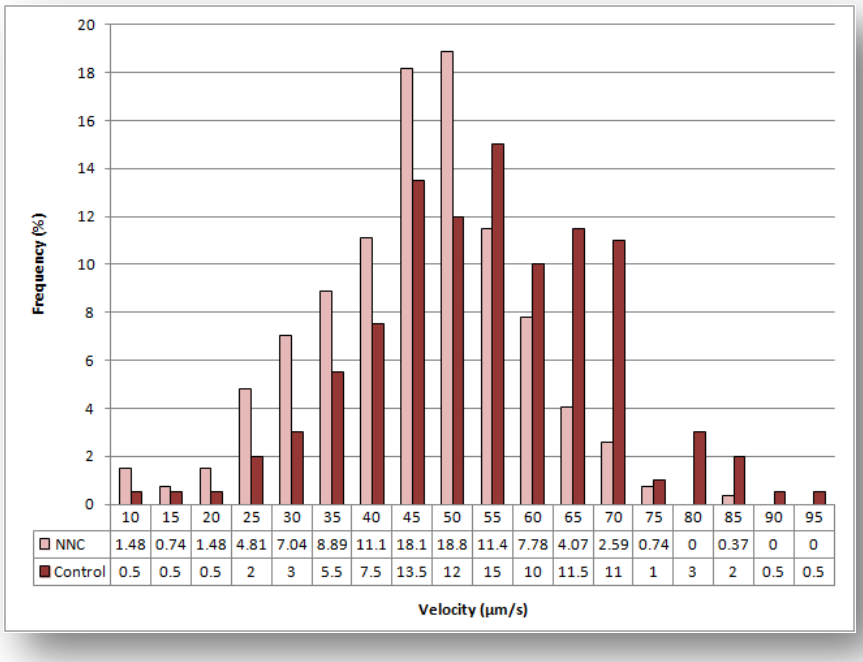

Figure 71 - Velocity (µm/s) distribution for sEBSS (control) or NNC-treated cells.

Chapter IV

Conclusions and future projects

Ca^{2+} signal propagation within sperm is essential to fertilisation. Without it, sperm is neither able to acquire the necessary motility type nor to undergo the exocytotic reaction that will allow degradation and perfuration of the surrounding layers of the oocyte. CatSper and ICS, especially RNE, contribute to this propagation probably by mediating Ca^{2+} signal from the midpiece to the flagellum and vice-versa. Pharmacological modulation of these channels with inhibitors such as Mibefradil and NNC or promoters like TMA or Progesterone allows a better understanding of CatSper's role on Ca^{2+} mobilisation. Furthermore, by inducing Ca^{2+} extrusion from ICS through stimulation with 4-AP or Thimerosal, the importance of stores in sperm can be also clarified.

In the present work, TMA proved to be a strong and reliable inducer of Ca^{2+} influx through pH-sensitive CatSper, by modulating intracellular pH. When added to cells, a typical response shows a rapid increase in Ca^{2+} levels followed by a steady plateau. Slight differences found between both concentrations tested and between the three times of stimulation were statistically non significant ($p > 0.05$).

As for 4-AP and Thimerosal, their addition causes intracellular Ca^{2+} rise, though it was not possible to determine if it was due to CatSper or efflux from the stores or even both. 4-AP seems to act similarly to TMA provoking an increase in fluorescence and eventual settling of a plateau; no statistically significant ($p > 0.05$) differences were found between the three concentrations, although the response to the highest [4-AP] presented a different kinetics. Thimerosal appears to reach a plateau faster than the previous compounds, although it settles at lower Ca^{2+} levels. When perfused in combination with either TMA or 4-AP, cells react with a first steep rise in fluorescence (higher when with 4-AP) and a second gradual increase after a fall above the plateau settled by 4-AP/TMA beforehand. No statistical significance ($p > 0.05$) was found between the three [4-AP].

Although Mibefradil showed a consistent inhibition of CatSper thus causing the decrease of intracellular Ca^{2+} below baseline levels, NNC presented at least three different responses: one similar to the Mibefradil one; the other, a partial inhibition with a plateau above baseline levels and a third causing a rise in Ca^{2+} levels. Causes for this kind of behaviour are yet unknown. P4 is also affected differently by both

compounds. When each is added to TMA or 4-AP separately, an inhibitory effect is seen, sometimes below the plateau settled by 4-AP/TMA beforehand (thus partially inhibiting cells) and others below baseline levels (full inhibition). No statistical significance ($p > 0.05$) was found between [4-AP] nor between [TMA].

With the motility studies, a change in swimming pattern can be seen when comparing sEBSS-treated sperm with TMA-treated and Mibefradil-treated (increased velocity) and NNC-treated (decreased velocity). Albeit Thimerosal and 4-AP treated cells presented some apparent differences when compared to sEBSS (control), no statistical significance ($p > 0.05$) was found when looking at velocity. Due to the reduced size of the sample, more experiments would be beneficial to confirm the stability of the statistics.

With this work, it is possible to conclude that there is a relevant intercommunication between CatSper and ICS that prevents the decrease of intracellular Ca^{2+} to abnormal levels. CatSper seem to be responsible for maintaining normal levels of intracellular Ca^{2+} and ICS (especially RNE) appear to contribute to this with an extra efflux of Ca^{2+} to the intracellular environment, possibly when the channels are overwhelmed or deactivated. Moreover, there seems to be a relation between $[Ca^{2+}]_i$ levels and flagellar beating, since after addition (to free swimming cells) of compounds who meddle with Ca^{2+} influx such as TMA, Mibefradil and NNC, sperm motility is altered. However, this relation (or not) is not documented so far.

Examples of possible future projects to develop on findings from the current work could be:

- longstanding experiments with M & P4 in order to explore its inhibitory effect on Ca^{2+} and on P4-induced responses;
- use of Ca^{2+} free medium instead of sEBSS to provoke emptying of ICS and better reveal its contribution to the rise of intracellular Ca^{2+} as well as the importance of extracellular Ca^{2+} in this increment.

Future work in motility studies that would be interesting to do:

- enhance the “n” of experiments and include more donors to allow for a sampling of human sperm population;

- use CASA (computed-aided sperm analysis) to evaluate other parameters such as percentage of progressively motile sperm, amplitude of lateral head movement, beat cross frequency, path linearity, accumulated distance, etc, with the same compounds and combinations of them
- use of caged IP_3 and NP-EGTA to test effects of Ca^{2+} and IP_3 bolus on sperm motility

Chapter V

References

Alberts B, Johnson A, Lewis J, Rafi M, Roberts K and Walter P (2007a) Molecular Biology of the Cell, Fifth Edition. *Garland Science Chapter 15, 835-964*

Alberts B, Johnson A, Lewis J, Rafi M, Roberts K and Walter P (2007b) Molecular Biology of the Cell, Fifth Edition. *Garland Science Chapter 21, 1269-1304*

Arnoult C, Villaz M and Florman HM (1998) Pharmacological Properties of the T-Type Ca^{2+} Current of Mouse Spermatogenic Cells. *Mol Pharm 53, 1104–1111*

Bedu-Addo K, Costello S, Harper CV, Machado-Oliveira G, Lefievre L, Ford C, Barratt C and Publicover S (2008) Mobilisation of stored calcium in the neck region of human sperm – a mechanism for regulation of flagellar activity. *Int J Dev Biol 52, 615-626*

Bonaccorsi L, Forti G and Baldi E (2001) Low-voltage-activated calcium channels are not involved in capacitation and biological response to progesterone in human sperm. Intern *Journ Androl 24, 341-351*

Brenker C, Goodwin N, Weyand I, Kashikar ND, Naruse M, Krähling M, Müller A, Kaupp UB and Strünker T (2012) The CatSper channel: a polymodal chemosensor in human sperm. *The EMBO Journal 31, 1654-1665*

Buffone MG, Calamera JC, Verstraeten SV and Doncel GF (2005) Capacitation-associated protein tyrosine phosphorylation and membrane fluidity changes are impaired in the spermatozoa of asthenozoospermic patients*. Reproduction 129, 697–705*

Carlson AE, Quill TA, Westenbroek RE, Schuh SM, Hille B and Babcock DF (2005) Identical Phenotypes of CatSper1 and CatSper2 Null Sperm. *J Biol Chem 280 (37), 32238–32244*

Carlson AE, Burnett LA, del Camino D, Quill TA, Hille B, Chong JA, Moran MM, and Babcock DF (2009) Pharmacological Targeting of Native CatSper Channels Reveals a Required Role in Maintenance of Sperm Hyperactivation. *PLoS ONE 4(8): e6844*

Catteral WA, Streissnig J, Snutch T and Perez-Reyes E (2003) International Union of Pharmacology. XL. Compendium of voltage-gated ion channels: calcium channels. *Pharmacol Rev 55, 579-581*

Chang H and Suarez SS (2011) Two Distinct Ca^{2+} Signaling Pathways Modulate Sperm Flagellar Beating Patterns in Mice. *Biol Reprod 85, 296-305*

Chiarella P, Puglisi R, Sorrentino V, Boitani C and Stefanini M (2004) Ryanodine receptors are expressed and functionally active in mouse spermatogenic cells and their inhibition interferes with spermatogonial differentiation. *J Cell Sci 117, 4127–4134*

Costello S, Michelangeli F, Nash K, Lefievre L, Morris J, Machado-Oliveira G, Barratt C, Kirkman-Brown J and Publicover S (2009) Ca^{2+}-stores in sperm: their identities and functions. *Reproduction 138, 425-437*

Cross NL and Razy-Faulkner P (1997) Control of Human Sperm Intracellular pH by Cholesterol and Its Relationship to the Response of the Acrosome to Progesterone. *Biol Reprod 56, 1169-1174*

De Blas G, Michaut M, Trevino CL, Tomes CN, Yunes R, Darszon A and Mayorga LS (2002) The intraacrosomal calcium pool plays a direct role in acrosomal exocytosis. *J Biol Chem 277, 49326–49331*

Garcia MA and Meizel S (1999) Progesterone-Mediated Calcium Influx and Acrosome Reaction of Human Spermatozoa: Pharmacological Investigation of T-Type Calcium Channels. *Biol Reprod 60, 102–109*

Gilbert SF (2000) Developmental Biology, Sixth Edition. Sinauer Associates Part II Chapter 7

Grimaldi M, Atzori M, Ray P and Alkon DL (2001) Mobilization of calcium from intracellular stores, potentiation of neurotransmitter-induced calcium transients, and capacitative calcium entry by 4-aminopyridine. *J Neurosci 21, 3135-3143*

Gu Y, Kirkman-Brown JC, Korcheva Y, Barratt CLR and Publicover SJ (2004) Multi-state, 4-aminopyridine-sensitive ion channels in human spermatozoa. *Dev Biol 274, 308–317*

Gunaratne HJ and Vacquier VD (2006) Evidence for a secretory pathway Ca^{2+}-ATPase in sea urchin spermatozoa. *FEBS Letters 580, 3900-3904*

Gunteski-Hamblin AM, Clarke DM and Shull GE (1992) Molecular cloning and tissue distribution of alternatively spliced mRNAs encoding possible mammalian homologues of the yeast secretory pathway calcium pump. *Biochemistry 31, 7600-7608*

Harper CV, Barratt CL and Publicover SJ (2004) Stimulation of human spermatozoa with progesterone gradients to stimulate approach to the oocyte. Induction of $[Ca^{2+}]_i$ oscillations and cyclical transitions in flagellar beating. *J Biol Chem 279 (44), 46315–46325*

Harper CV and Publicover SJ (2005) Reassessing the role of progesterone in fertilization-compartmentalized calcium signalling in human spermatozoa?. *Human Reproduction 20 (10), 2675–2680*

Harper C, Wootton L, Michelangeli F, Lefièvre L, Barratt C and Publicover S (2005) Secretory pathway Ca^{2+}-ATPase (SPCA1) Ca^{2+} pumps, not SERCAs, regulate complex $[Ca^{2+}]_i$ signals in human spermatozoa. *J Cell Sci 118, 1673-1685*

Harper CV, Barratt CLR, Publicover SJ and Kirkman-Brown JC (2006) Kinetics of the Progesterone-Induced Acrosome Reaction and Its Relation to Intracellular Calcium Responses in Individual Human Spermatozoa. *Biol Reprod 75, 933–939*

Herrick SB, Schweissinger DL, Kim SW, Bayan KR, Mann S and Cardullo RA (2005) The acrosomal vesicle of mouse sperm is a calcium store. *J Cell Physiol 202, 663–671*

Ho HC and Suarez SS (2001a) An inositol 1,4,5-trisphosphate receptor-gated intracellular Ca^{2+} store is involved in regulating sperm hyperactivated motility. *Biol Reprod 65, 1606–1615*

Ho HC and Suarez SS (2001b) Hyperactivation of mammalian spermatozoa: function and regulation. *Reproduction 122, 519–526*

Ho HC, Granish KA and Suarez SS (2002) Hyperactivated Motility of Bull Sperm Is Triggered at the Axoneme by Ca^{2+} and Not cAMP. *Dev Biol 250, 208–217*

Ho HC and Suarez SS (2003) Characterization of the Intracellular Calcium Store at the Base of the Sperm Flagellum That Regulates Hyperactivated Motility. *Biol Reprod 68, 1590-1596*

Huang L, Keyser BM Tagmose TM, Hansen JB, Taylor JT, Zhuang H, Zhang M, Ragsdale DS and Li M (2004) NNC 55-0396 [(1*S*,2*S*)-2-(2-(*N*-[(3-Benzimidazol-2-yl)propyl]-*N*methylamino)ethyl)-6-fluoro-1,2,3,4-tetrahydro-1-isopropyl-2-naphtyl cyclopropanecarboxylate dihydrochloride]: A New Selective Inhibitor of T-Type Calcium Channels. *JPET 309, 193-199*

Jimenez-Gonzalez C, Michelangeli F, Harper CV, Barratt CL and Publicover SJ (2006) Calcium signalling in human spermatozoa: A specialized 'toolkit' of channels, transporters and stores. *Hum Reprod Update 12 (3), 253–267*

Kirkman-Brown JC, Bray C, Stewart PM, Barratt CLR and Publicover SJ (2000) Biphasic Elevation of $[Ca^{2+}]_i$ in Individual Human Spermatozoa Exposed to Progesterone. *Dev Biol 222, 326–335*

Kirkman-Brown JC, Punt EL, Barratt CL and Publicover SJ (2002) Zona pellucida and progesterone-induced Ca^{2+} signalling and acrosome reaction in human spermatozoa. *J Androl 23 (3), 306–315*

Kirkman-Brown JC, Barratt CL and Publicover SJ (2003) Nifedipine reveals the existence of two discrete components of the progesterone-induced $[Ca^{2+}]_i$ transient in human spermatozoa. *Dev Biol 259, 71–82*

Kirkman-Brown JC, Barratt CL and Publicover SJ (2004) Slow calcium oscillations in human spermatozoa. *Biochem J 378, 827–832*

Krausz C, Bonaccorsi L, Maggio P, Luconi M, Criscuoli L, Fuzzi , Pellegrini S, Forti G and Baldi E (1996) Two functional assays of sperm responsiveness to progesterone and their predictive values in in-vitro fertilization. *Hum Reprod 11(8), 1661-1667*

Kuroda Y, Kaneko S, Yoshimura Y, Nozawa S and Mikoshiba K (1999) Are there inositol 1,4,5-triphosphate (IP_3) receptors in human sperm?. *Life Sci 65 (2), 135–143*

Lishko PV, Botchkina IL and Kirichok Y (2011) Progesterone activates the principal Ca^{2+} channel of human sperm. *Nature 471, 387-391*

Marquez B, Ignotz G and Suarez SS (2007) Contributions of extracellular and intracellular Ca^{2+} to regulation of sperm motility: release of intracellular stores can hyperactivate CatSper1 and CatSper2 null sperm. *Dev Biol 303, 214–221*

Michelangeli F, Ogunbayo OA and Wootton LL (2005) A plethora of interacting organellar Ca^{2+} stores. *Curr Opin Cell Biol 17, 135-140*

Mitchison TJ and Mitchison HM (2010) Cell biology: How cilia beat. *Nature 463, 308-309*

Naaby-Hansen S, Wolkowicz MJ, Klotz K, Bush LA, Westbrook VA, Shibahara H, Shetty J, Coonrod SA, Reddi PP, Shannon J, Kinter M, Sherman NE, Fox J, Flickinger CJ and Herr JC (2001) Co-localization of the inositol 1,4,5-trisphosphate receptor and calreticulin in the equatorial segment and in membrane bounded vesicles in the cytoplasmic droplet of human spermatozoa. *Mol Hum Reprod 7(10), 923–933*

Ohmuro J and Ishijima S (2006) Hyperactivation Is the Mode Conversion From Constant-Curvature Beating to Constant-Frequency Beating Under a Constant Rate of Microtubule Sliding. *Mol Reprov Dev 73, 1412–1421*

Putney JW Jr (1990) Receptor-regulated calcium entry. *Pharmacol Ther 48, 427-434*

Quill TA, Sugden SA, Rossi KL, Doolittle LK, Hammer RE and Garbers DL (2003) Hyperactivated sperm motility driven by CatSper2 is required for fertilization. *Proc Natl Acad Sci USA 100, 14869–14874*

Rossato M, Di Virgilio F, Rizzuto R, Galeazzi C and Foresta C (2001) Intracellular calcium store depletion and acrosome reaction in human spermatozoa: role of calcium and plasma membrane potential. *Mol Hum Reprod 7, 119-128*

Schuh K, Cartwright EJ, Jankevics E, Bundschu K, Liebermann J, Williams JC, Armesilla AL, Emerson M, Oceandy D, Knobeloch K and Neyses L (2003) Plasma Membrane Ca^{2+} ATPase 4 Is Required for Sperm Motility and Male Fertility. *J Biol Chem 279 (27), 28220-28226*

Strünker T, Goodwin N, Brenker C, Kashikar ND, Weyand I, Seifert R and Kaupp UB (2011) The CatSper channel mediates progesterone-induced Ca^{2+} influx in human sperm. *Nature 471, 382-386*

Suarez SS (2008) Control of hyperactivation in sperm. *Hum Reprod Update 14 (6), 647–657*

Treviño CL, Felix R, Castellano LE, Gutiérrez C, Rodríguez D, Pacheco J, López-González I, Gomora JC, Tsutsumi V, Hernández-Cruz A, Fiordelisio T, Scaling AL, Darszon A (2004) Expression and diferential cell distribution of low-threshold Ca^{2+} channels in mammalian male germ cells and sperm. *FEBS Letters 563, 87-92*

Visconti PE, Westbrook VA, Chertihin O, Demarco I, Sleight S and Diekman AB (2002) Novel signaling pathways involved in sperm acquisition of fertilizing capacity. *J Reprod Immunol 53, 133–150*

Walensky LD and Snyder SH (1995) Inositol 1,4,5-triphosphate receptors selectively localized to the acrosomes of mammalian sperm. *J Cell Biol 130 (4), 857-869*

Wennemuth G, Babcock DF and Hille B (2003) Calcium clearance mechanisms of mouse sperm. *J Gen Physiol 122, 115-128*

World Health Organization laboratory manual for the examination and processing of human semen, Fifth Edition (2010) Chapter 2

Wu S, Zhang M, Vest PA, Bhattacharjee A, Liu L and Li M (2000) A mibefradil metabolite is a potent intracellular blocker of L-type Ca^{2+} currents in pancreatic β-cells. *J Pharmacol Exp Ther 292, 939–943*